Nuclear Surface Unveiled by Knockout Reactions.

Arun K Jain

Nuclear Physics Division, B.A.R.C., Mumbai.

N-N Interaction has a complicated nature (provided to it by the strong coupling finite mass mesons), it has strong short range repulsion (almost a hard core of ~ 0.5 to 0.6 fm) and a finite short range, but a comparatively longer range, ~2 fm strong attraction.

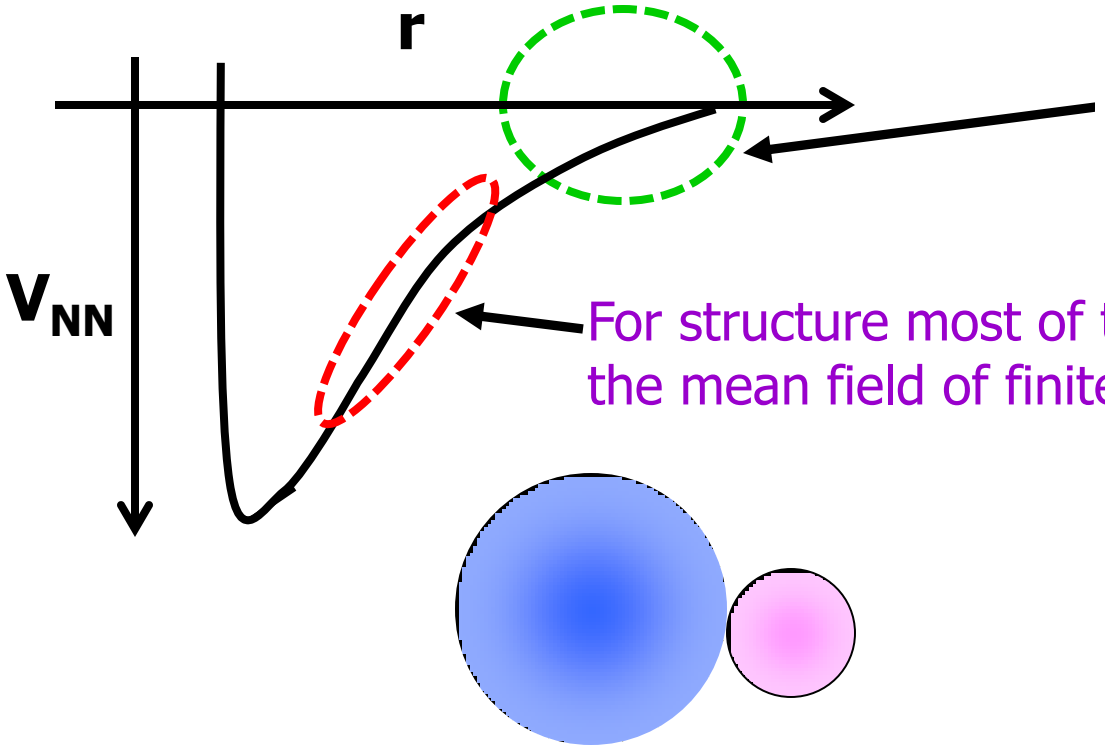

This longer range residual interaction leads to clustering

For structure most of the N-N interaction leads to the mean field of finite range Woods Saxon type.

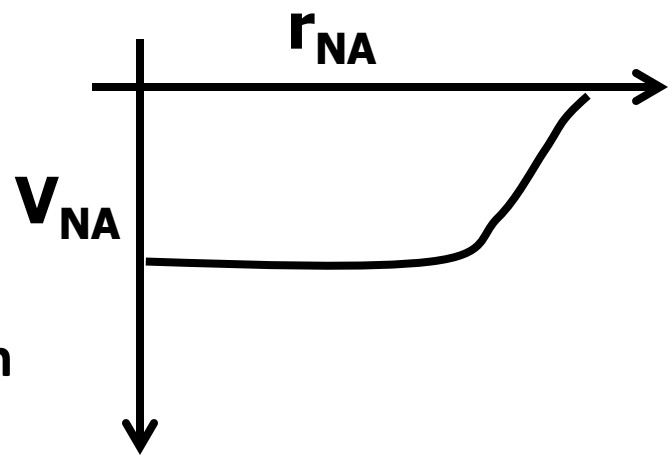

Clustering due to long range residual interaction

Knockout Reaction Kinematics

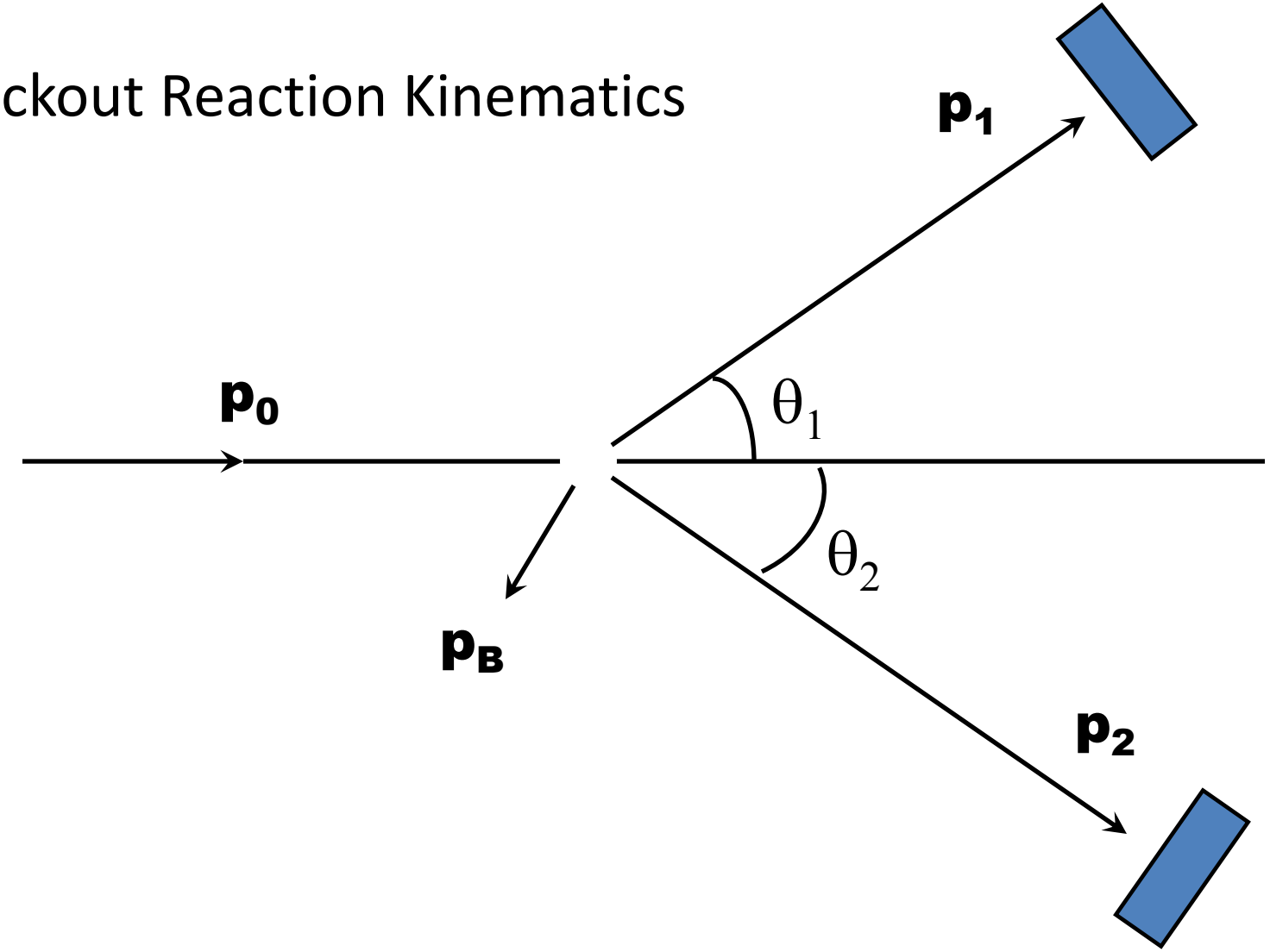

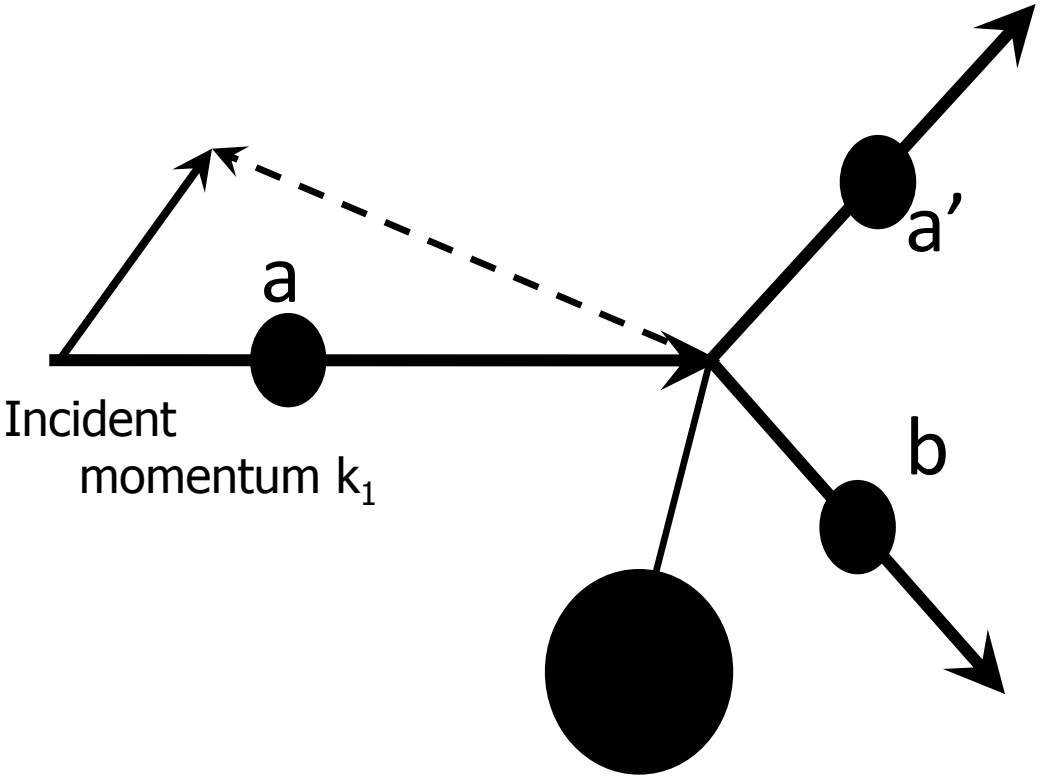

Knockout Reaction

A(a, a'b)B

$\vec{k}_1\ \vec{k}'_1\vec{k}'_2$

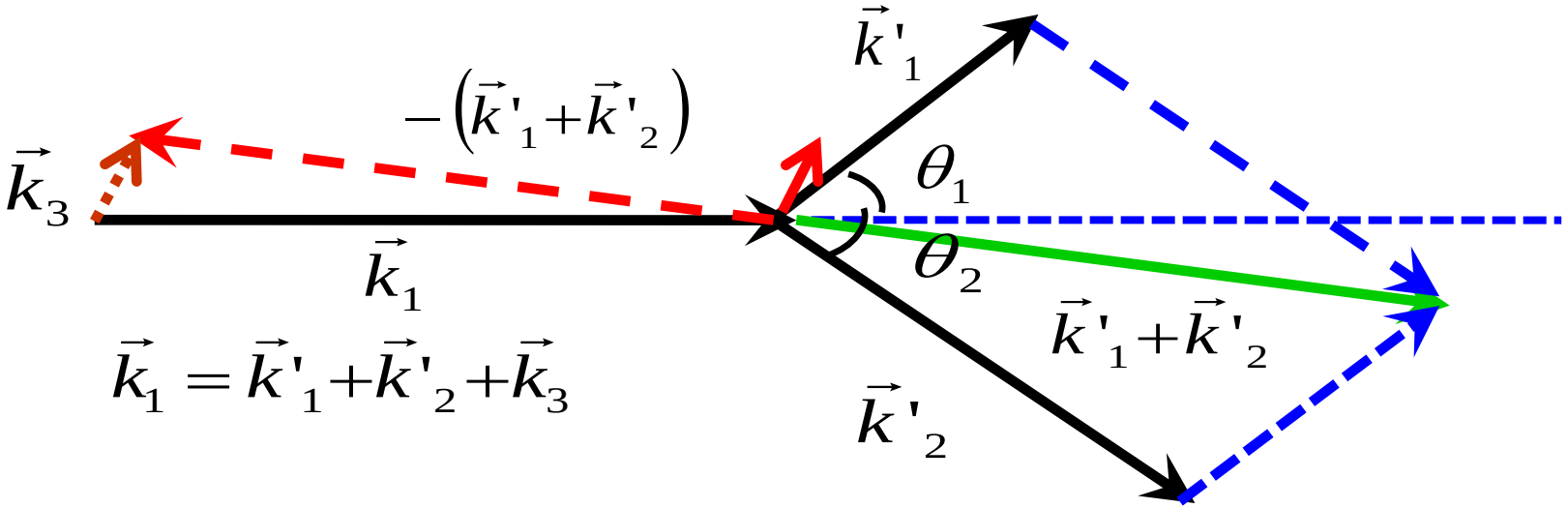

If b were free then

$\boldsymbol{k_3 = - k_3 = 0}$

$$\vec{k}_1 = \vec{k}'_1 + \vec{k}'_2$$

$E_1 = E'_1 + E'_2$

If the particle is bound by a few *MeV*, then

$$E_0 = E'_1 + E'_2 + Q$$

as the Q is (- *ve*)

E'_1 and E'_2 are $<$ E_1 and E_2 respectively.

Hence k'_1 and k'_2 are $<$ k_1 and k_2 respectively.

and θ_1 and θ_2 of $\boldsymbol{k'_1}$ and $\boldsymbol{k'_2}$ will be

slightly $<$ that of free scattering.

Zero Range Knockout

Zero Range Knockout

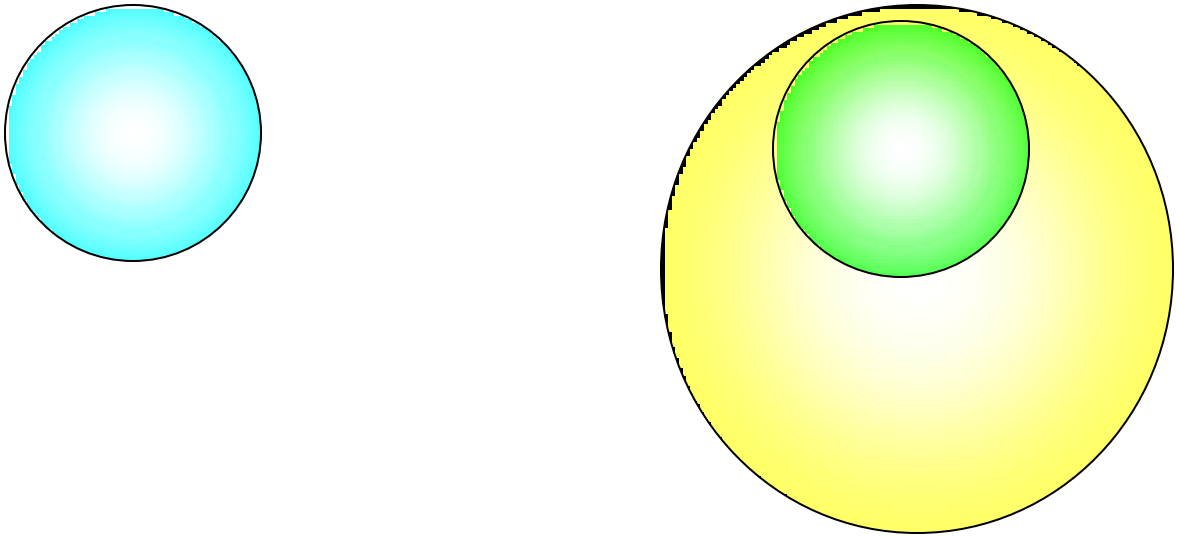

Zero Range Knockout

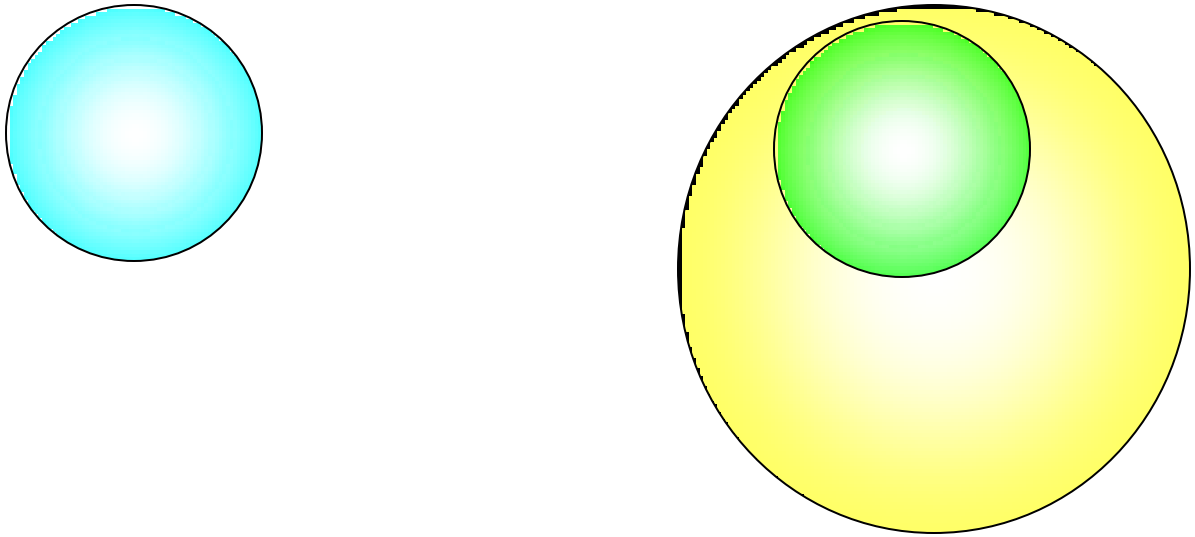

Zero Range Knockout

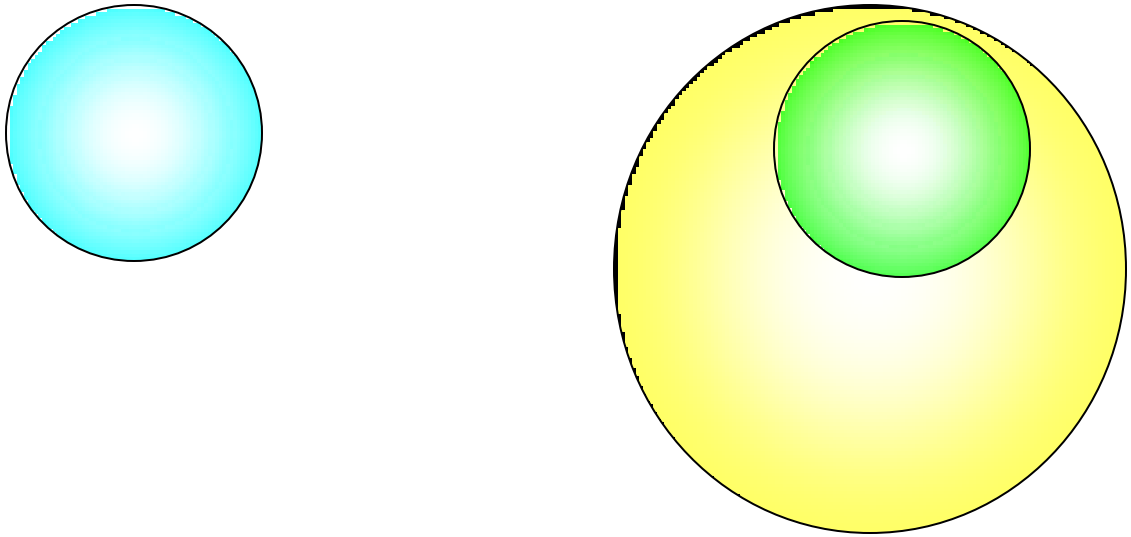

Zero Range Knockout

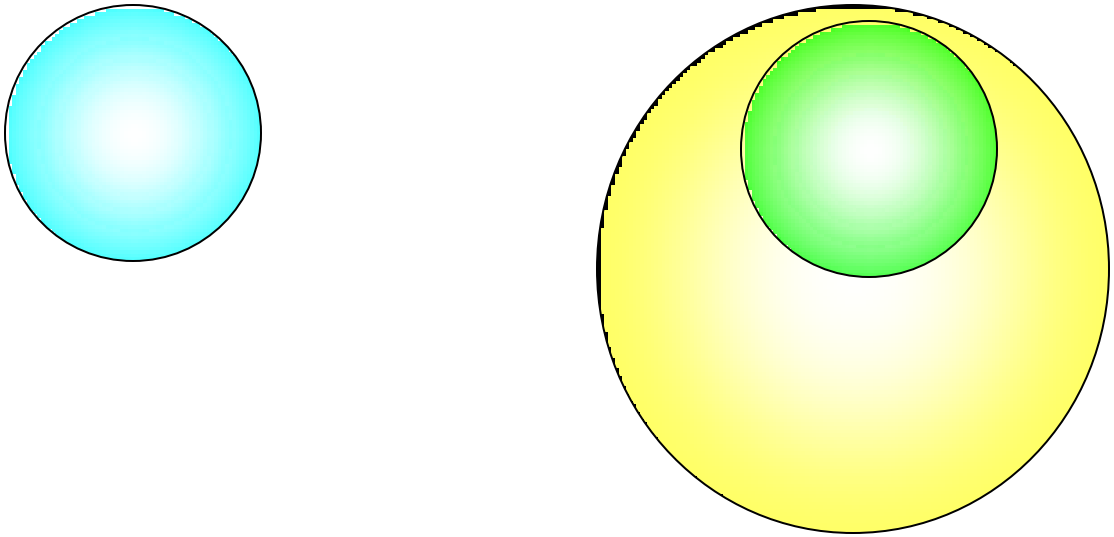

Zero Range Knockout

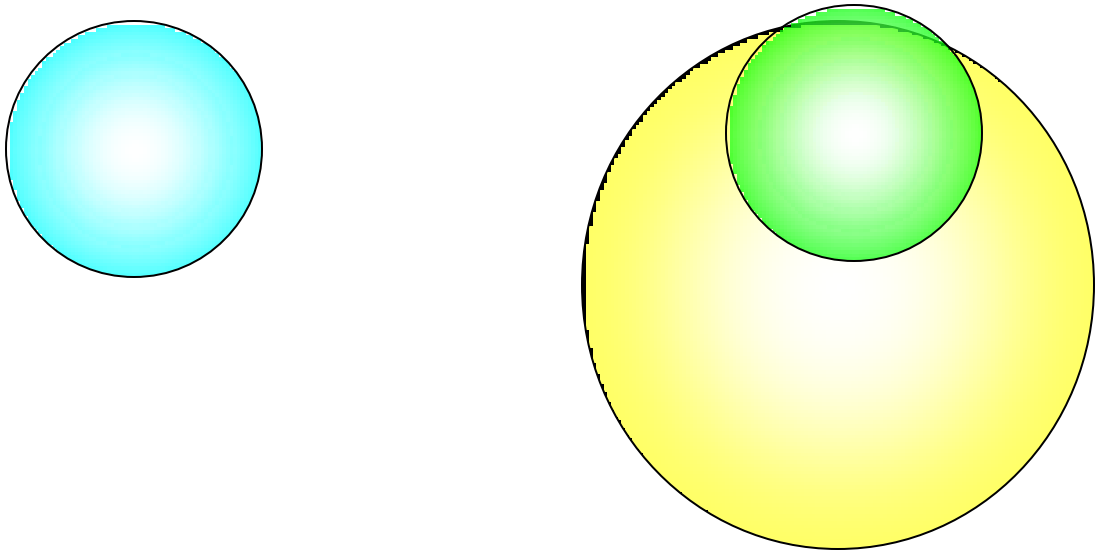

Zero Range Knockout

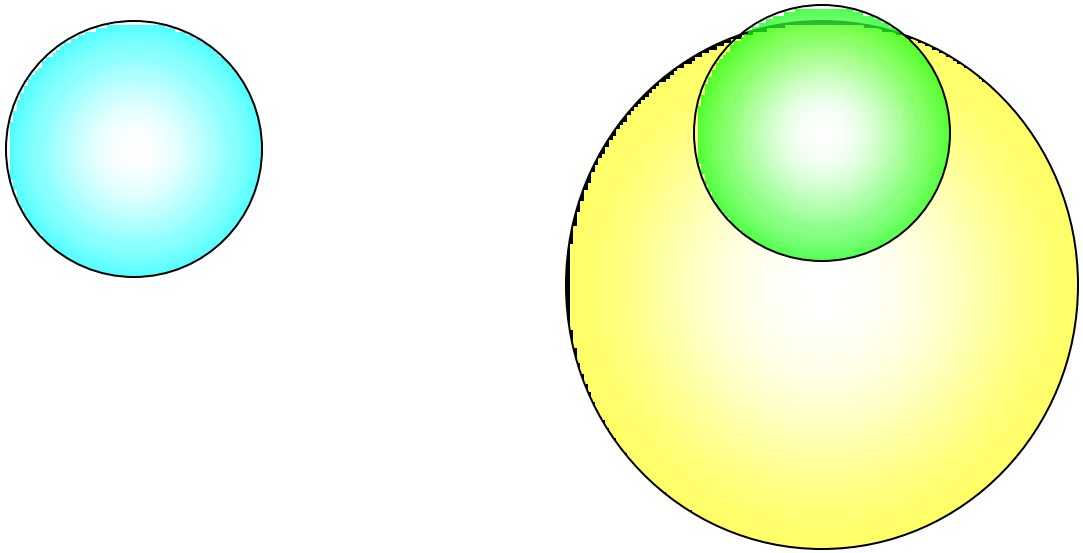

Zero Range Knockout

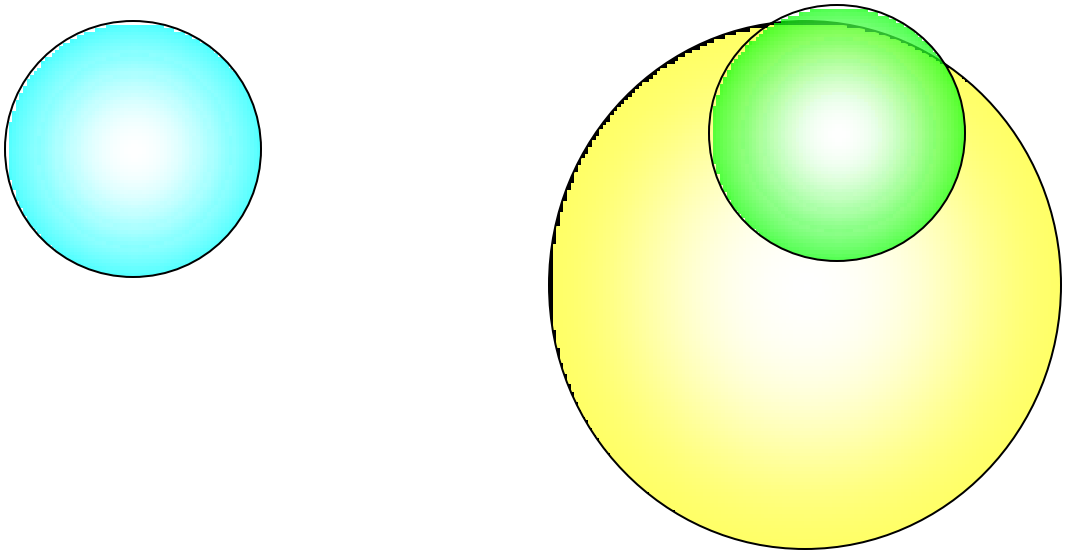

Zero Range Knockout

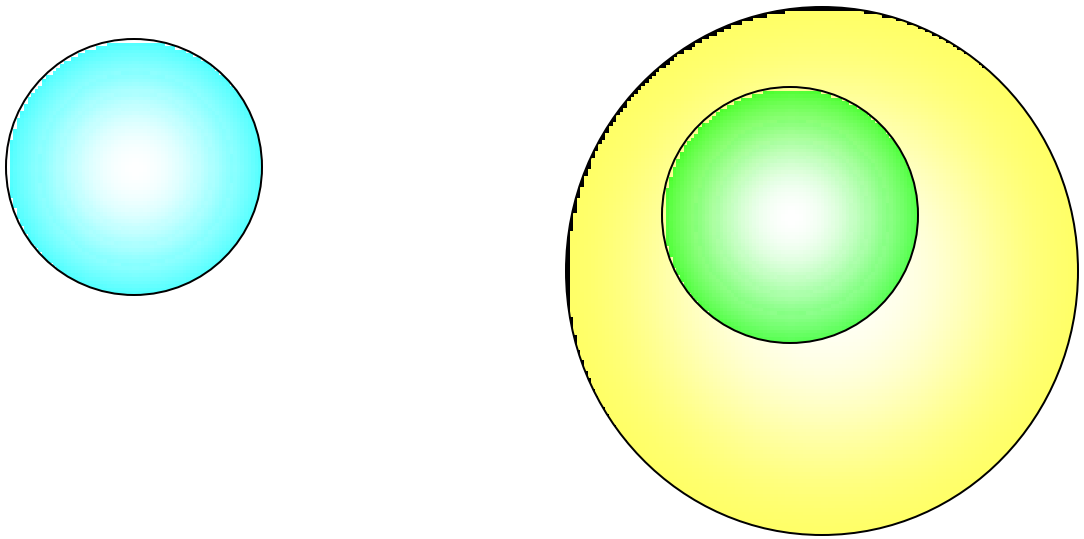

Zero Range Knockout

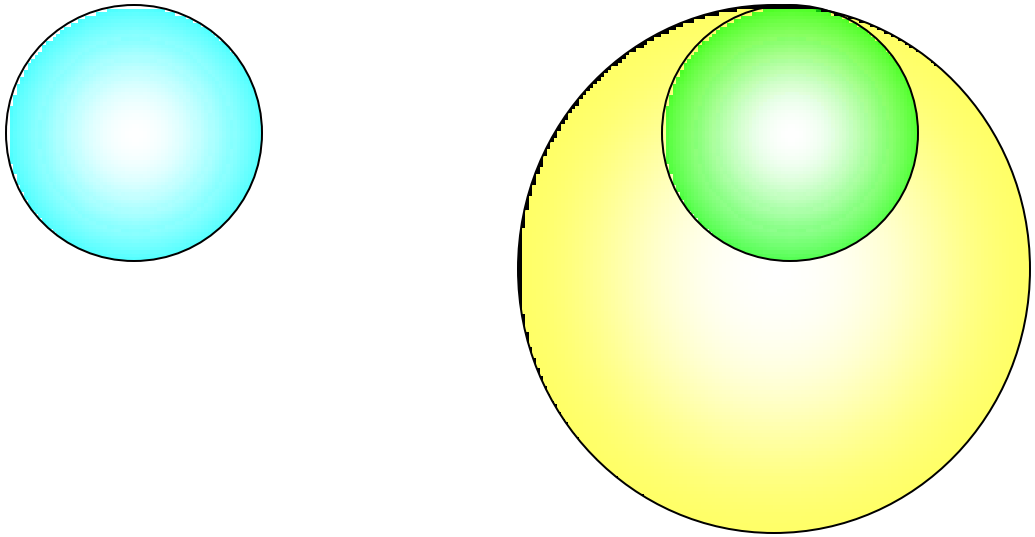

Zero Range Knockout

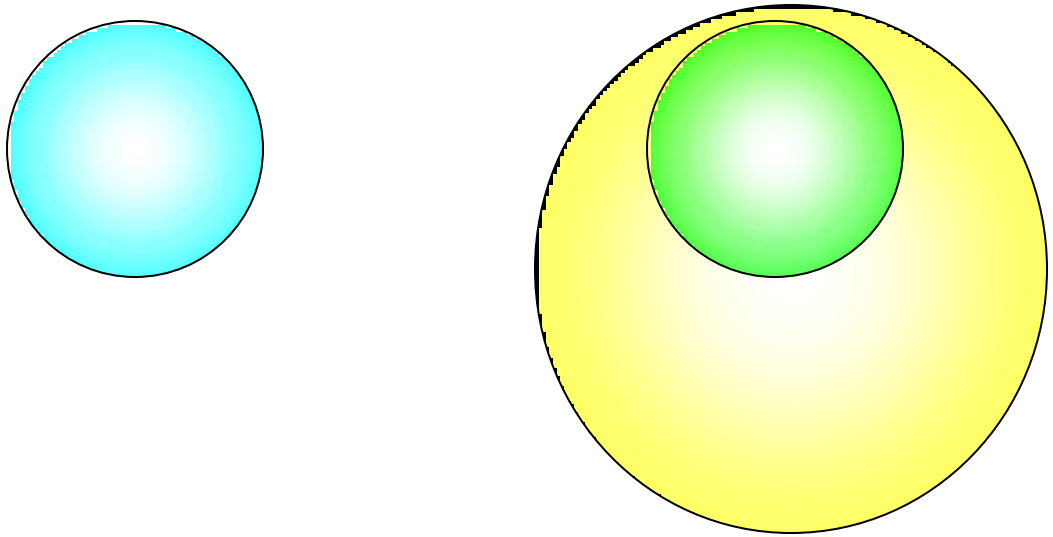

Zero Range Knockout

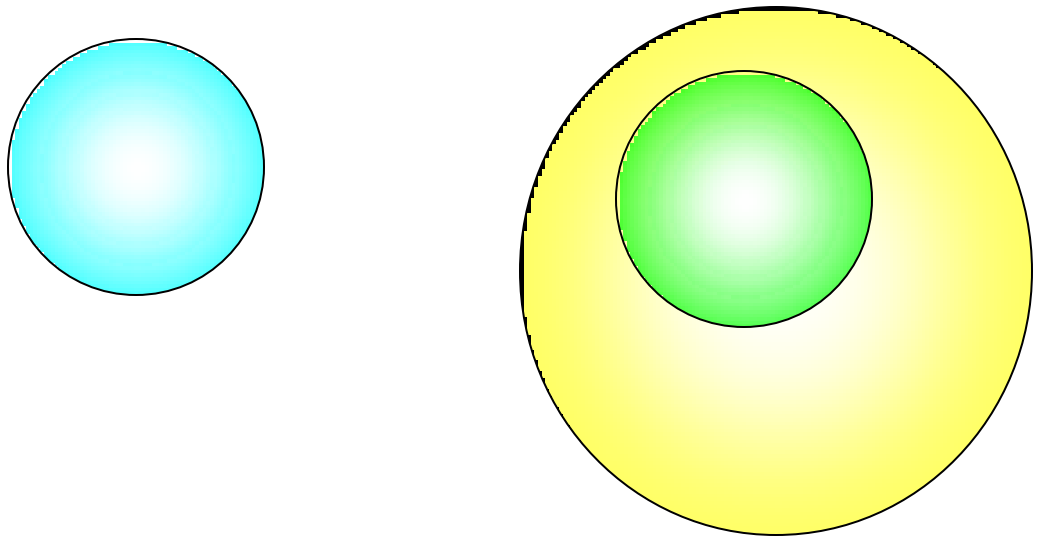

Zero Range Knockout

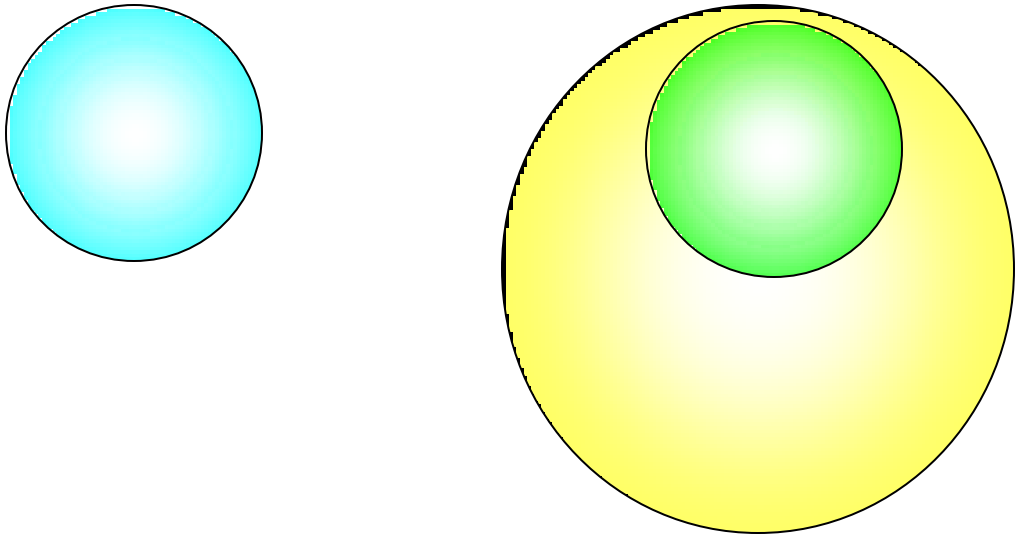

Zero Range Knockout

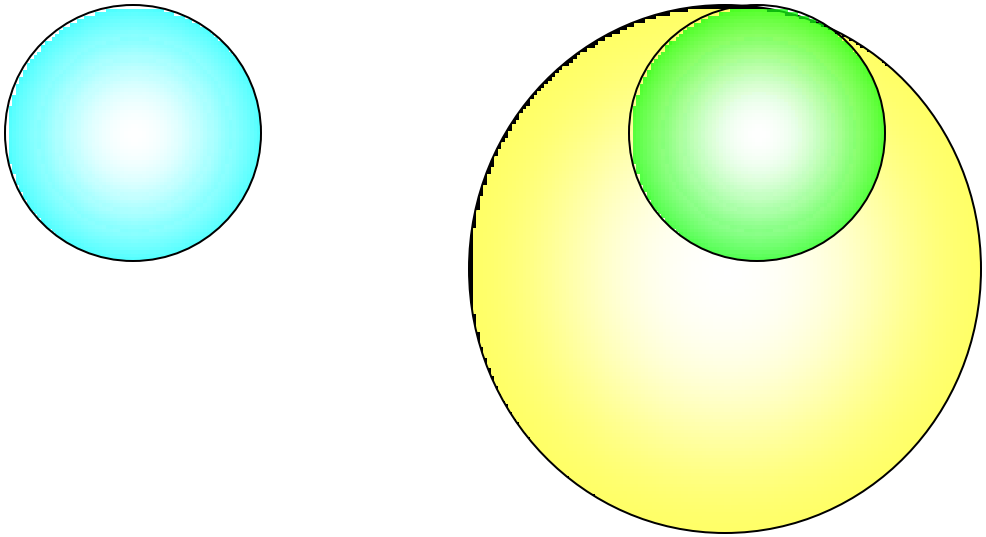

Zero Range Knockout

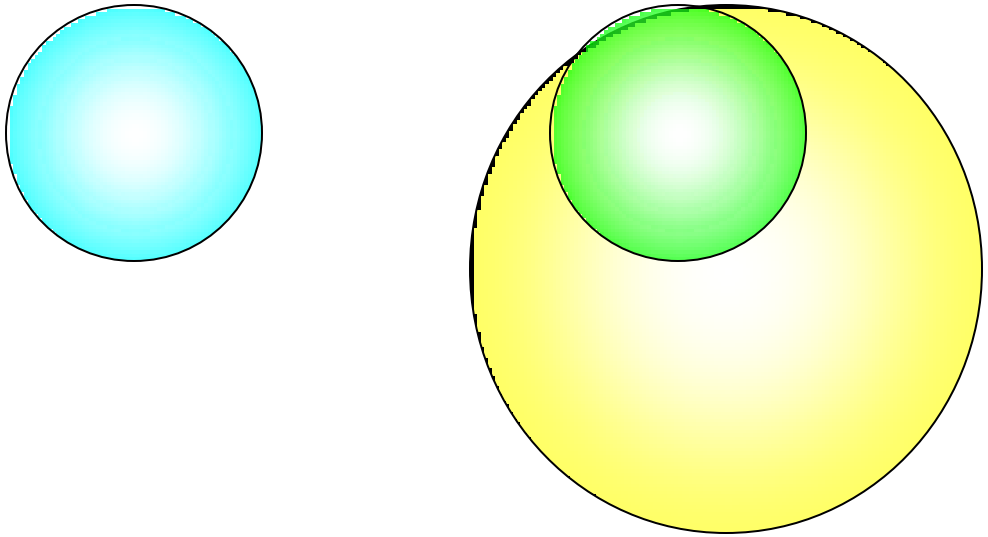

Zero Range Knockout

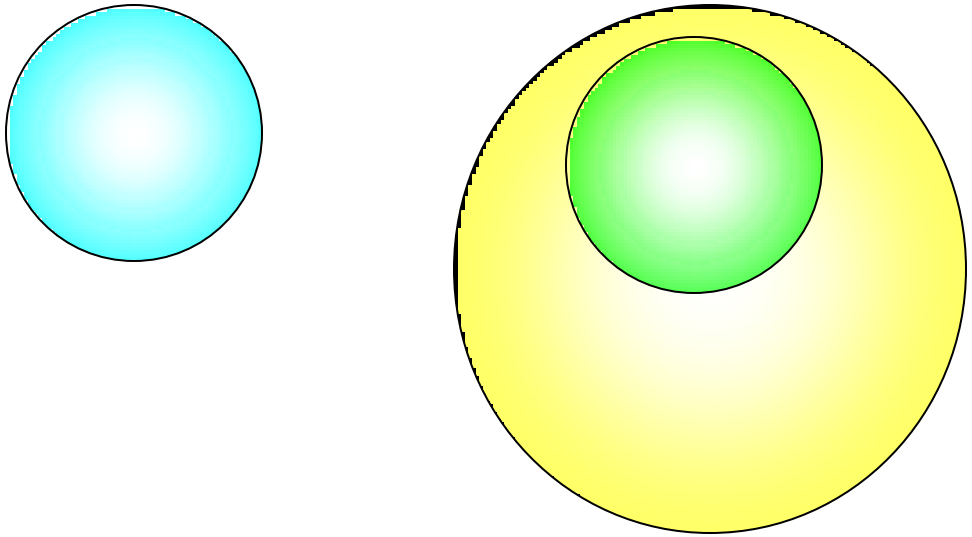

Zero Range Knockout

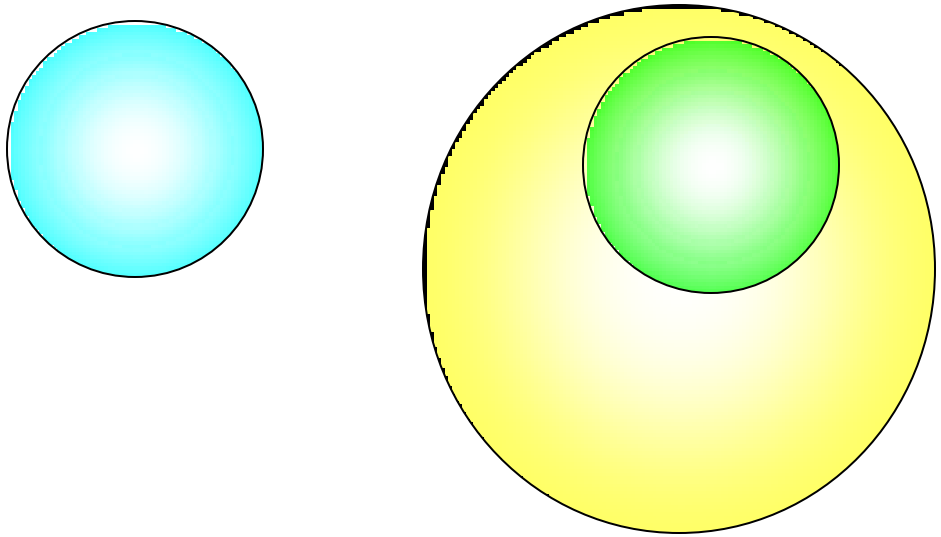

Zero Range Knockout

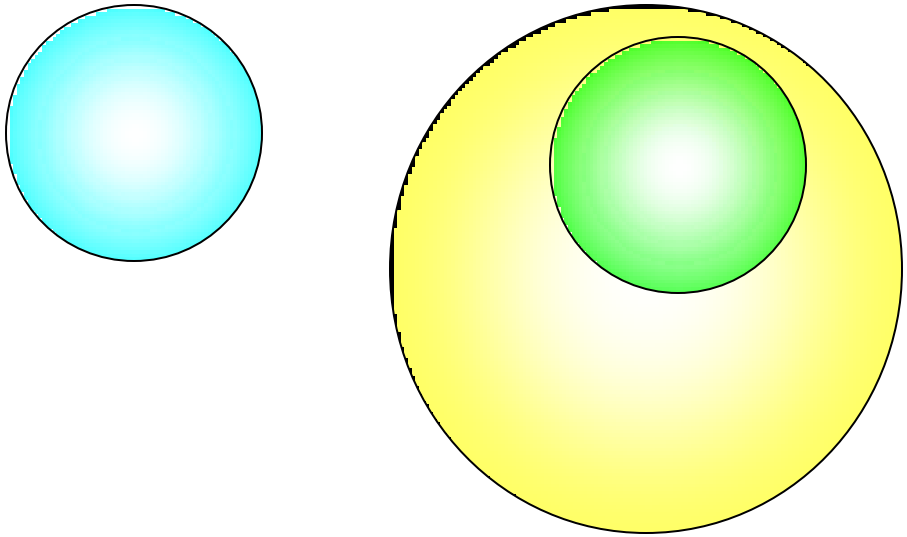

Zero Range Knockout

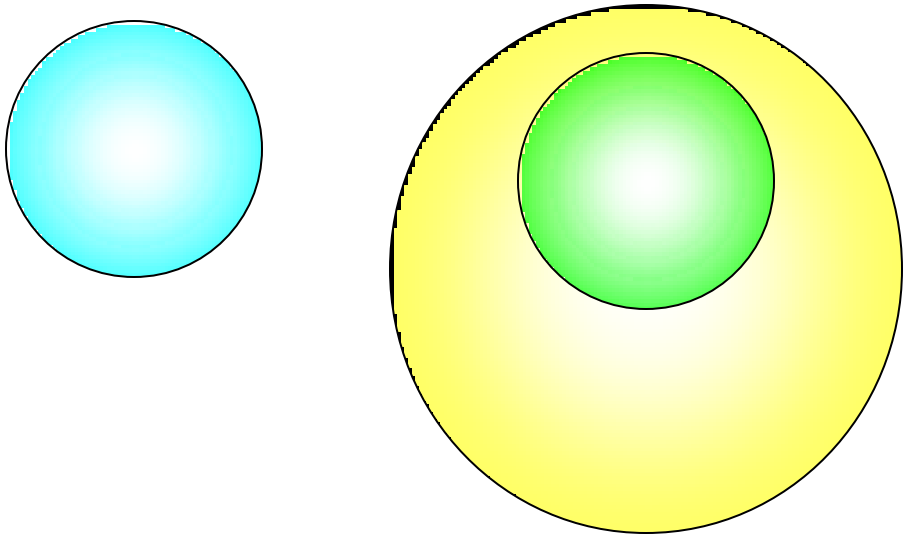

Zero Range Knockout

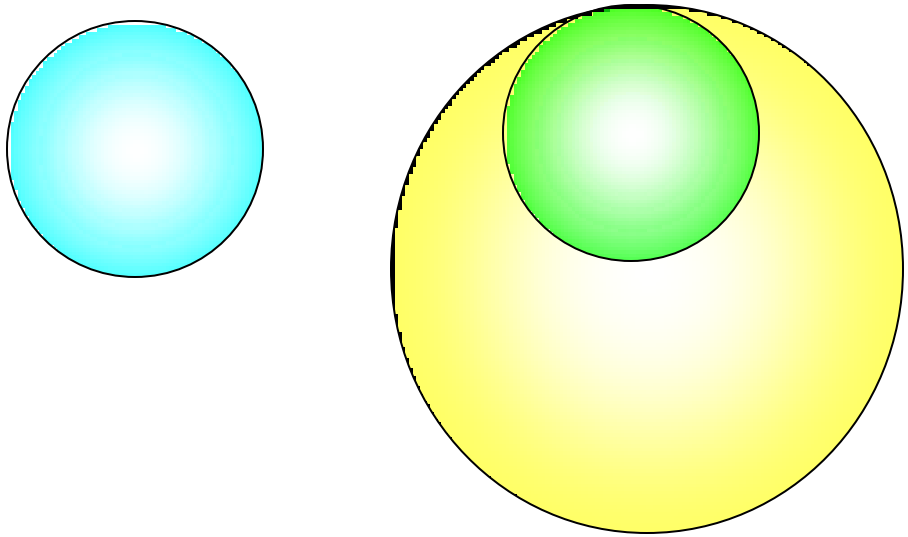

Zero Range Knockout

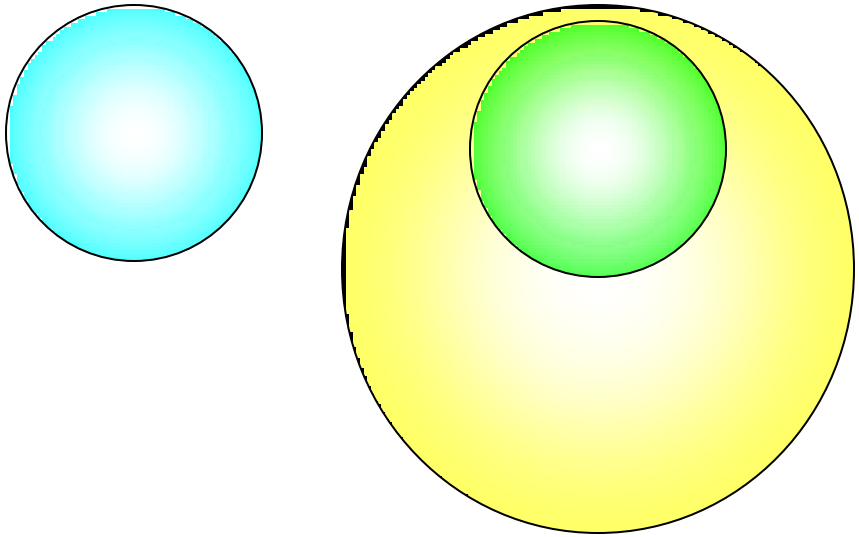

Zero Range Knockout

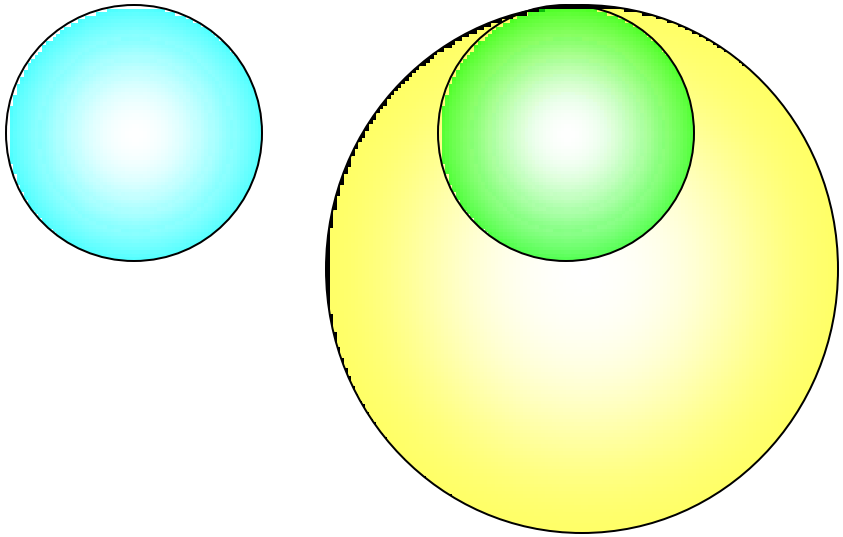

Zero Range Knockout

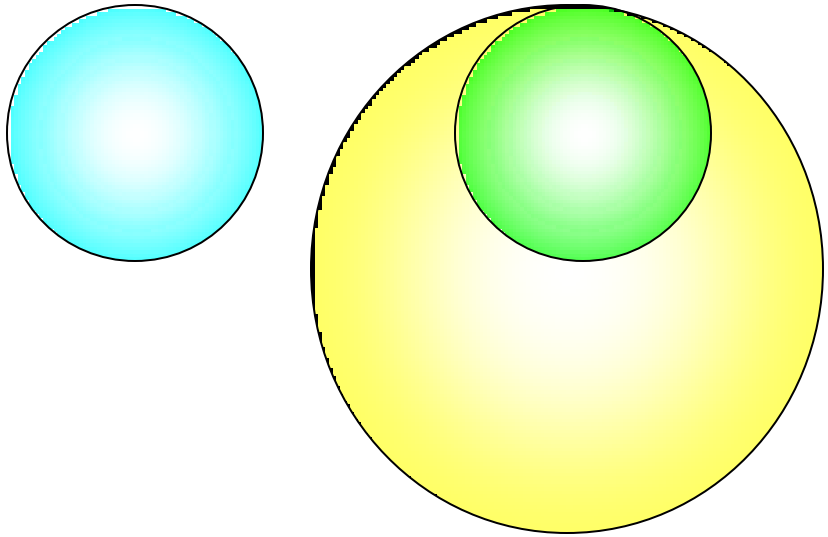

Zero Range Knockout

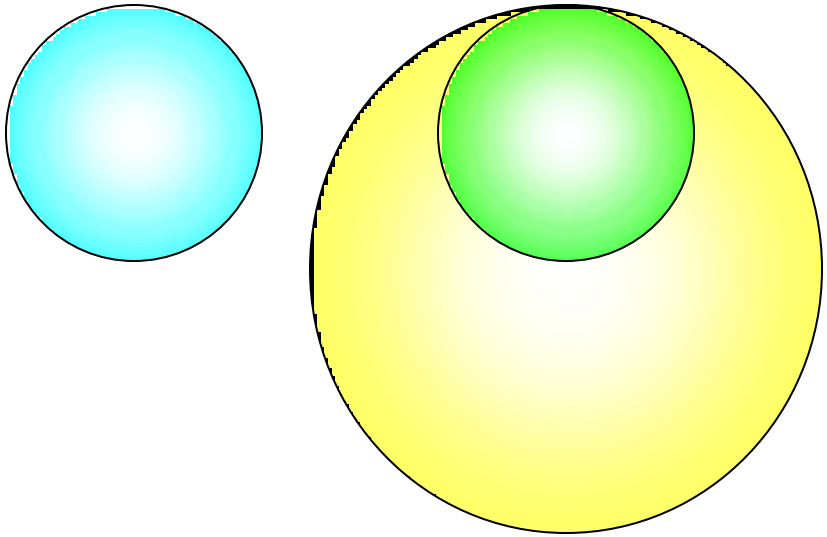

Zero Range Knockout

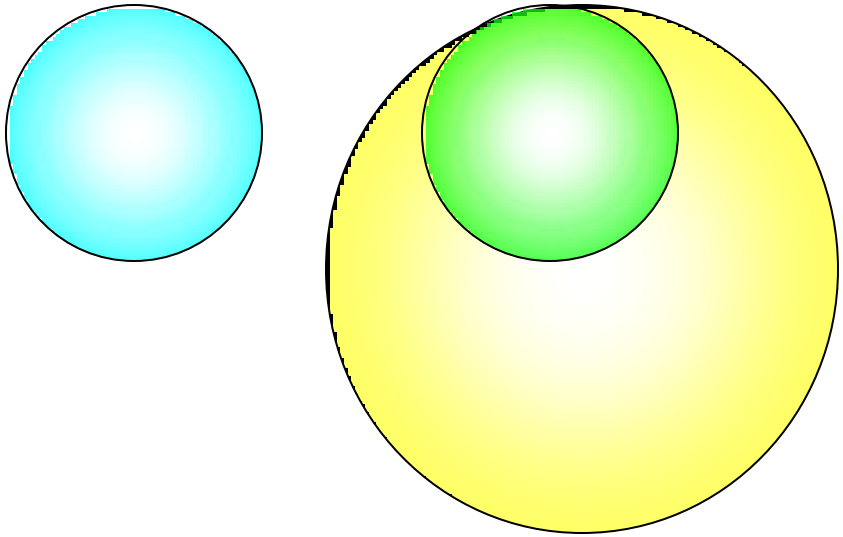

Zero Range Knockout

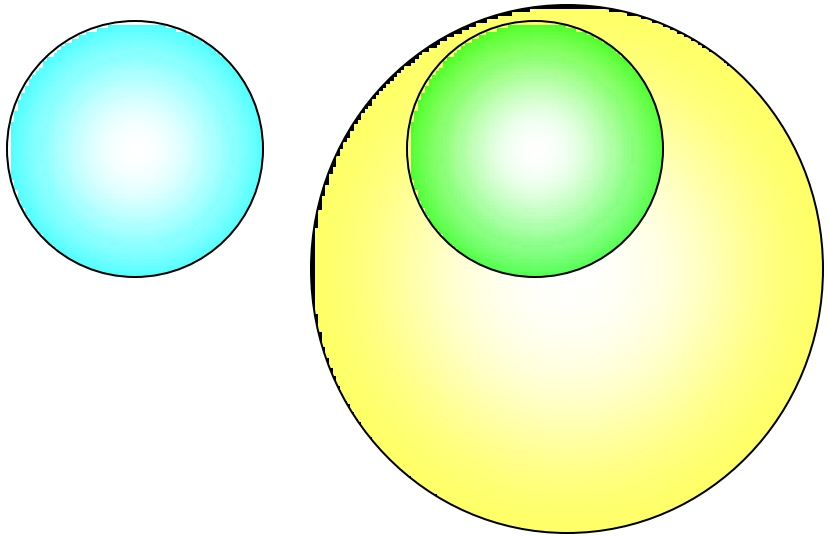

Zero Range Knockout

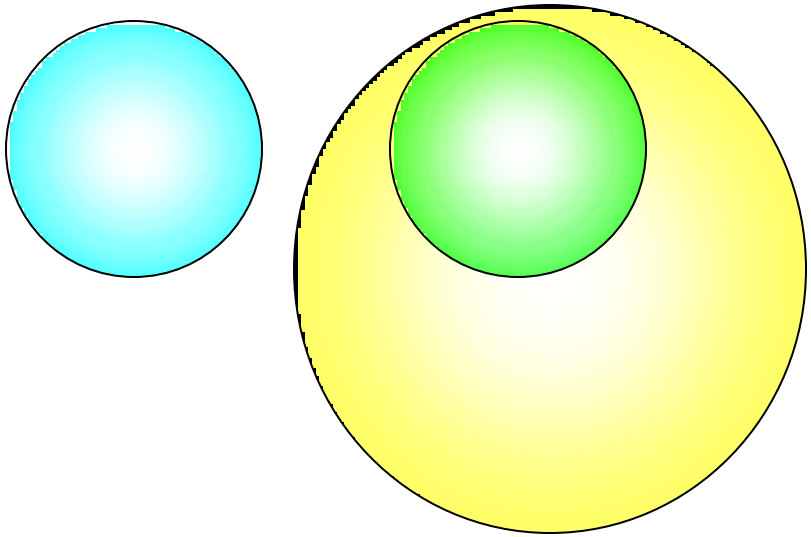

Zero Range Knockout

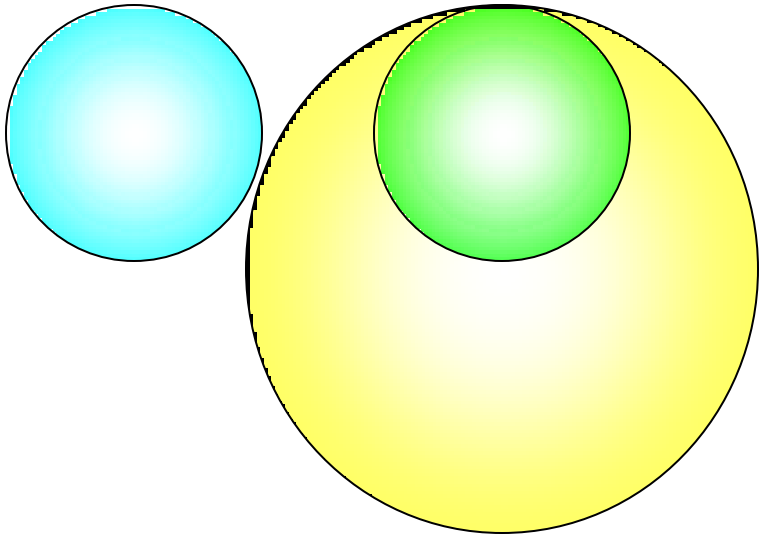

Zero Range Knockout

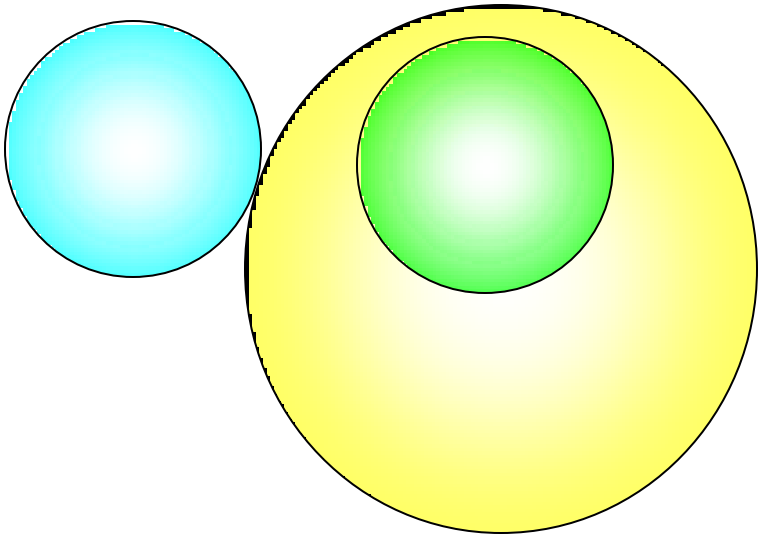

Zero Range Knockout

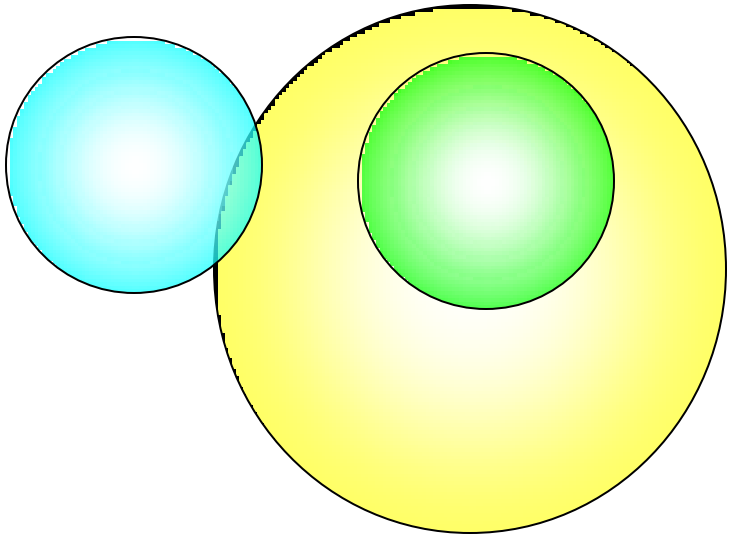

Zero Range Knockout

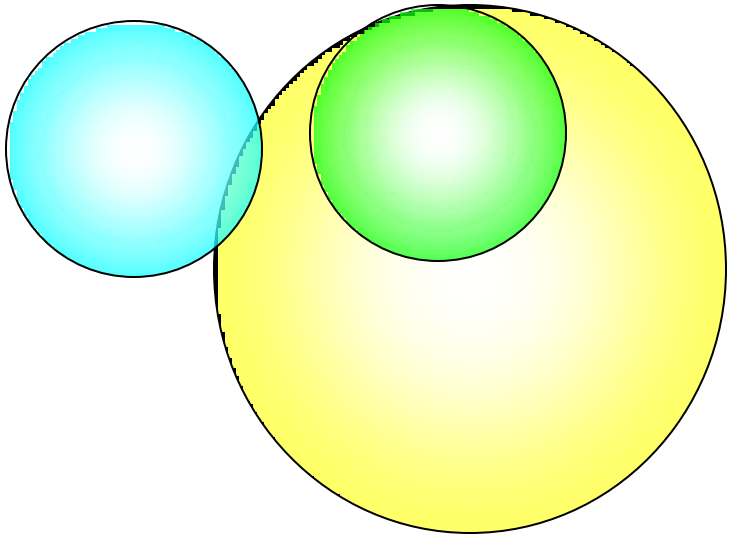

Zero Range Knockout

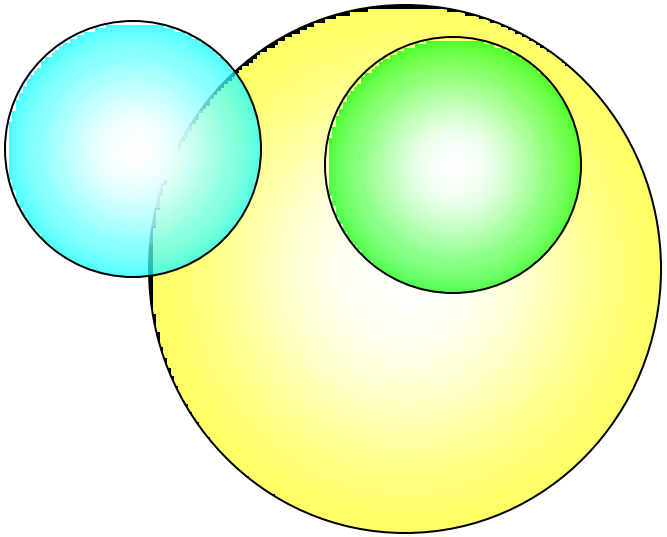

Zero Range Knockout

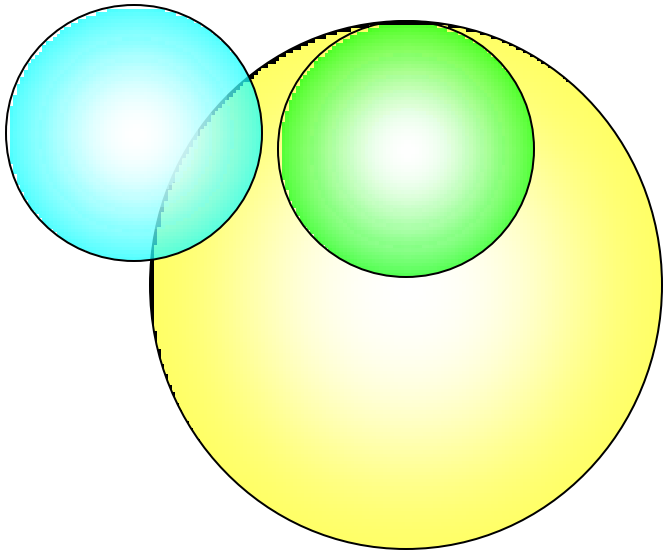

Zero Range Knockout

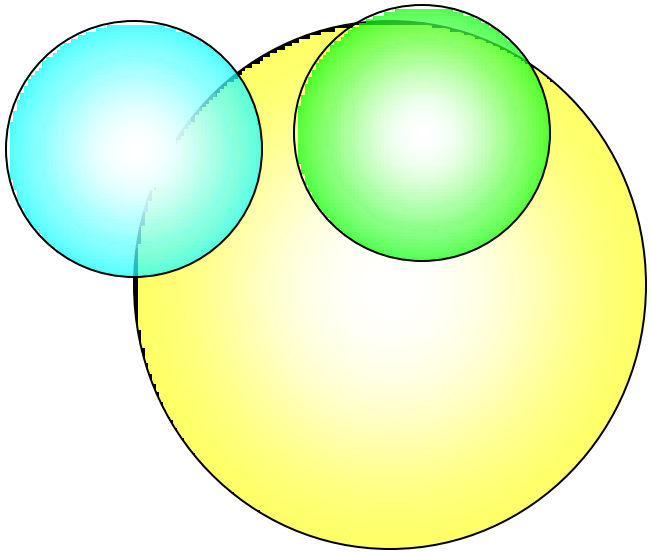

Zero Range Knockout

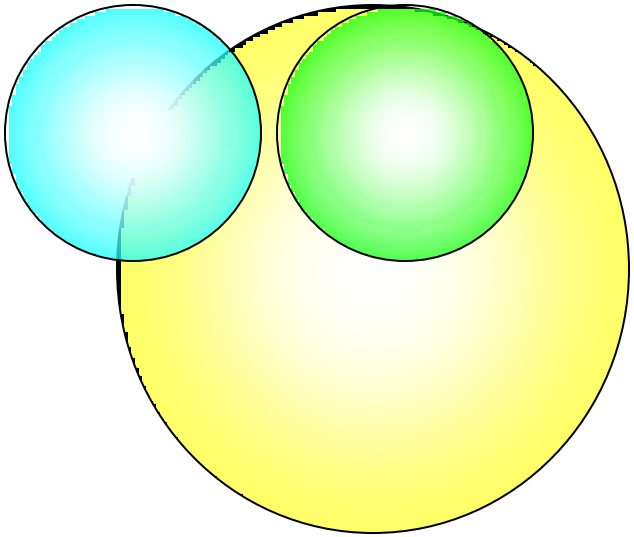

Zero Range Knockout

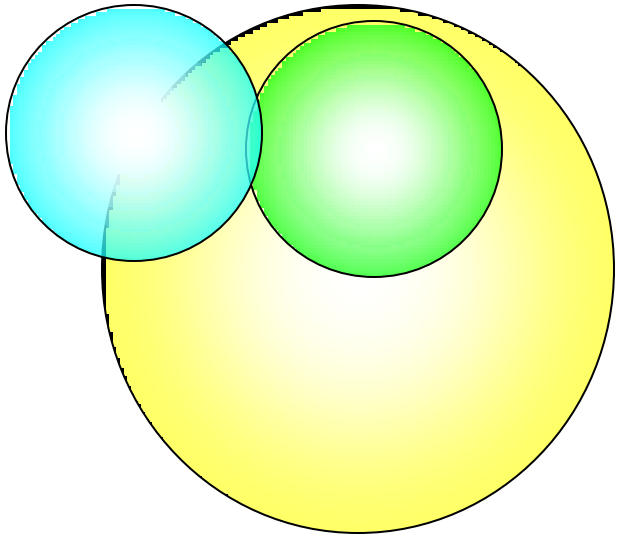

Zero Range Knockout

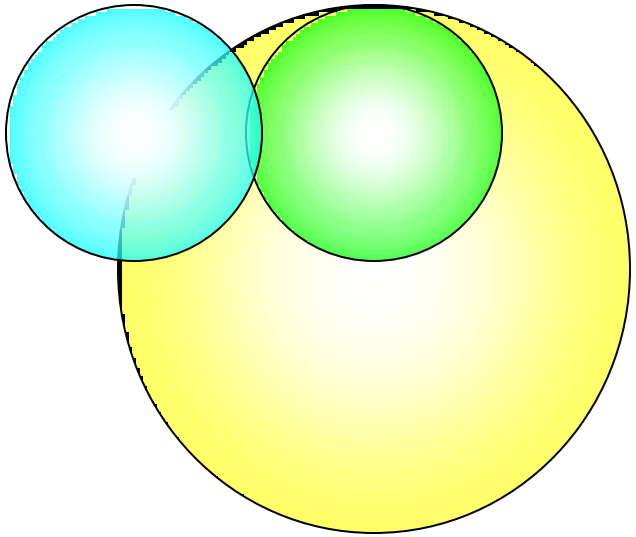

Zero Range Knockout

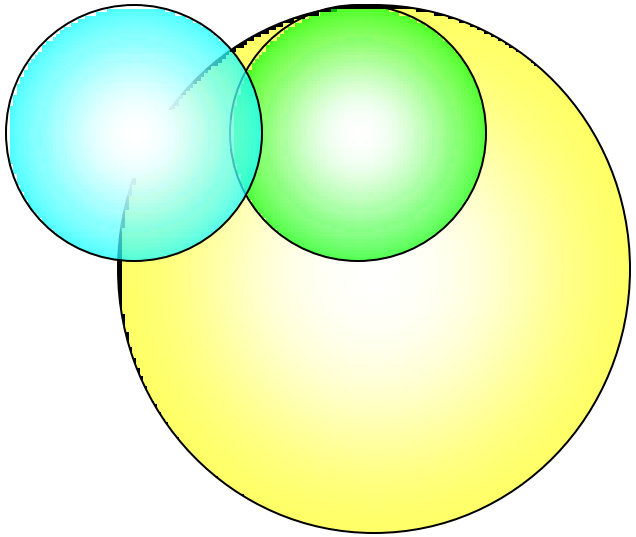

Zero Range Knockout

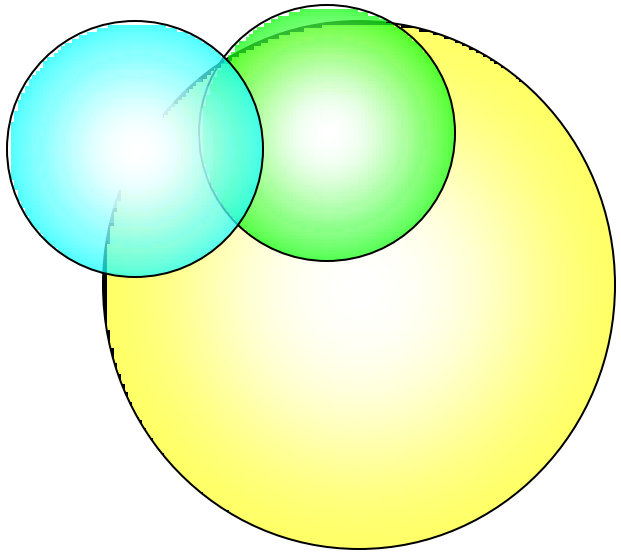

Zero Range Knockout

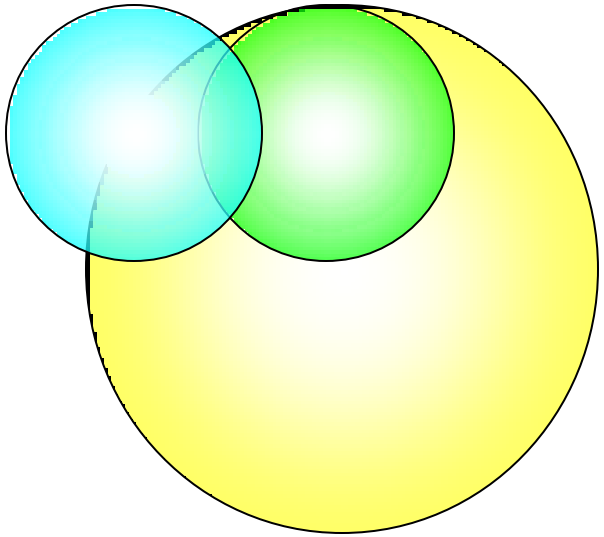

Zero Range Knockout

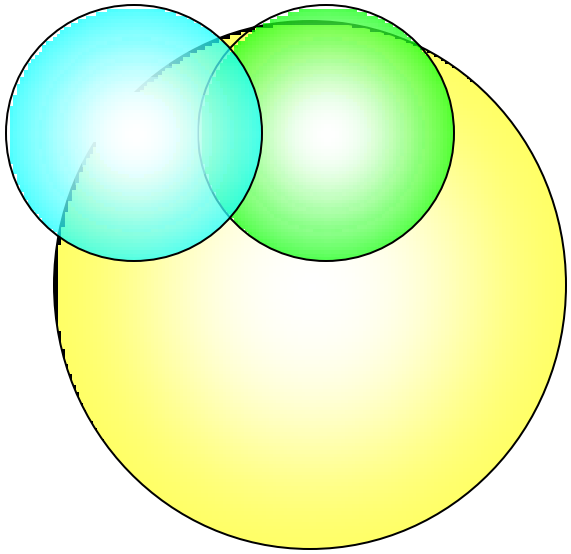

Zero Range Knockout

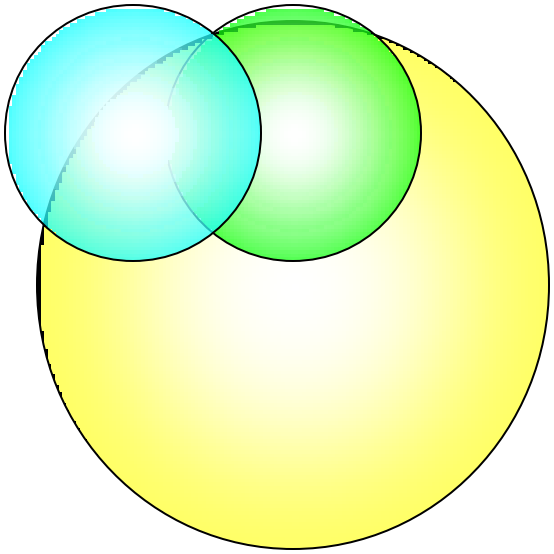

Zero Range Knockout

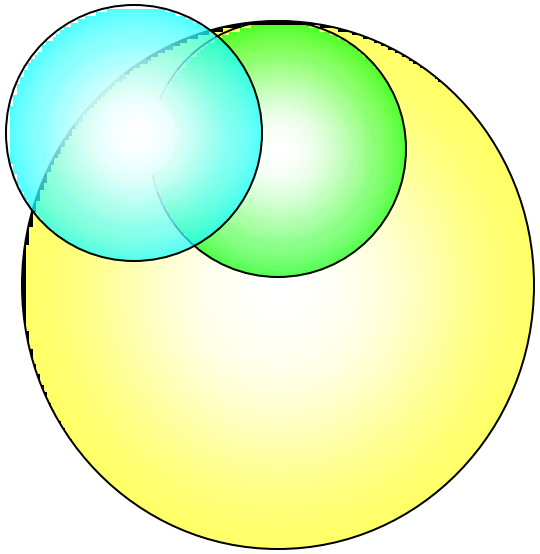

Zero Range Knockout

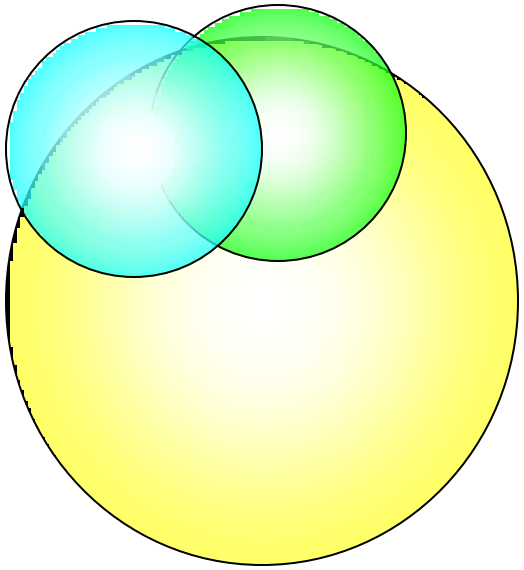

Zero Range Knockout

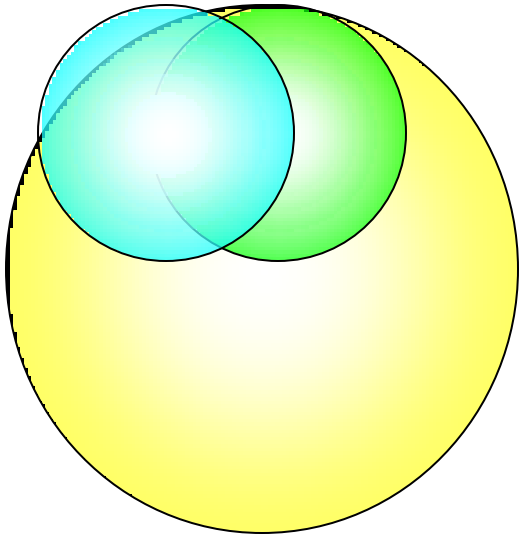

Zero Range Knockout

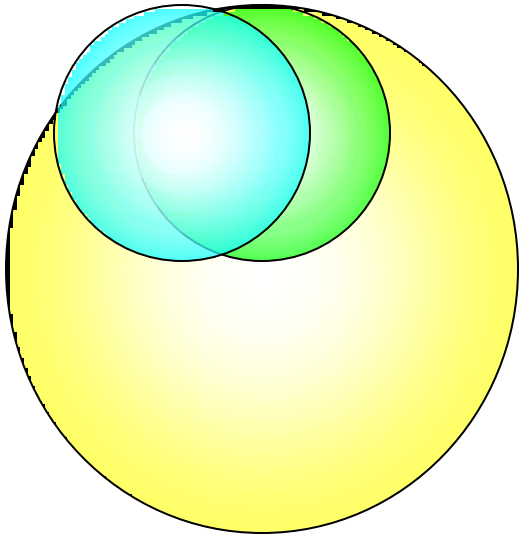

Zero Range Knockout

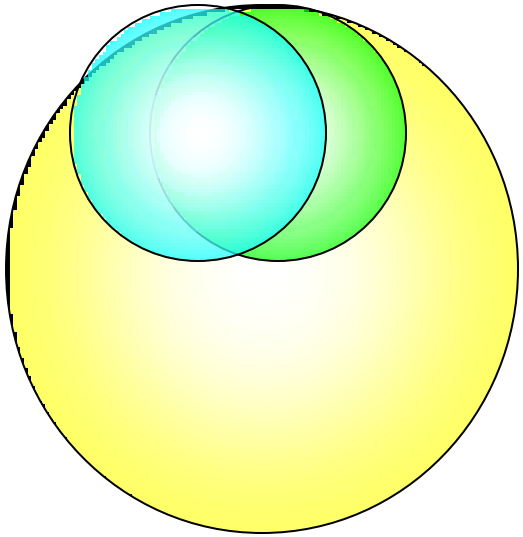

Zero Range Knockout

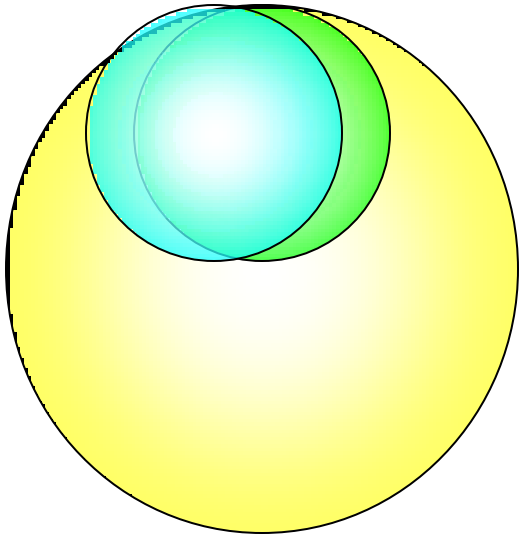

Zero Range Knockout

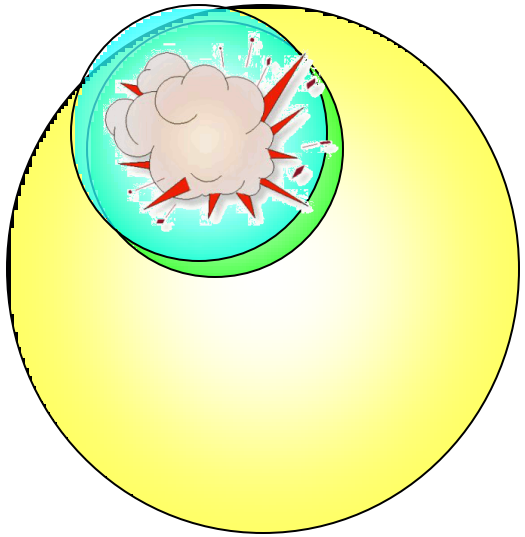

Zero Range Knockout

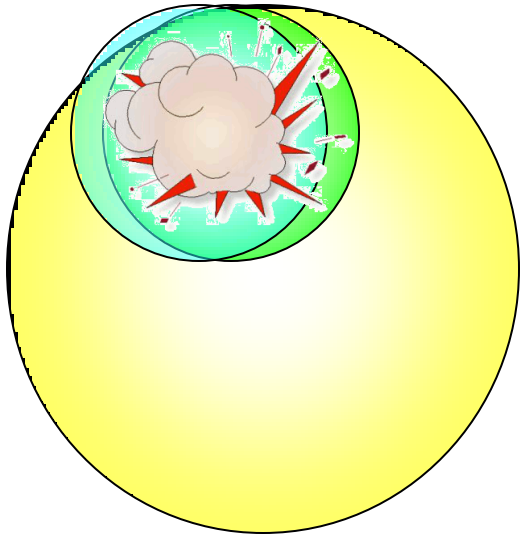

Zero Range Knockout

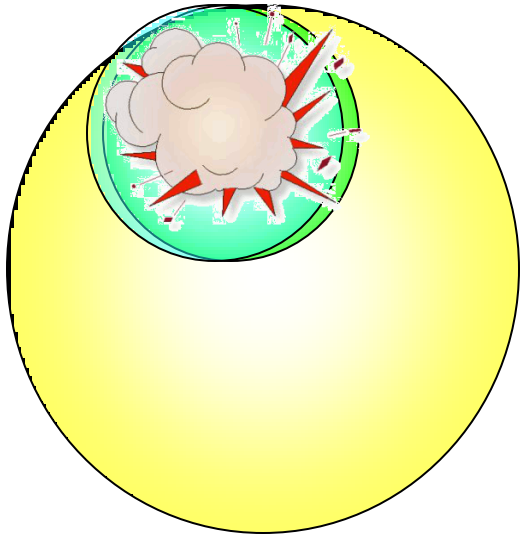

Zero Range Knockout

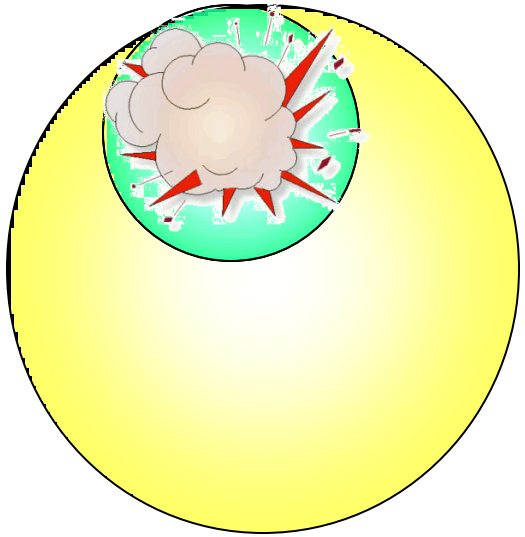

Zero Range Knockout

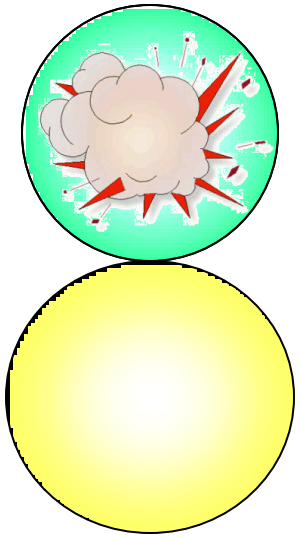

Zero Range Knockout

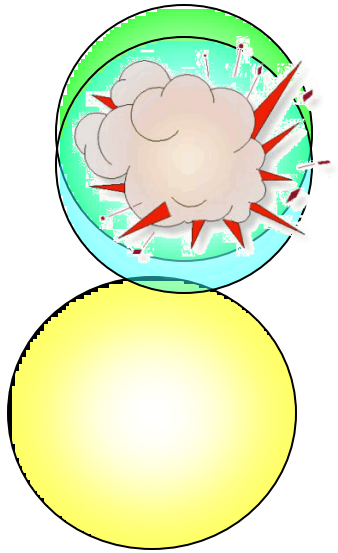

Zero Range Knockout

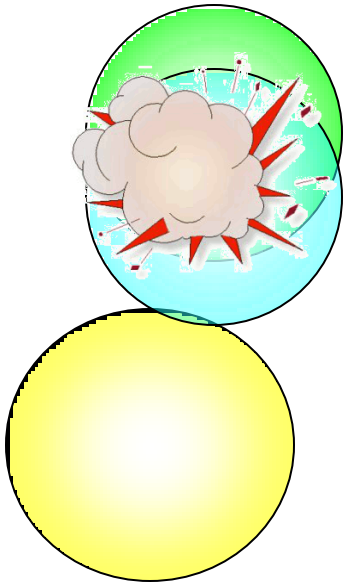

Zero Range Knockout

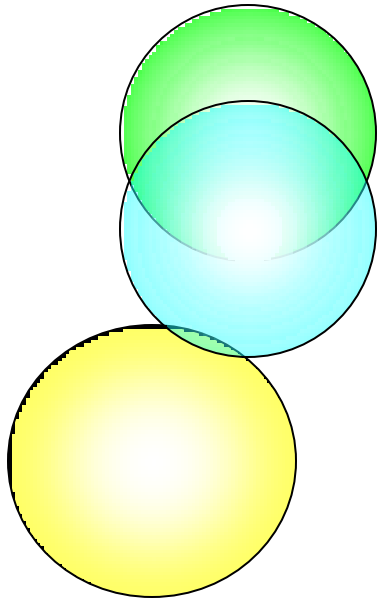

Zero Range Knockout

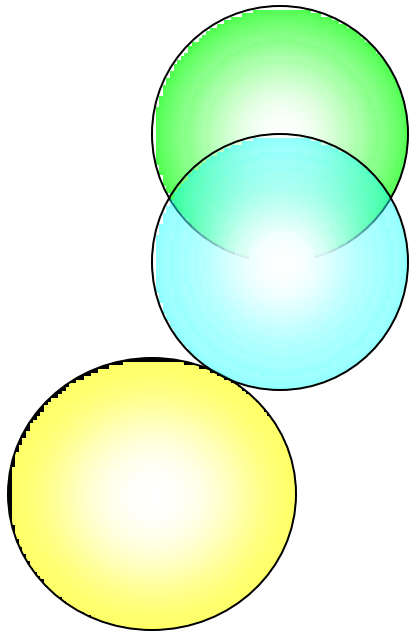

Zero Range Knockout

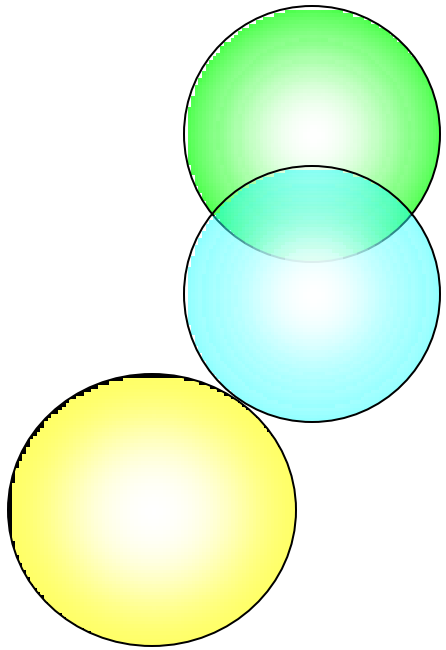

Zero Range Knockout

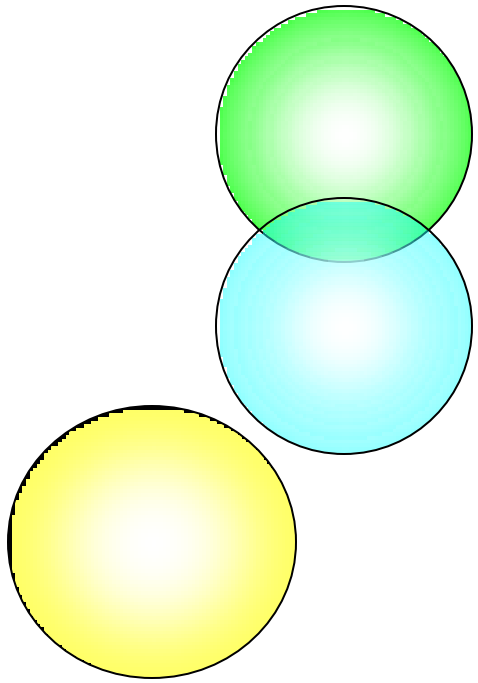

Zero Range Knockout

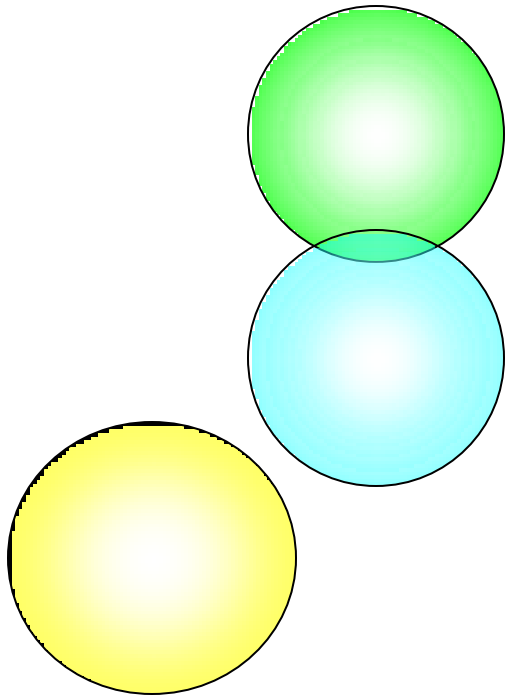

Zero Range Knockout

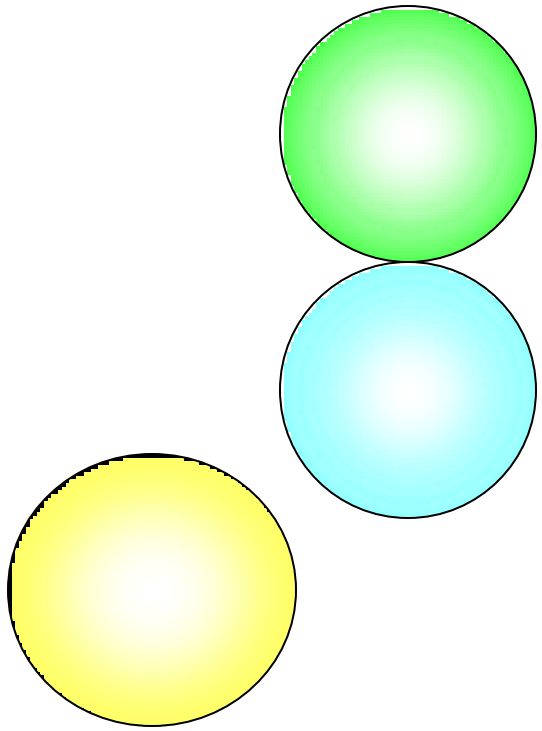

Zero Range Knockout

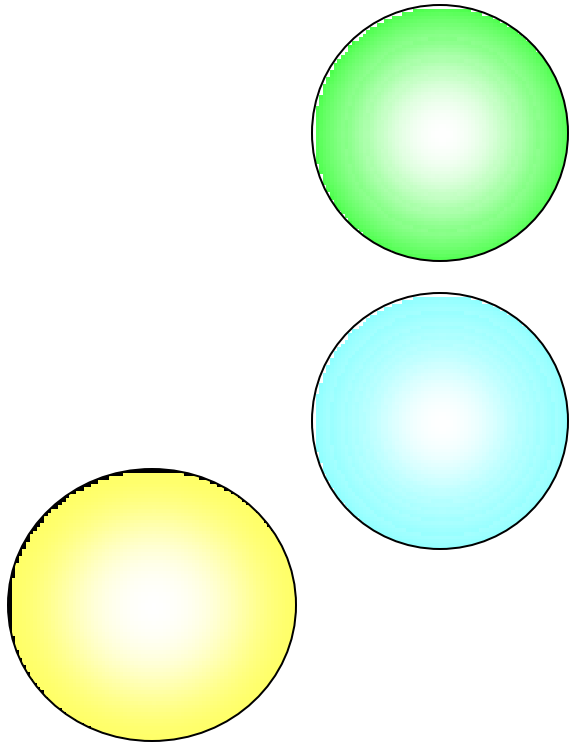

Zero Range Knockout

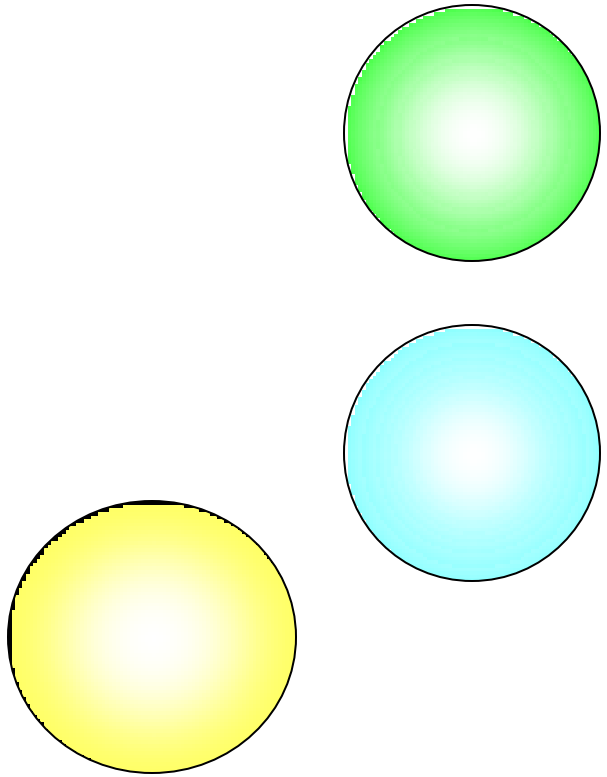

Zero Range Knockout

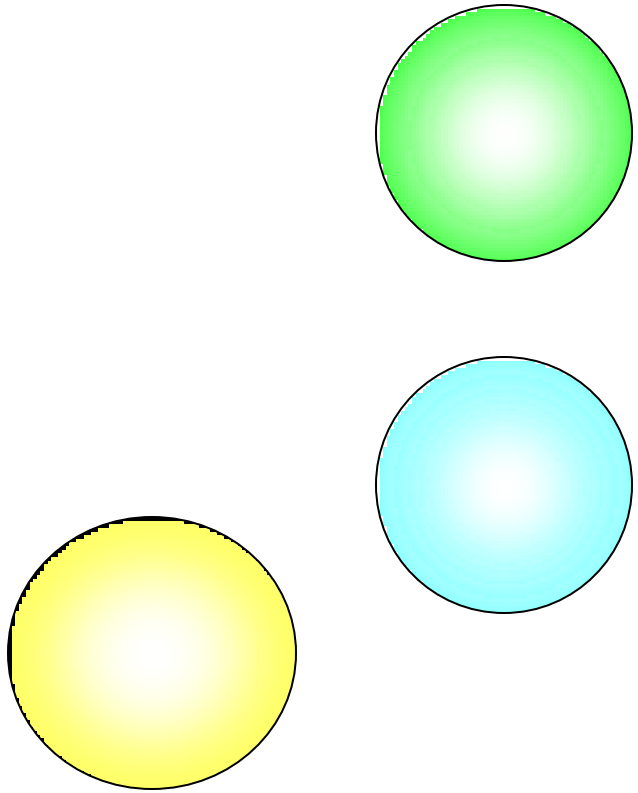

Zero Range Knockout

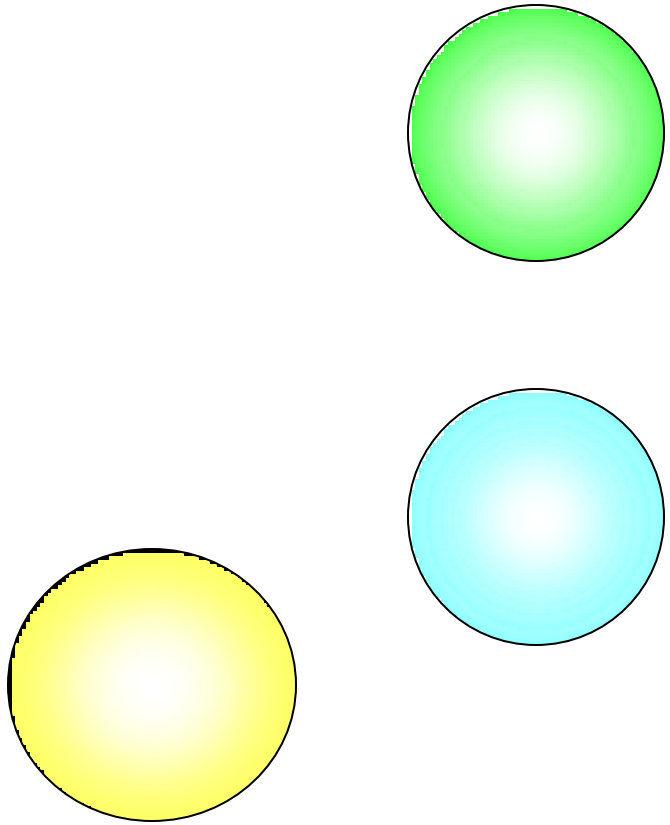

Zero Range Knockout

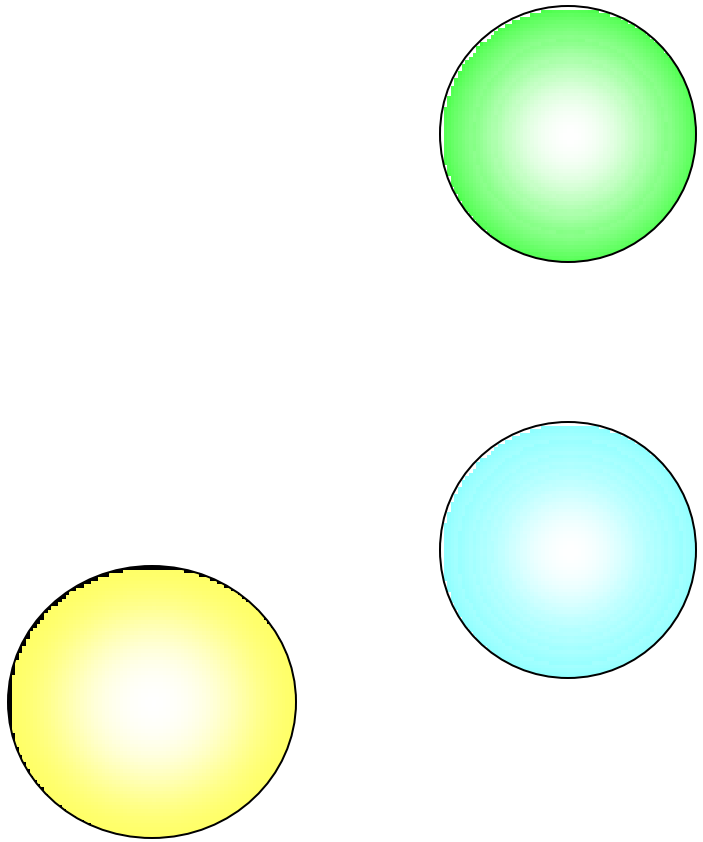

Zero Range Knockout

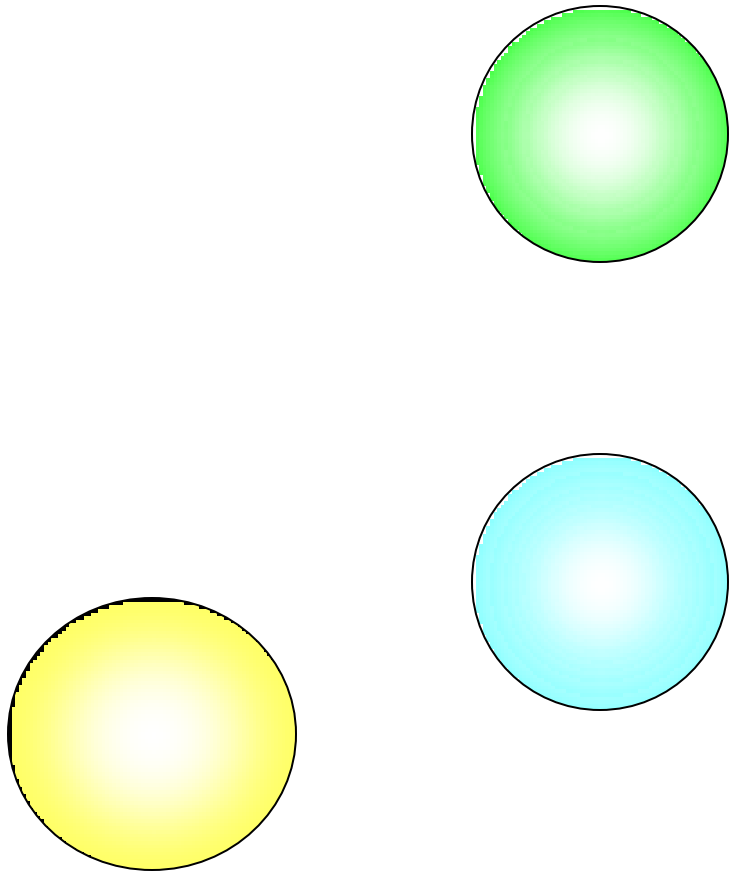

Zero Range Knockout

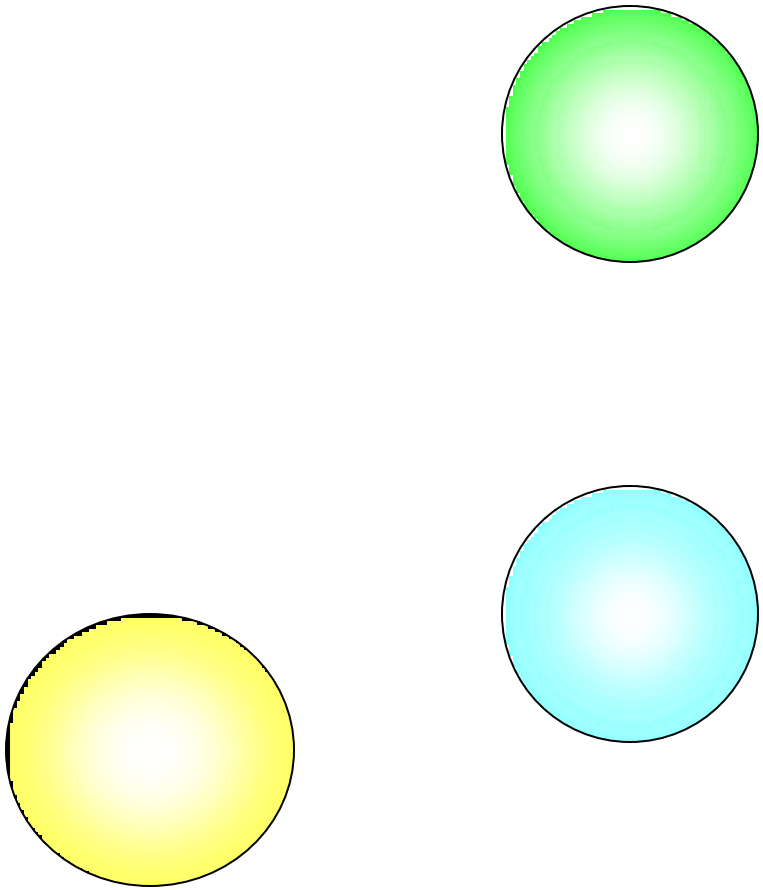

Zero Range Knockout

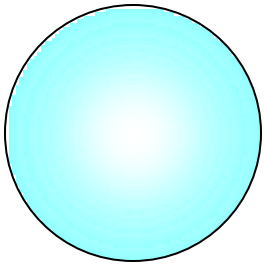

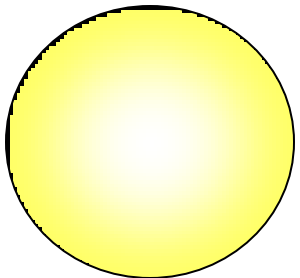

Zero Range Knockout

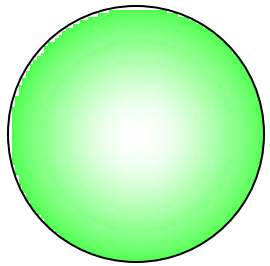

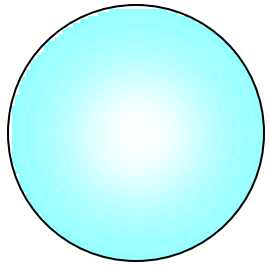

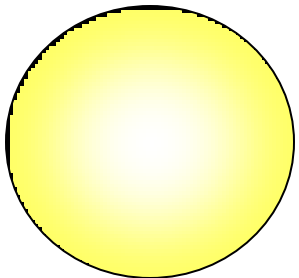

Zero Range Knockout

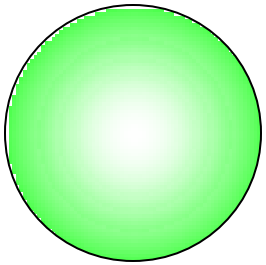

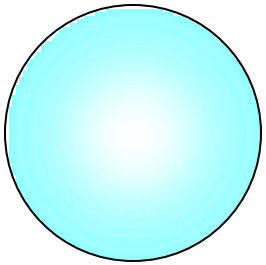

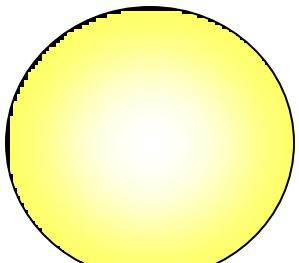

Zero Range Knockout

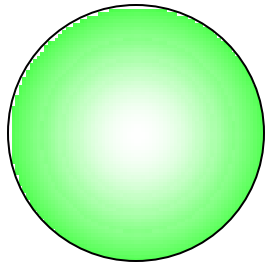

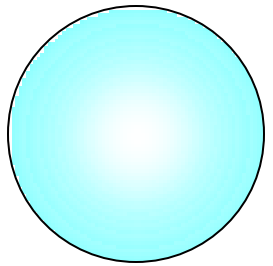

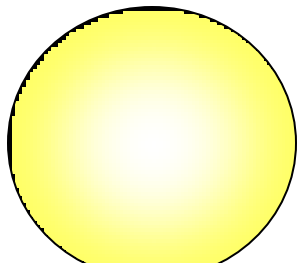

Zero Range Knockout

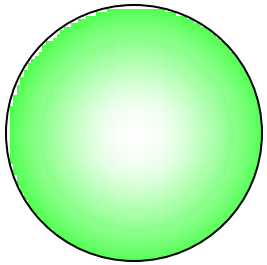

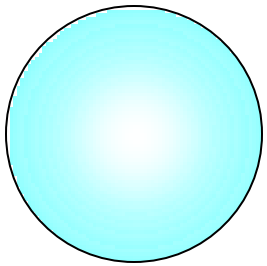

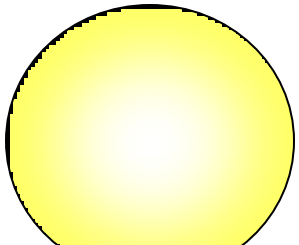

Zero Range Knockout

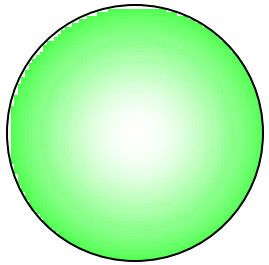

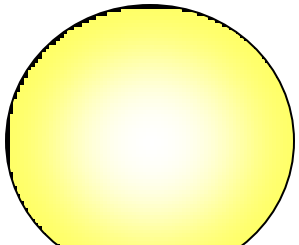

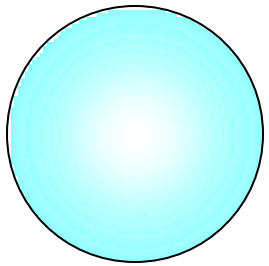

Zero Range Knockout

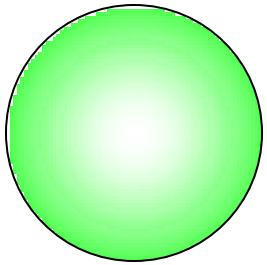

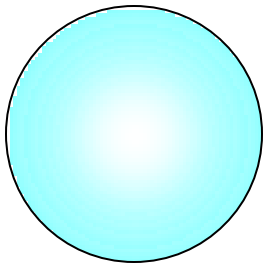

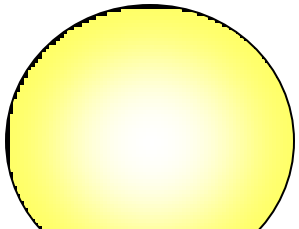

Zero Range Knockout

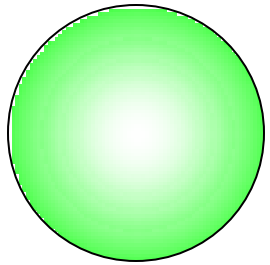

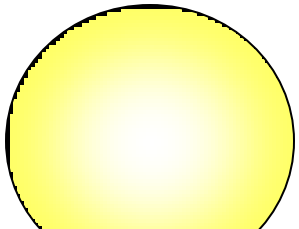

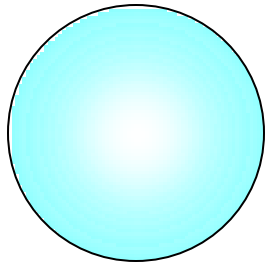

Zero Range Knockout

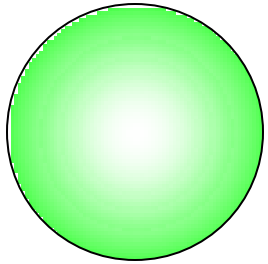

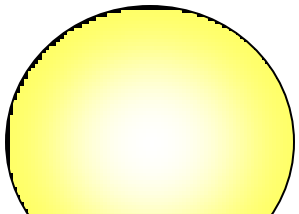

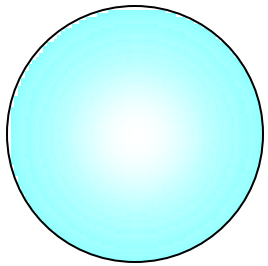

Zero Range Knockout

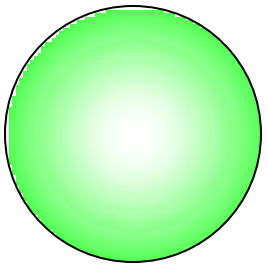

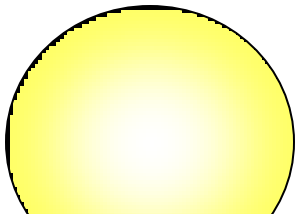

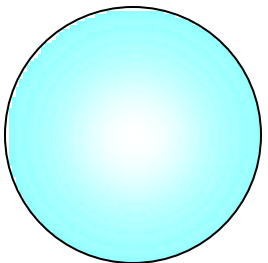

Zero Range Knockout

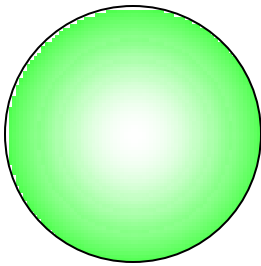

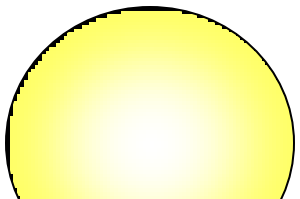

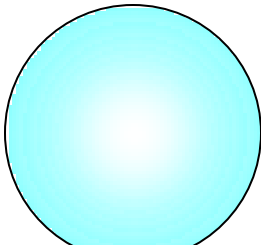

Zero Range Knockout

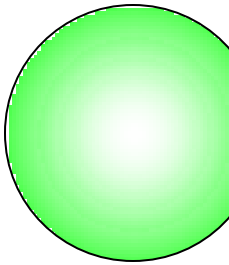

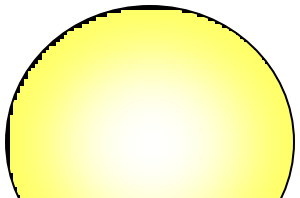

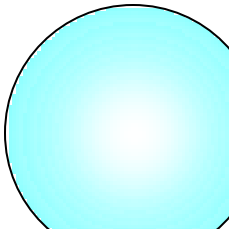

Zero Range Knockout

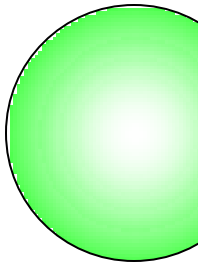

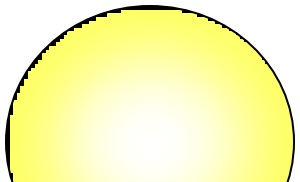

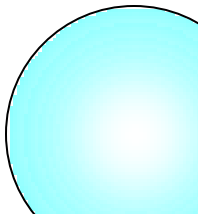

Zero Range Knockout

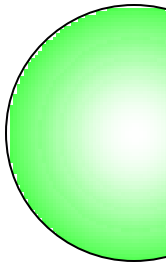

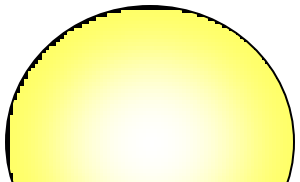

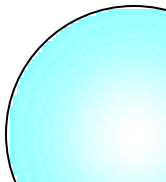

Zero Range Knockout

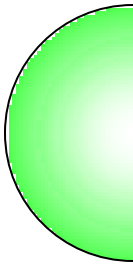

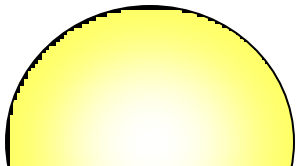

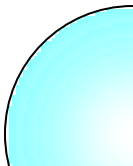

Zero Range Knockout

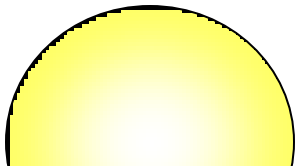

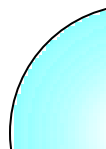

Zero Range Knockout

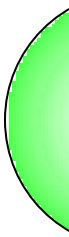

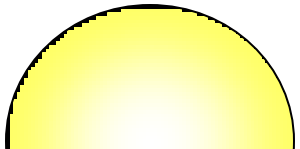

From Transfer Reactions one obtains reasonable relative spectroscopic factors.

For Knockout Reactions one uses quasi free scattering approx. or Distorted Wave Impulse Approximation (DWIA).

(α,2α) , knockout reaction cross section

= product of kinematic factor,

α-α Cross section and

Distorted wave form factor,

(~Fourier transform of Wfn).

$$\frac{d^3\sigma}{d\Omega_1 d\Omega_2 dE_1} = KF \cdot S_{LJ} \cdot \left(\frac{d\sigma}{d\Omega}\right)_{ab} \sum_{\Lambda} \left| T_{BA}^{LJ}(Q) \right|^2 \cdot$$

S_{LJ} is the cluster spectroscopic factor for specific L and J.

The transition amplitude may be written as :

$$T_{BA}^{LJ}(Q) = (2L+1)^{-1/2} \int \chi_{aB}^{(-)^*}(\vec{k}_{aB}, \vec{R}) \cdot \chi_{bB}^{(-)^*}(\vec{k}_{bB}, \vec{R}) \cdot \chi_{aA}^{(+)}(\vec{k}_{aA}, \varepsilon\vec{R}) \cdot \phi_{LJ}(\vec{R}) d\vec{R}.$$

Here ε = B/A.

Ground State spectroscopic factors S_a for $^{16}O(\alpha, 2\alpha)^{12}C$

Eα	S_{o+}	$\sigma_{PW} / \sigma_{DW}$
Theory	**0.23**	-
850 *MeV*	**< 1.8**	5.4
90 *MeV*	**15**	~1500
52.5 *MeV*	**150**	~3200

Ground State spectroscopic factors S_a for $^{12}C(\alpha, 2\alpha)^{8}Be$ at **139 MeV** and **200 MeV**

	139 *MeV*	**200 *MeV***	**Ratio**
	17	**0.48**	35
Theory	**0.55**	**0.55**	

Discrepancy between Proton and Alpha inducted Cluster Knockout Reactions

Here Spectroscopic Factor *Sα* is seen to be almost ~2-orders of magnitude too large

Reaction	θ_1-θ_2	P3 (MeV/c)	Spectroscopic factor (Sα)
$^{16}O(p,pd)^{14}N$	40.1^0-40.0^0	~41	0.43
$^{16}O(p,pt)^{13}N$	40.1^0-40.0^0	~51	3.4
$^{16}O(\alpha,\alpha d)^{14}N$	9.0^0-43.99^0	~4	55
$^{16}O(\alpha,\alpha t)^{13}N$	25.81^0-43.99^0	~13	53
$^{16}O(\alpha,\alpha t)^{13}C$	25.81^0-43.99^0	~2	55

Finite Range Knockout

Knockout using Short Finite Range Repulsion

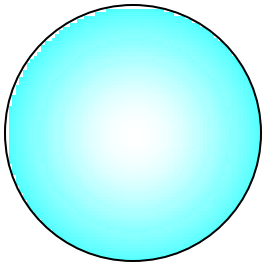

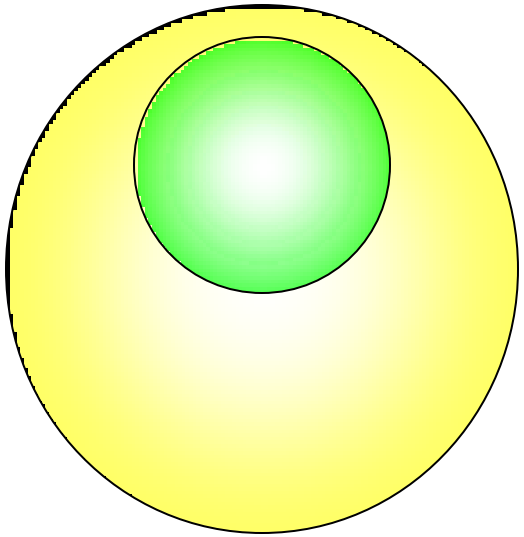

Knockout using Short Finite Range Repulsion

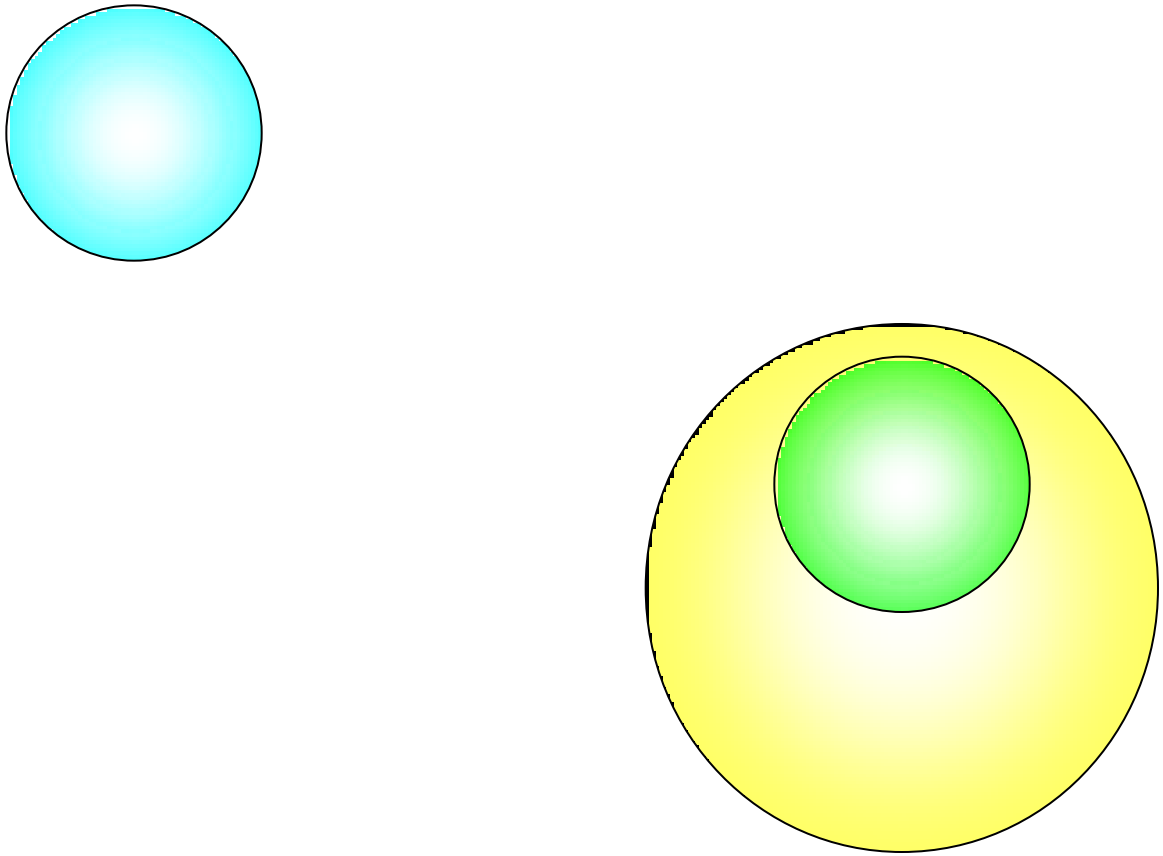

Knockout using Short Finite Range Repulsion

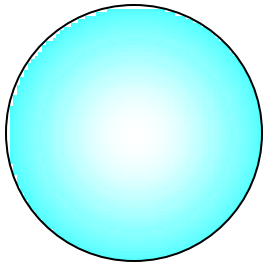

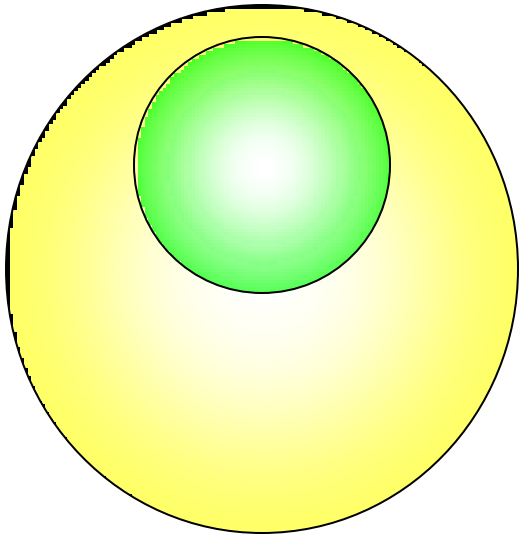

Knockout using Short Finite Range Repulsion

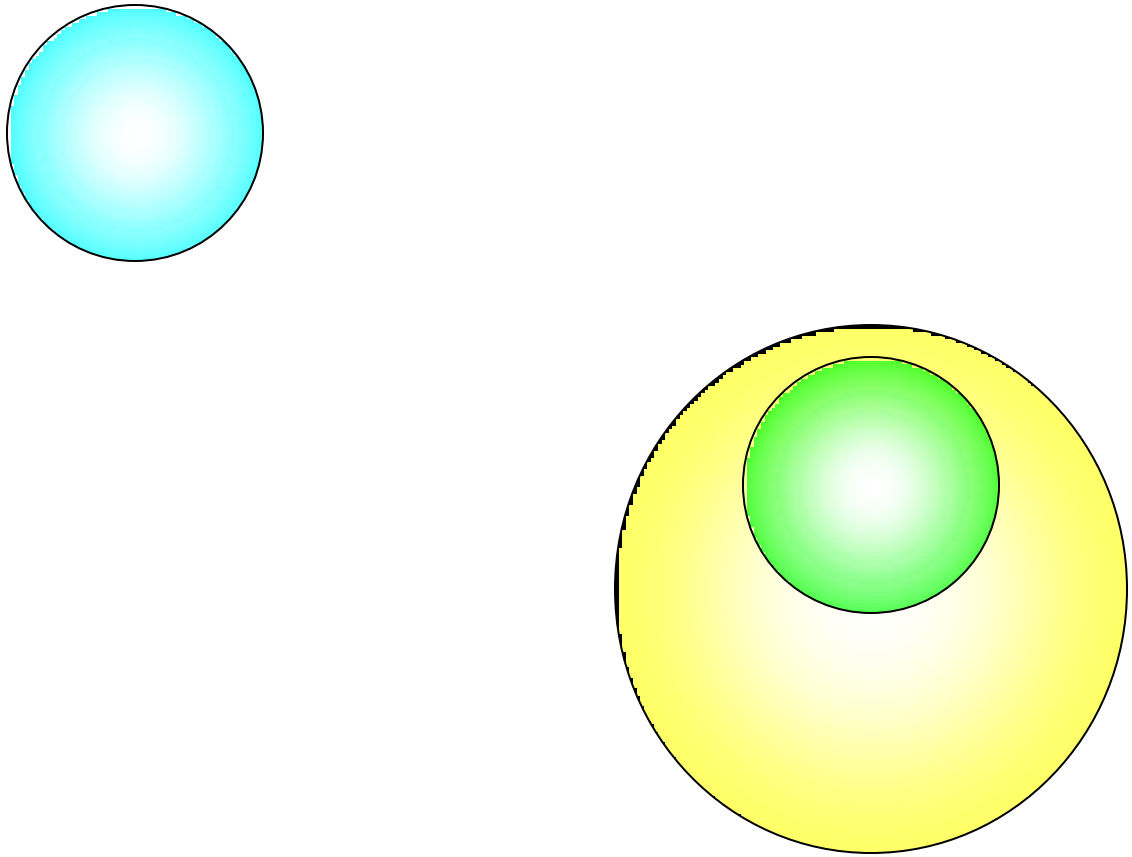

Knockout using Short Finite Range Repulsion

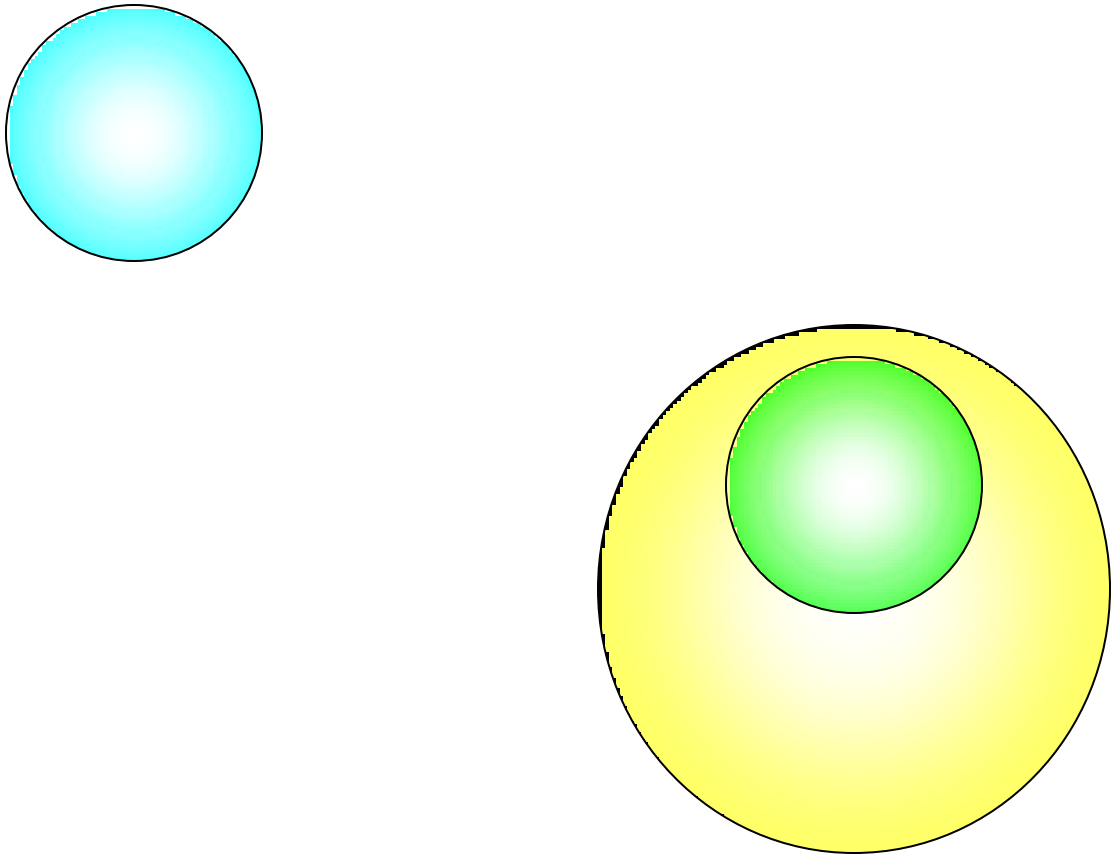

Knockout using Short Finite Range Repulsion

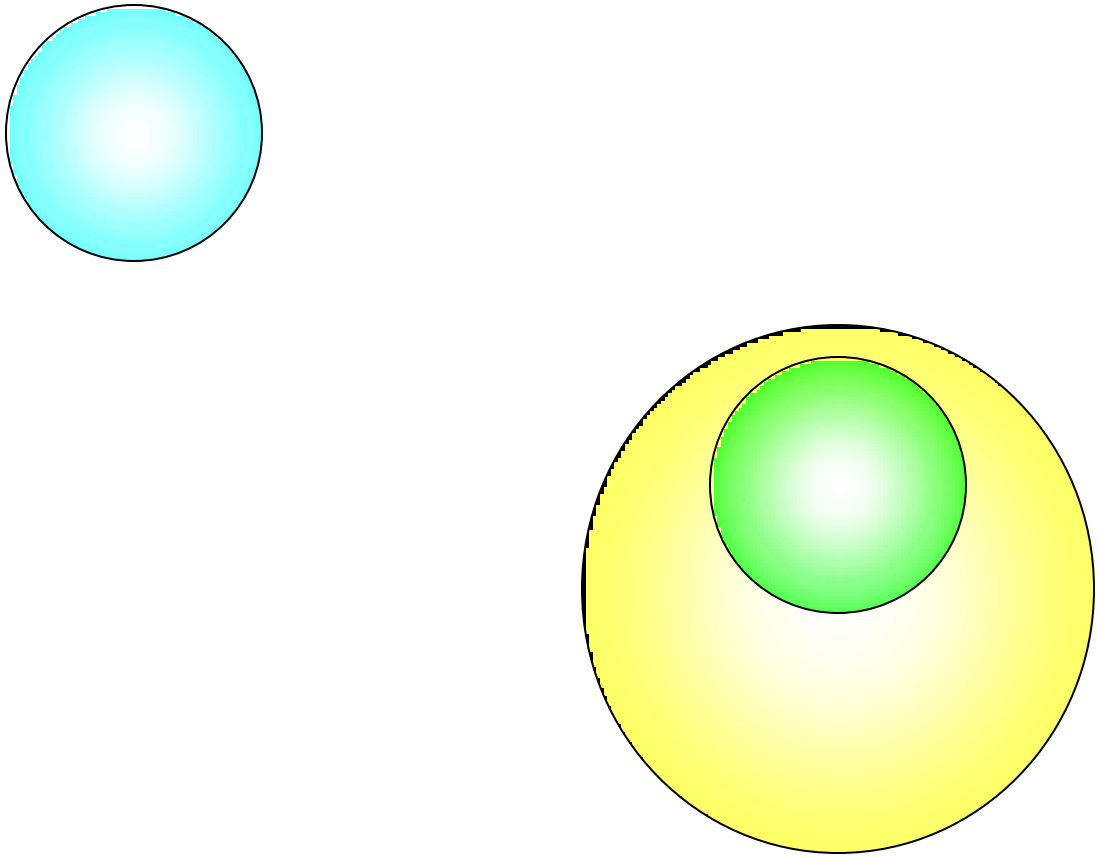

Knockout using Short Finite Range Repulsion

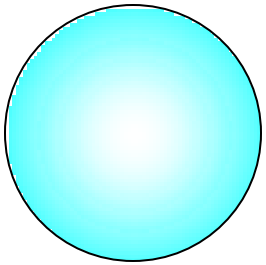

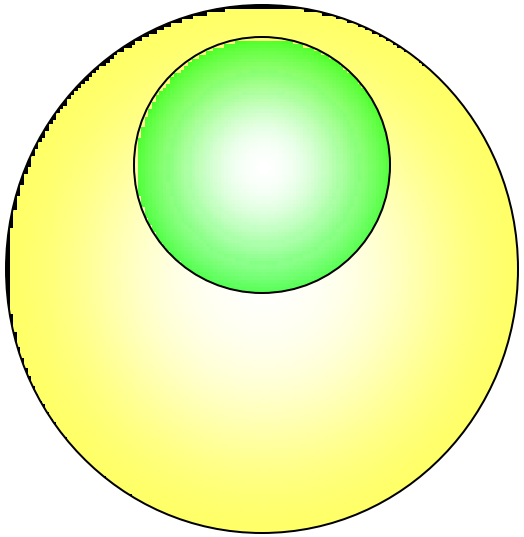

Knockout using Short Finite Range Repulsion

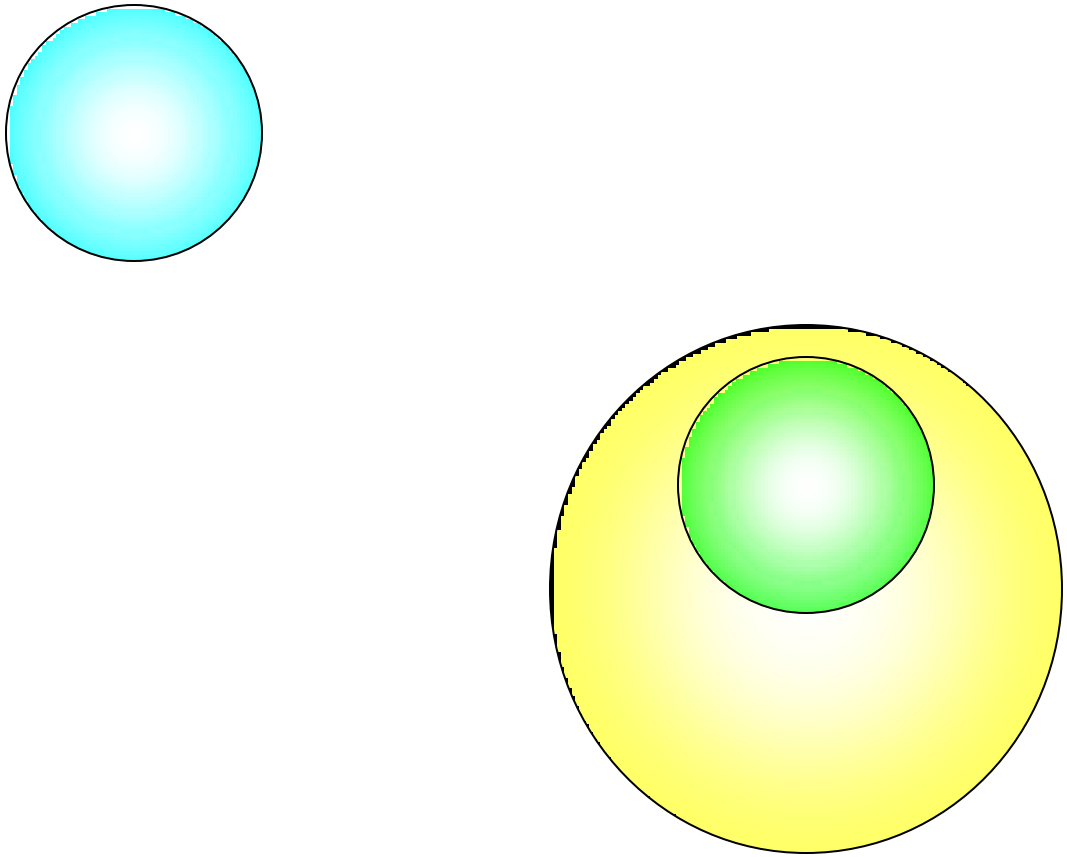

Knockout using Short Finite Range Repulsion

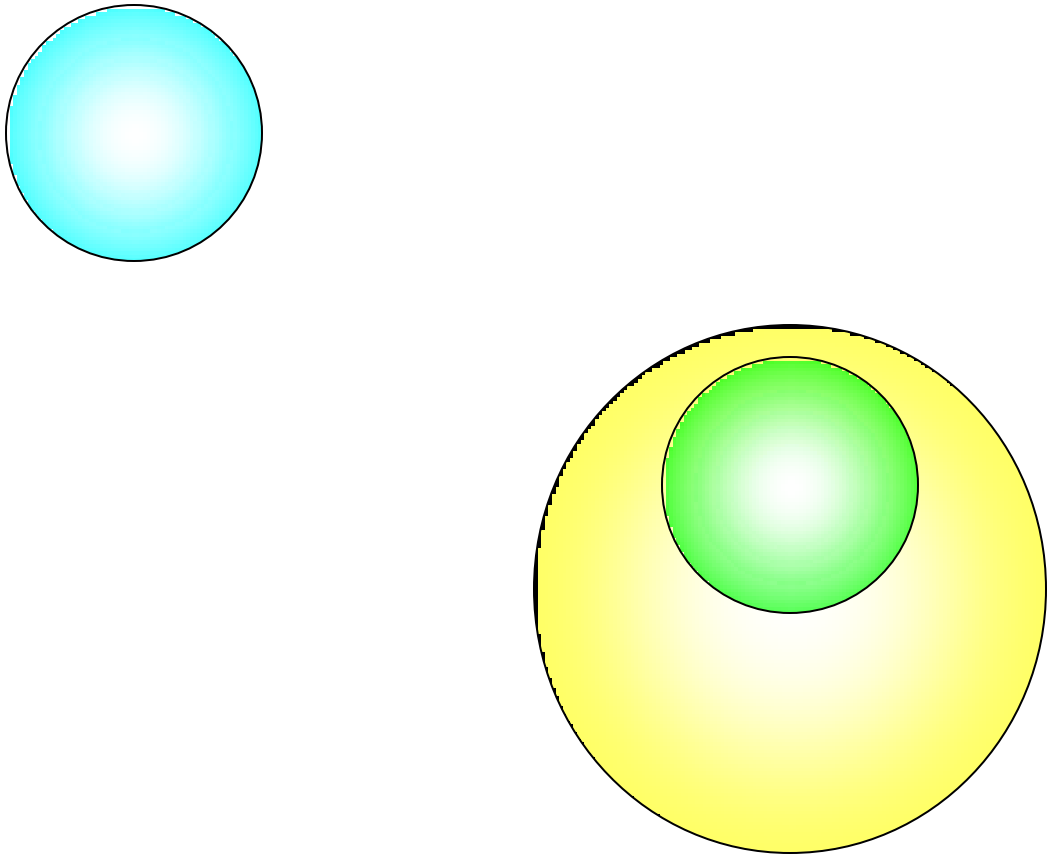

Knockout using Short Finite Range Repulsion

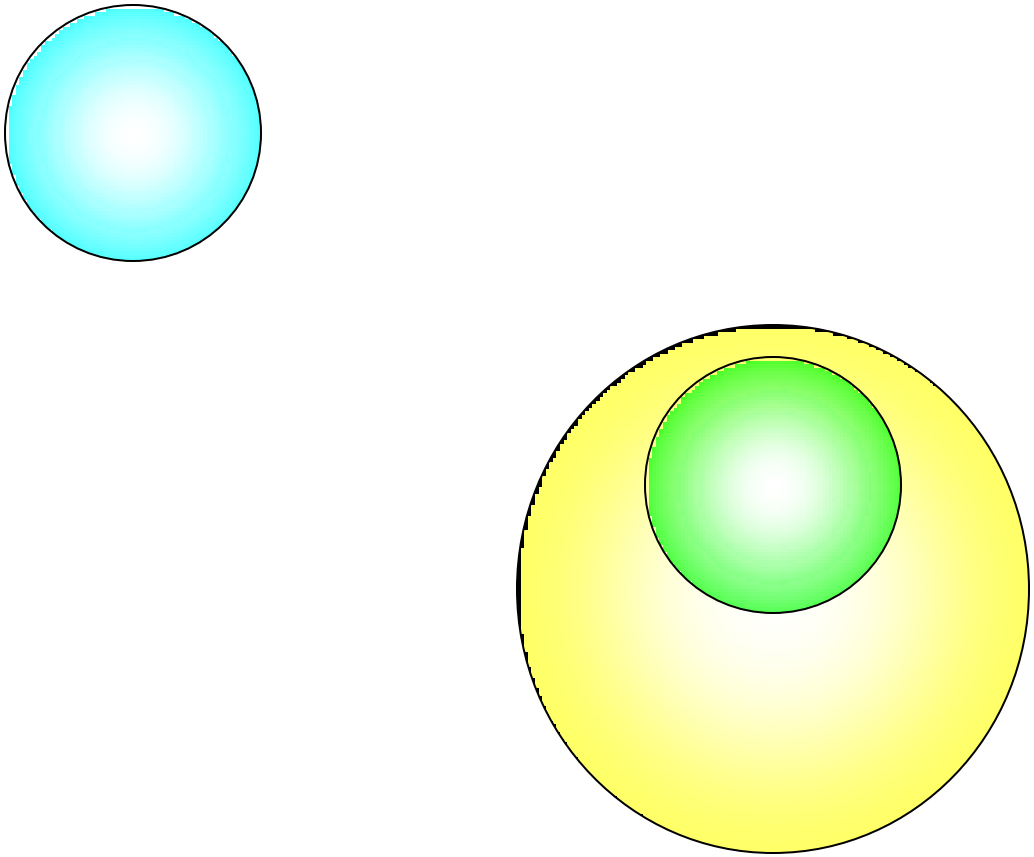

Knockout using Short Finite Range Repulsion

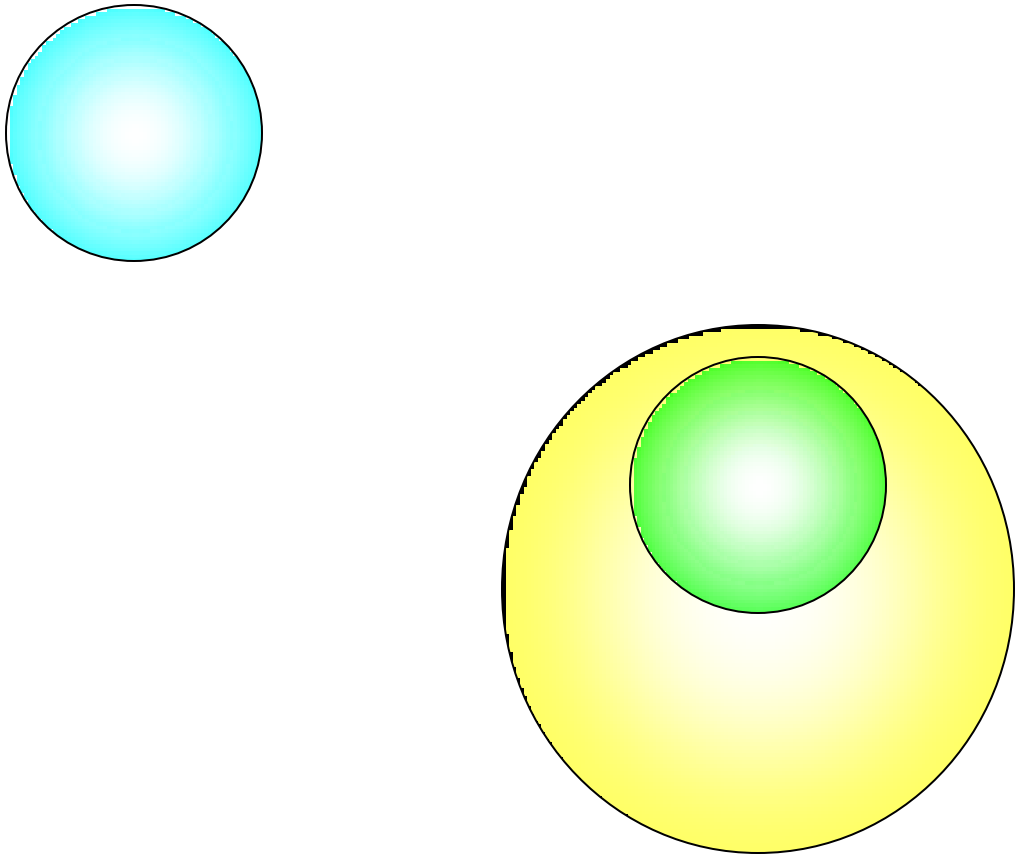

Knockout using Short Finite Range Repulsion

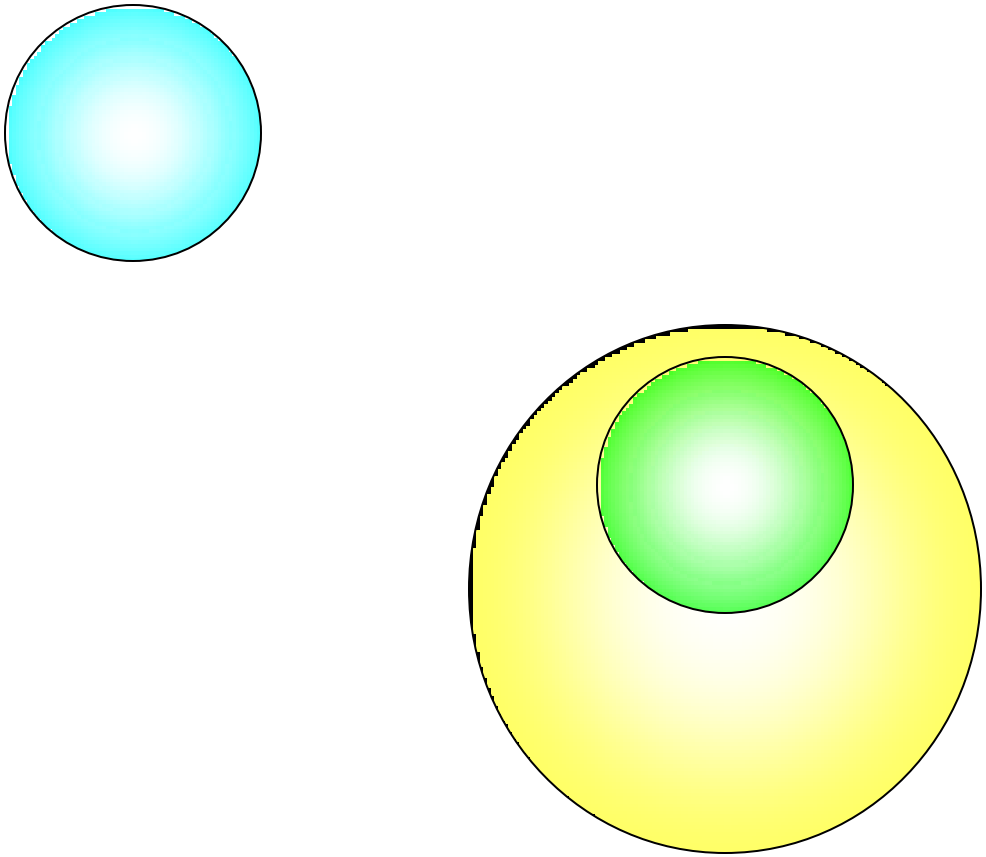

Knockout using Short Finite Range Repulsion

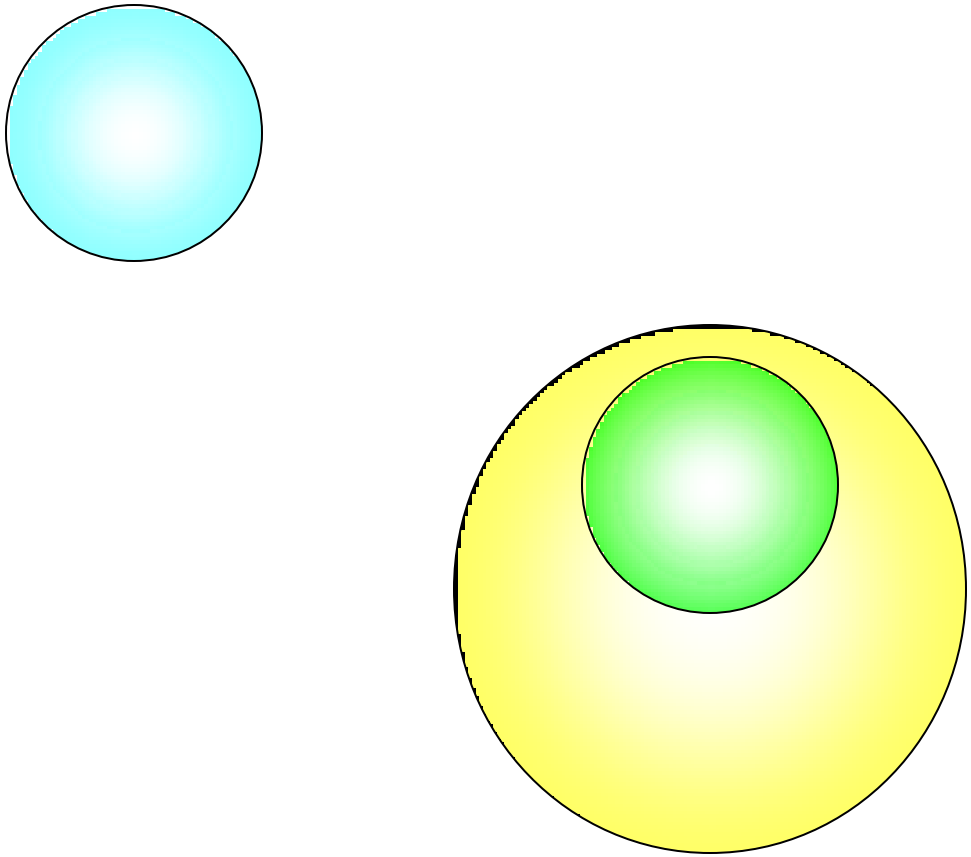

Knockout using Short Finite Range Repulsion

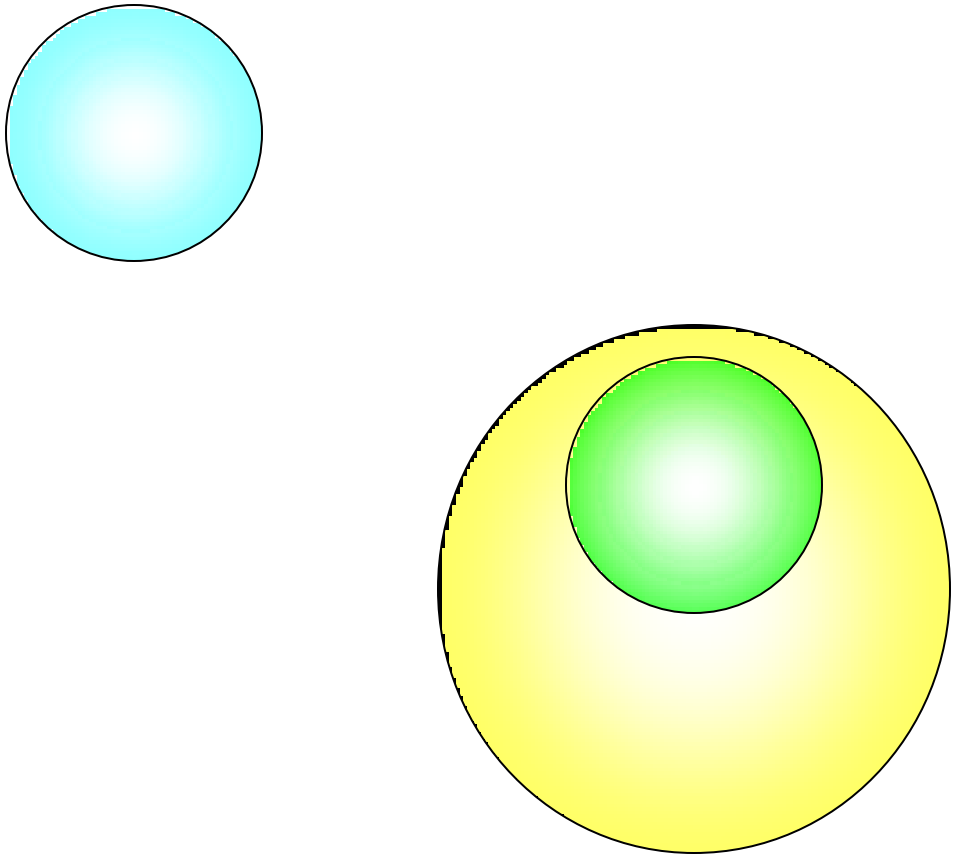

Knockout using Short Finite Range Repulsion

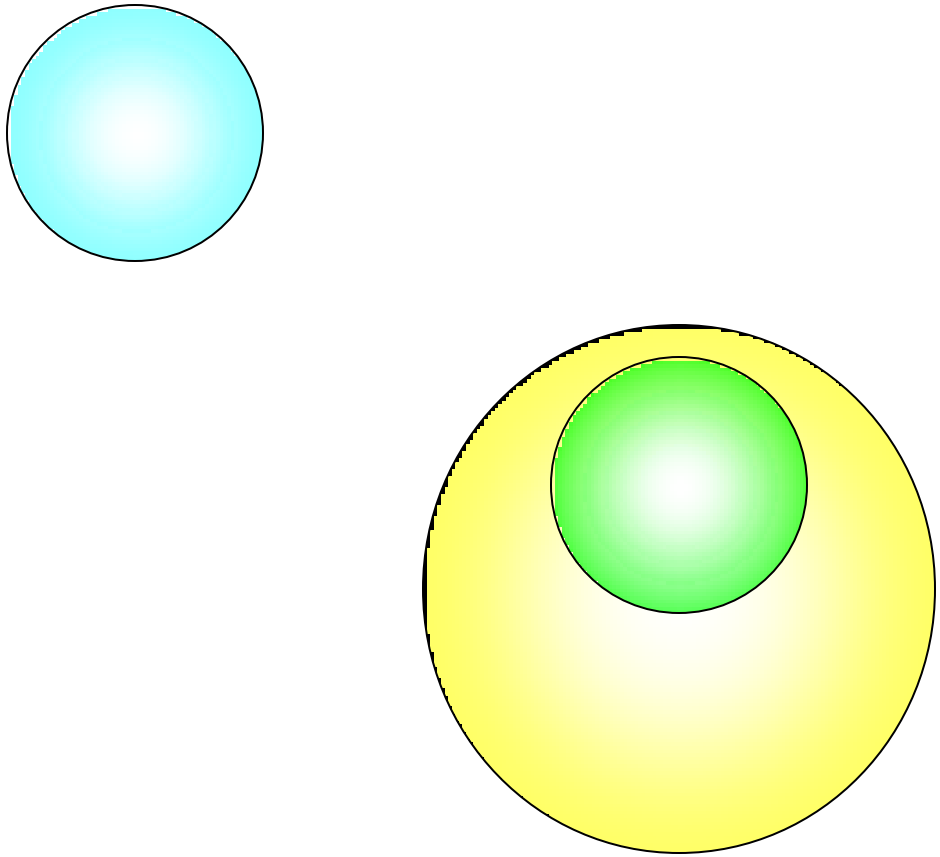

Knockout using Short Finite Range Repulsion

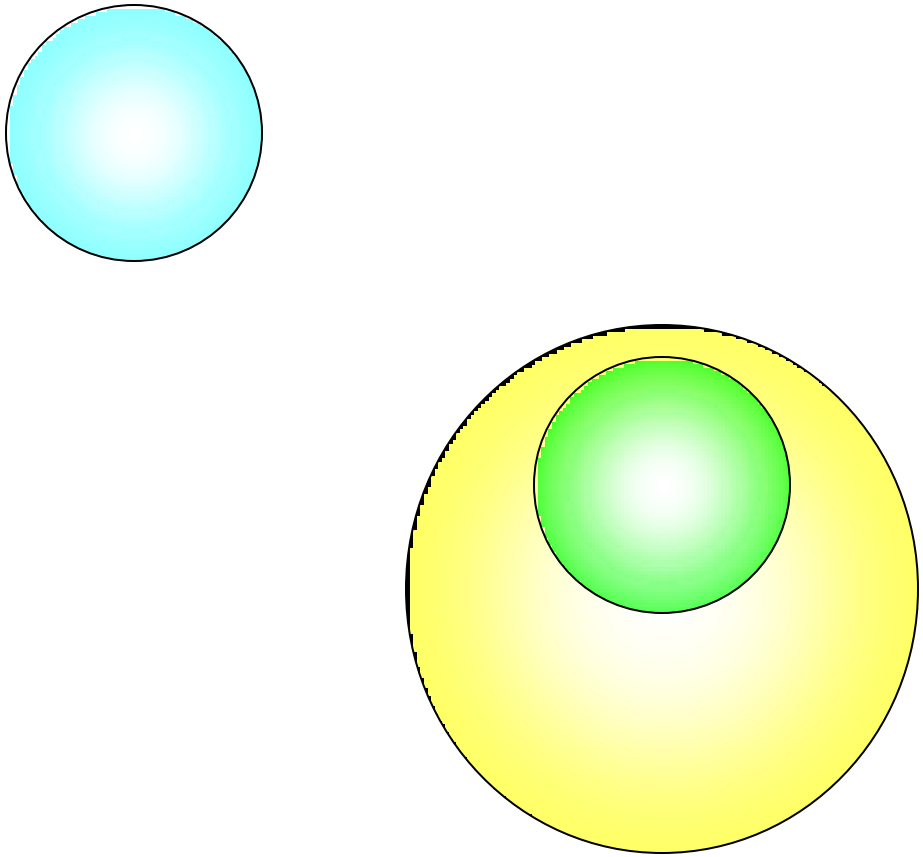

Knockout using Short Finite Range Repulsion

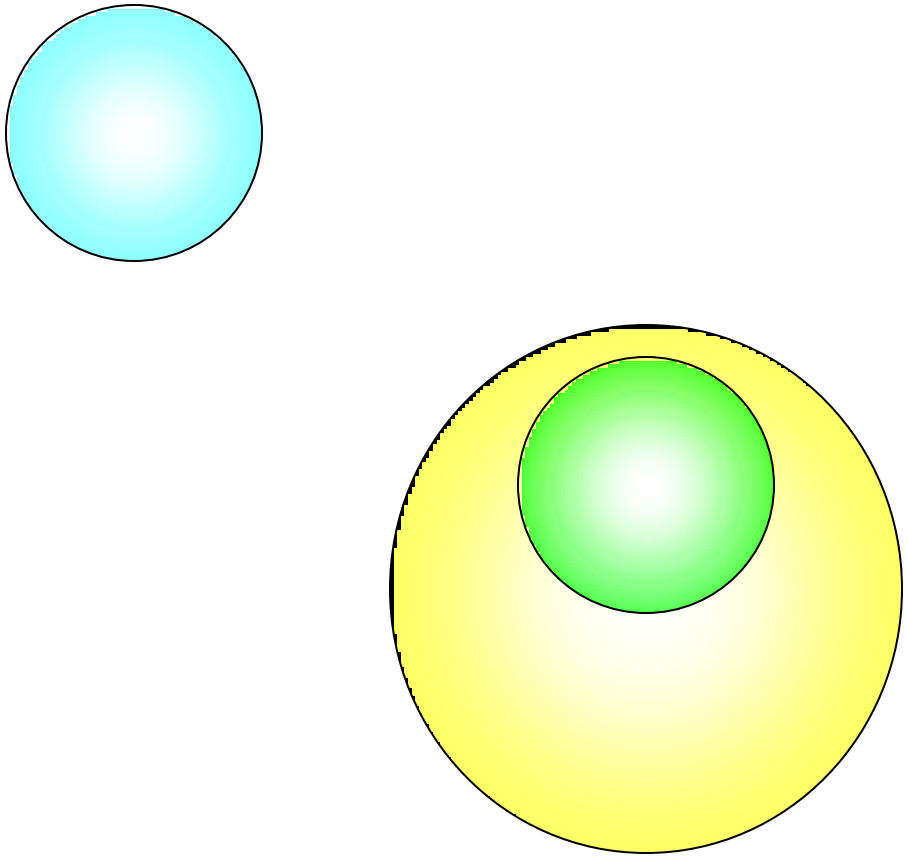

Knockout using Short Finite Range Repulsion

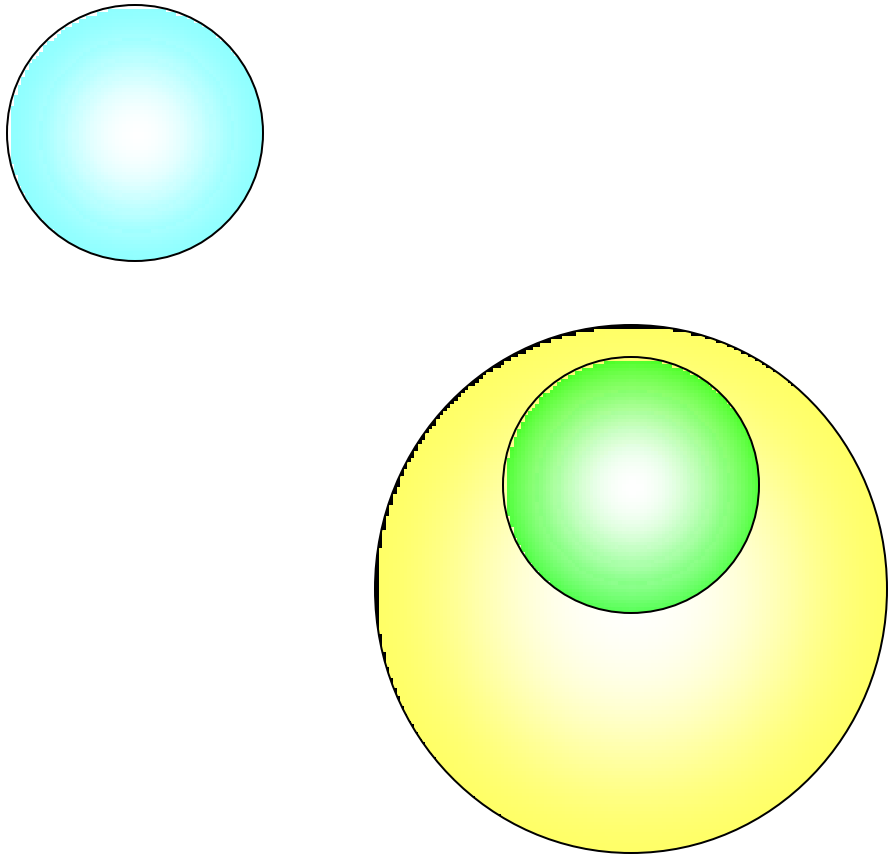

Knockout using Short Finite Range Repulsion

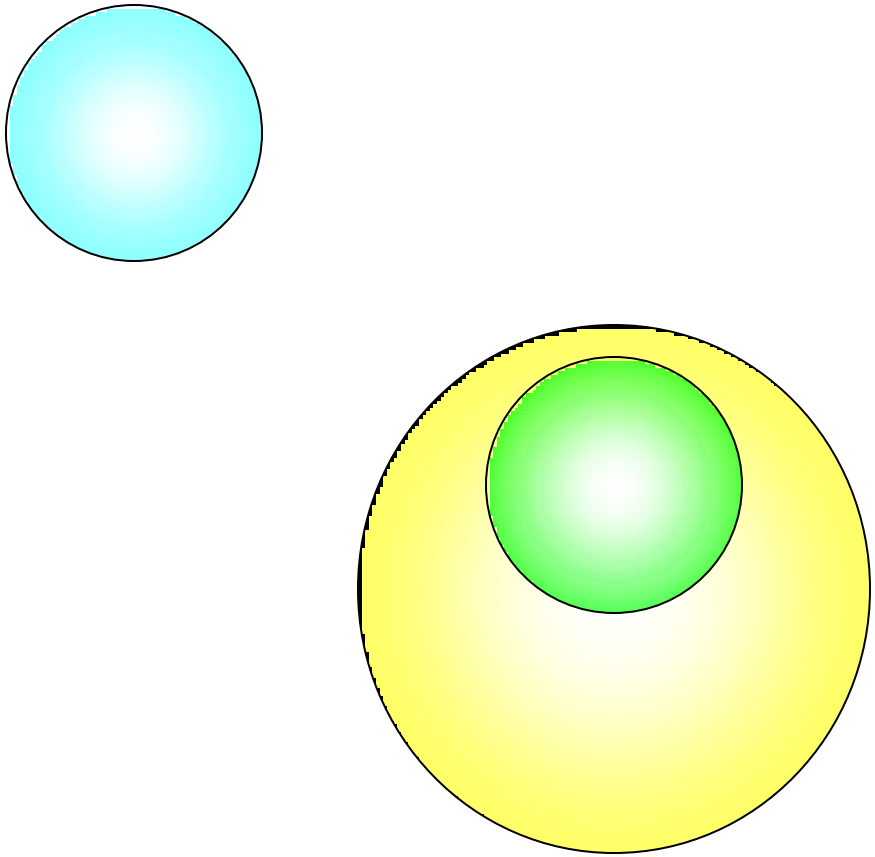

Knockout using Short Finite Range Repulsion

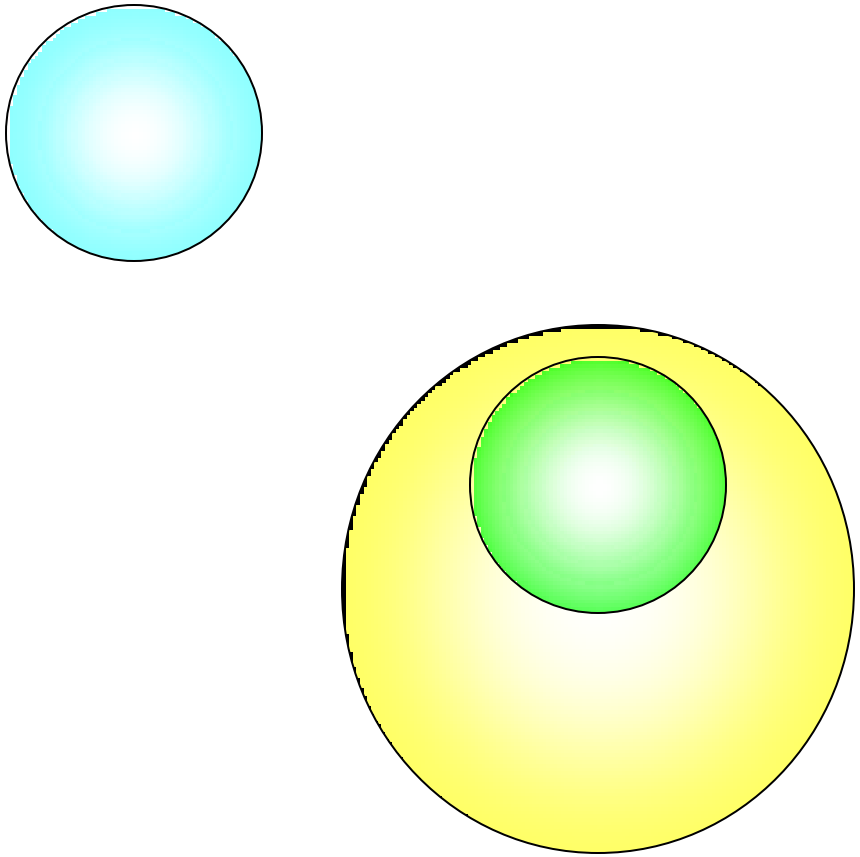

Knockout using Short Finite Range Repulsion

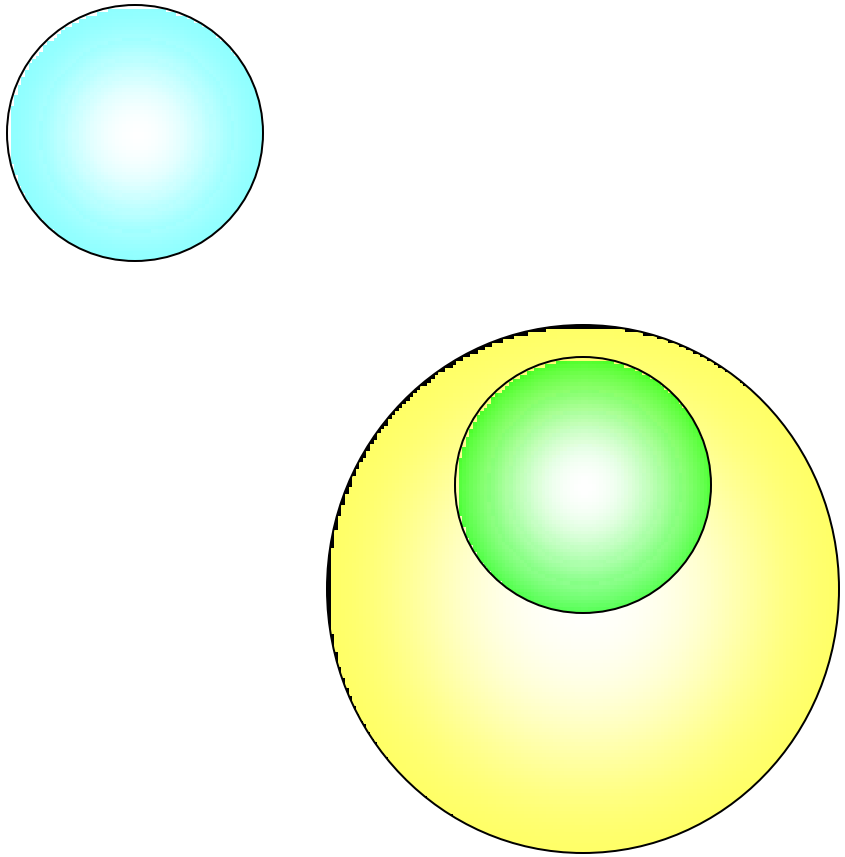

Knockout using Short Finite Range Repulsion

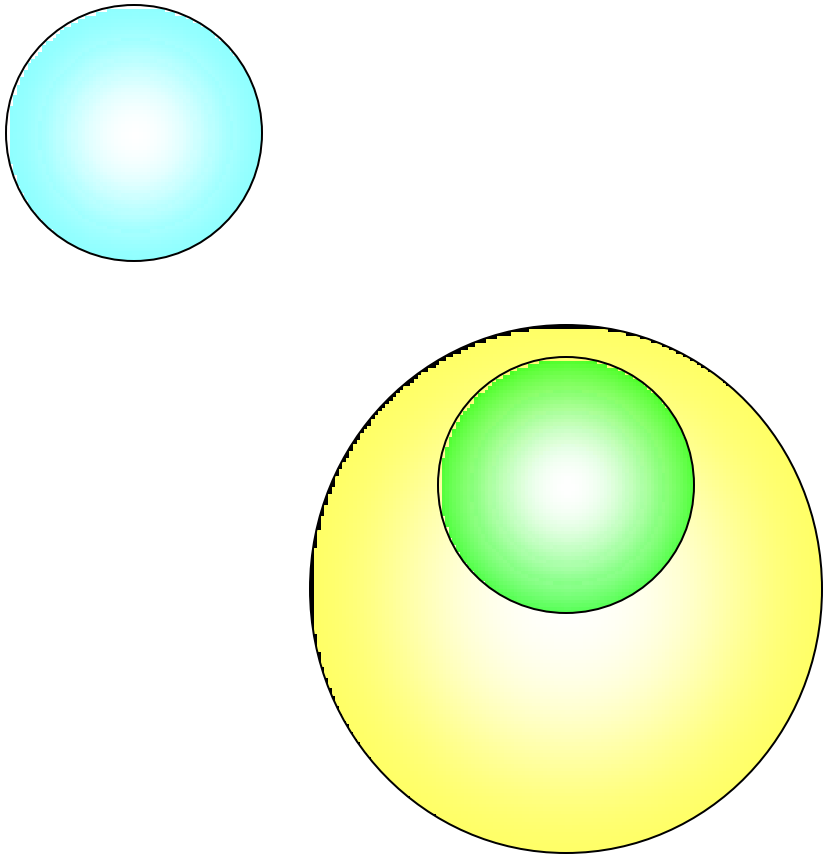

Knockout using Short Finite Range Repulsion

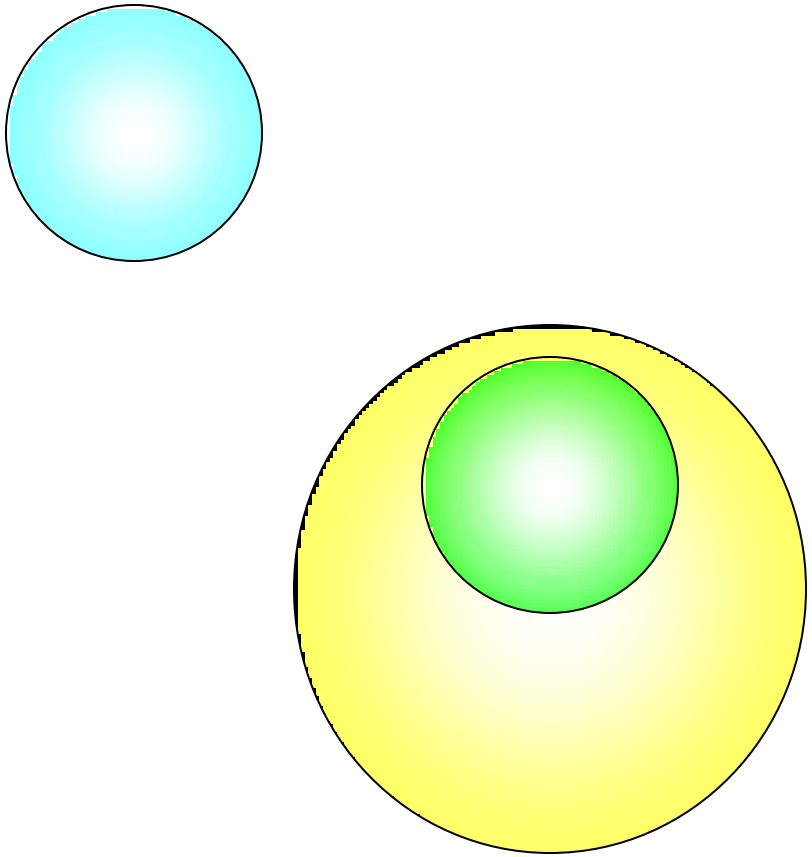

Knockout using Short Finite Range Repulsion

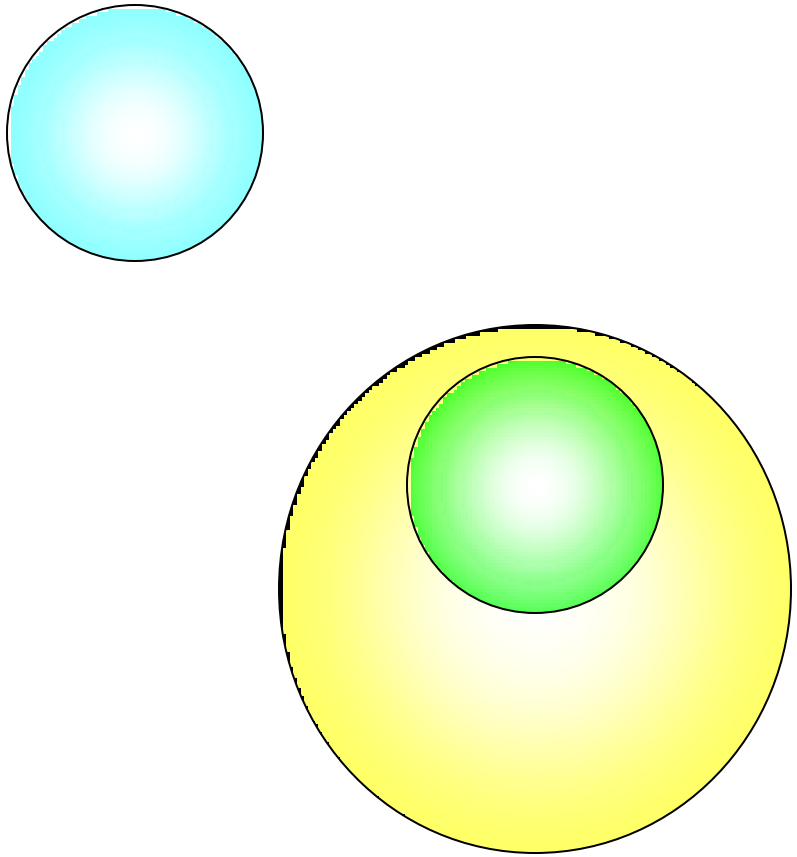

Knockout using Short Finite Range Repulsion

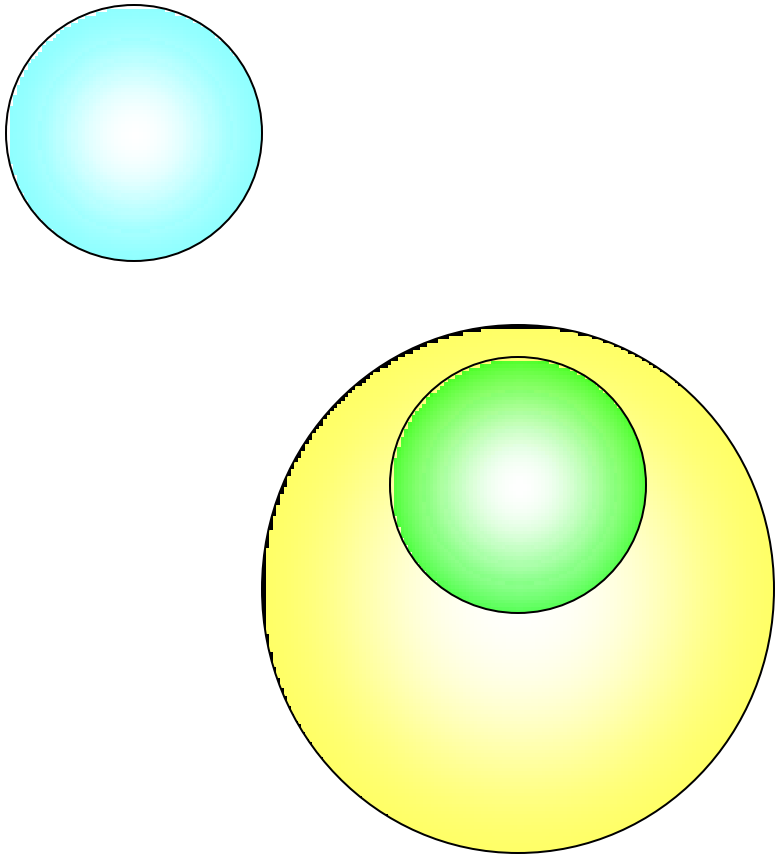

Knockout using Short Finite Range Repulsion

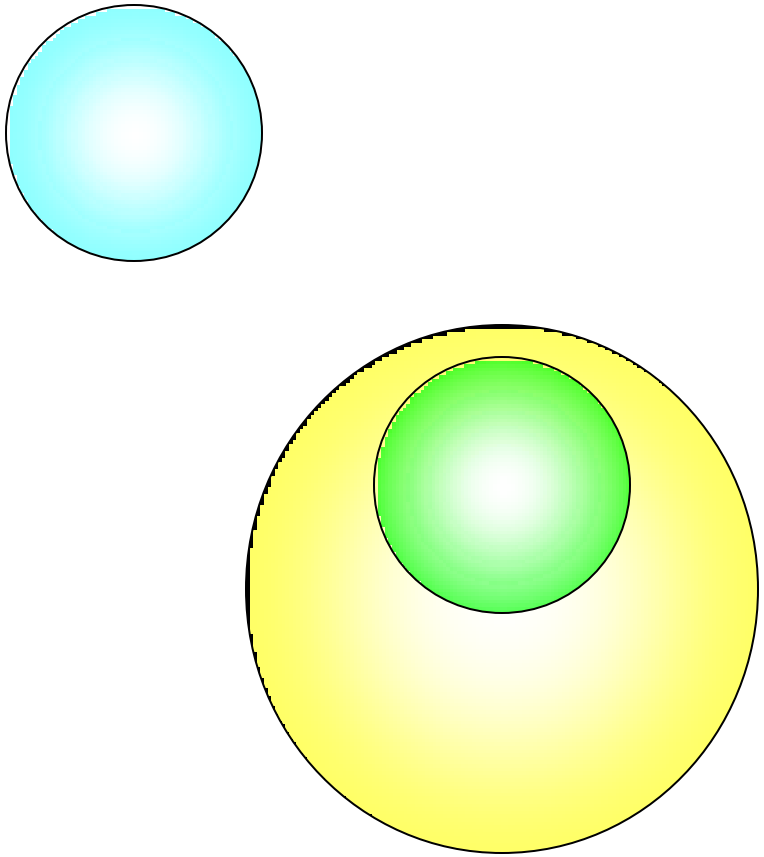

Knockout using Short Finite Range Repulsion

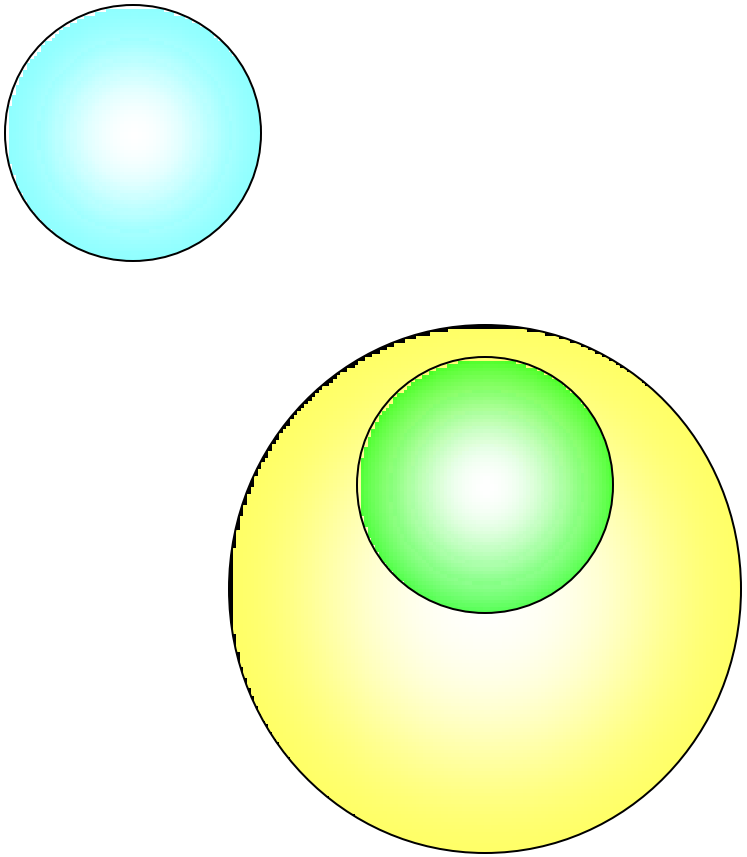

Knockout using Short Finite Range Repulsion

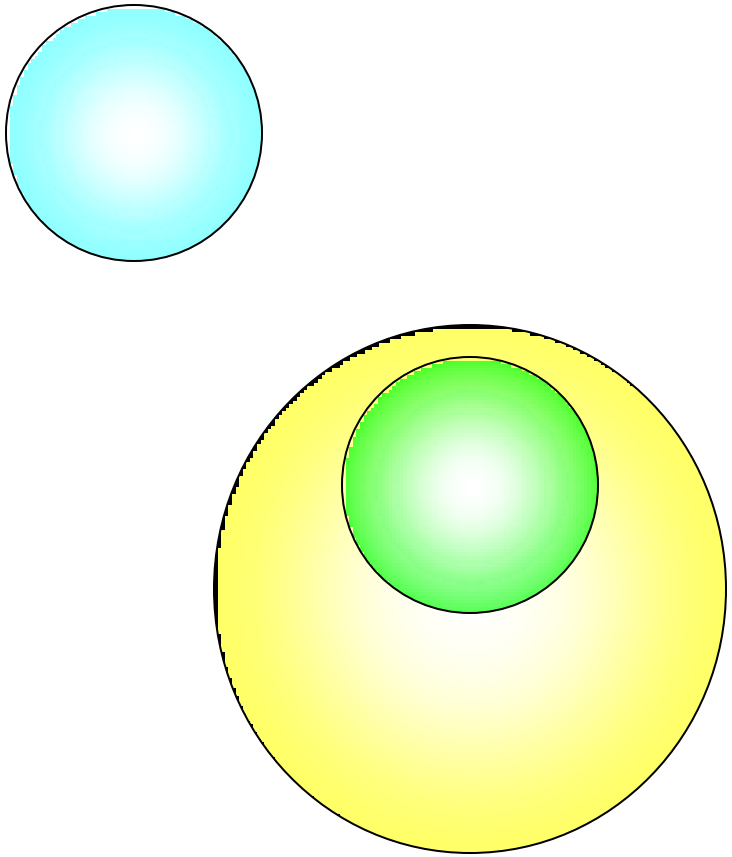

Knockout using Short Finite Range Repulsion

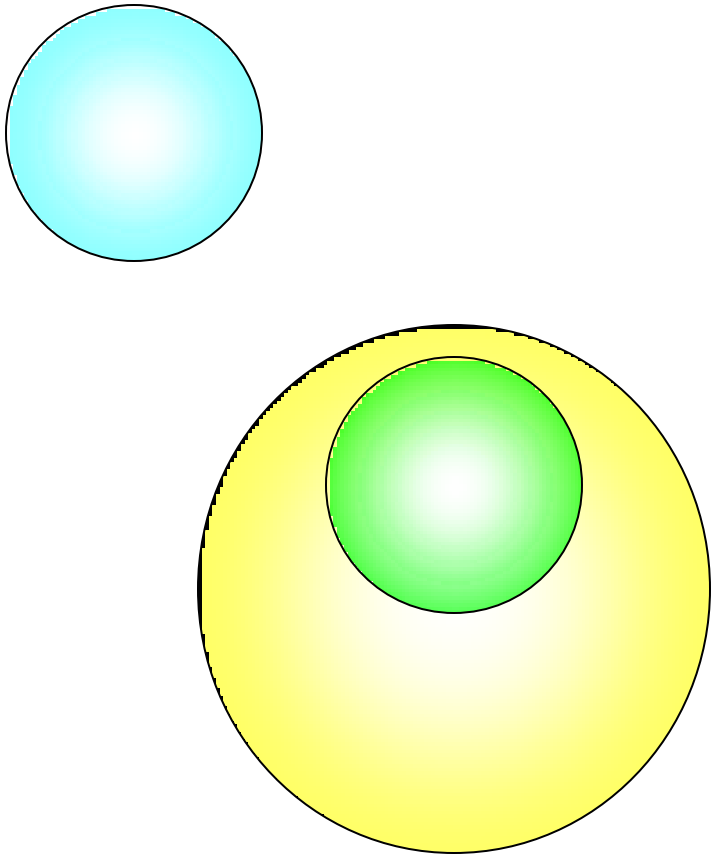

Knockout using Short Finite Range Repulsion

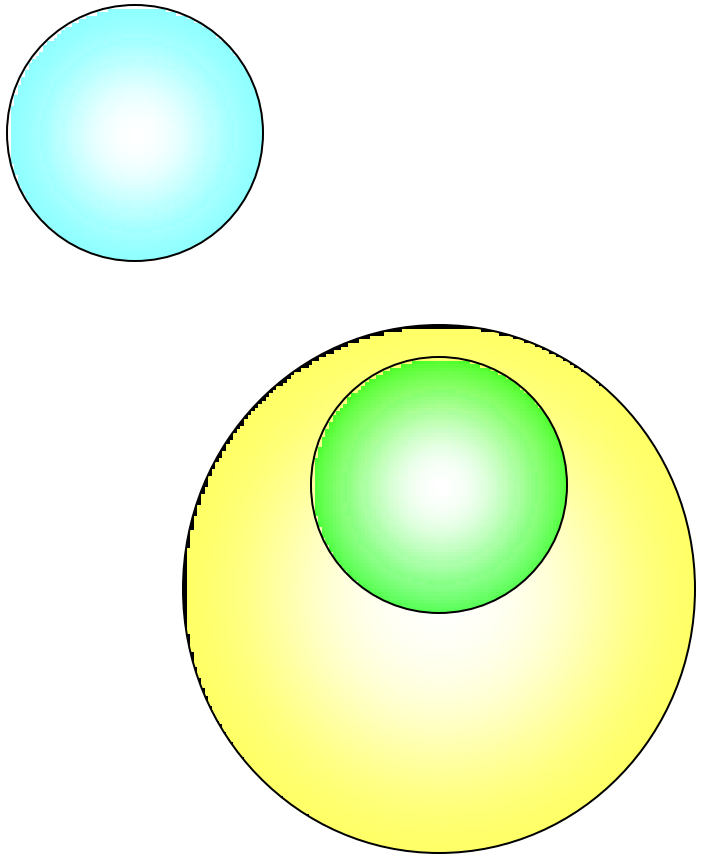

Knockout using Short Finite Range Repulsion

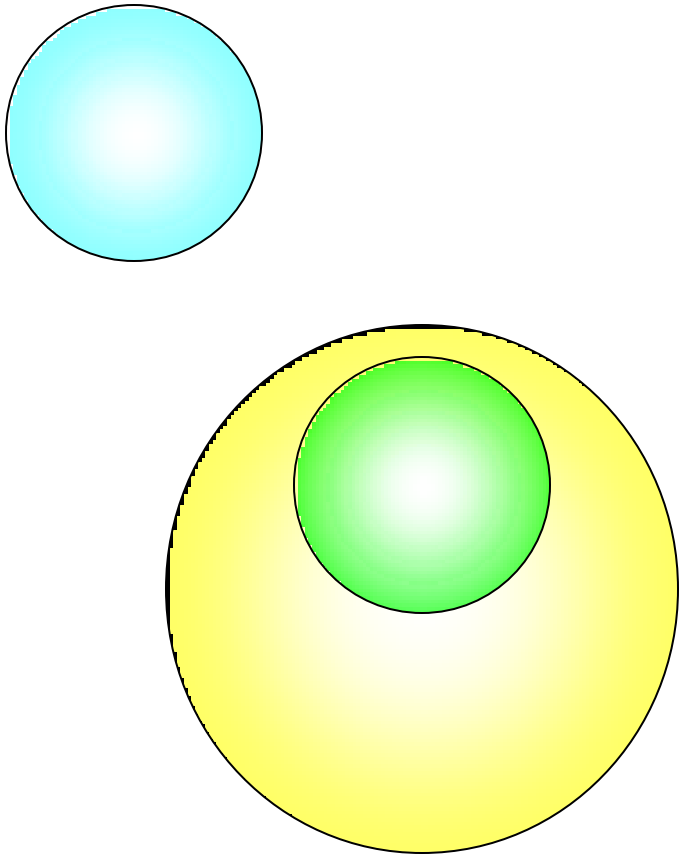

Knockout using Short Finite Range Repulsion

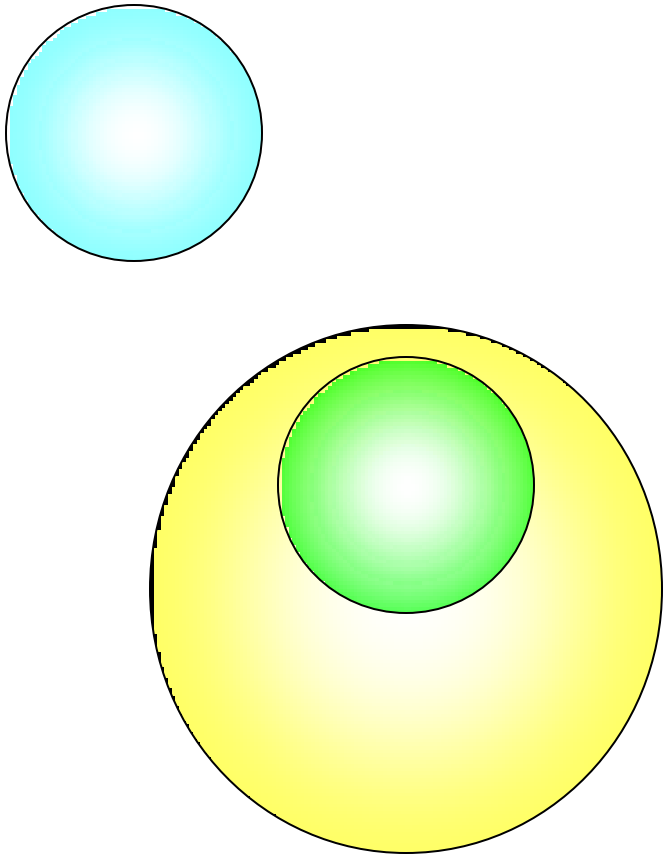

Knockout using Short Finite Range Repulsion

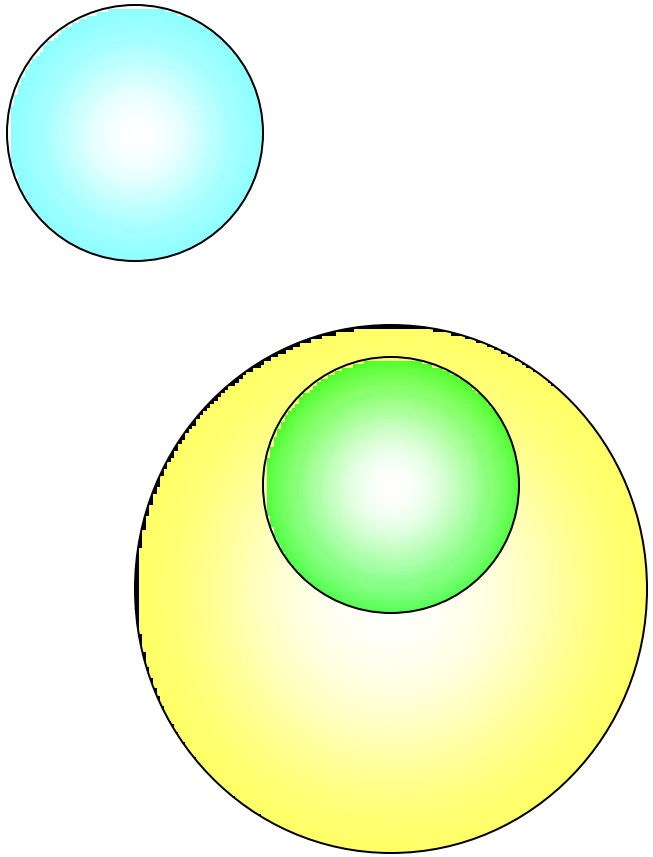

Knockout using Short Finite Range Repulsion

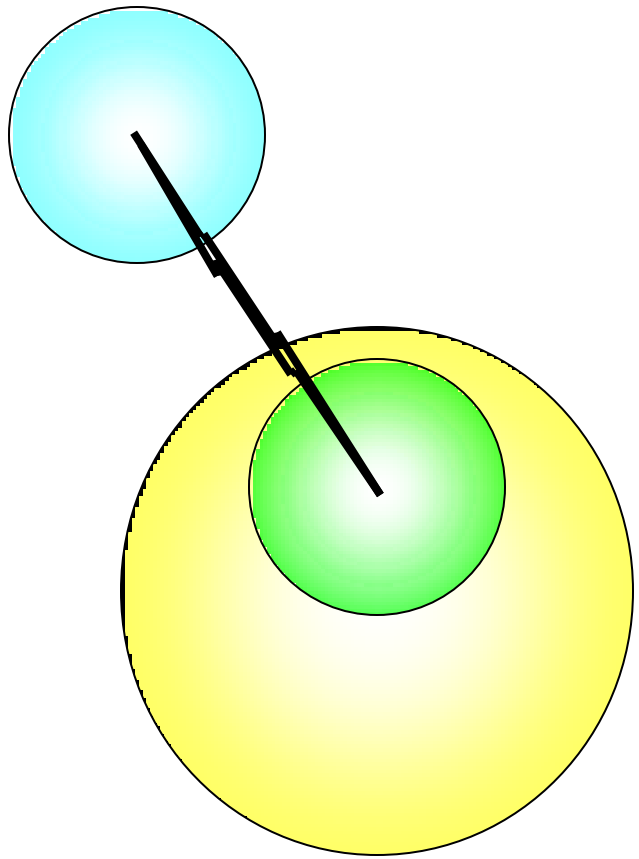

Knockout using Short Finite Range Repulsion

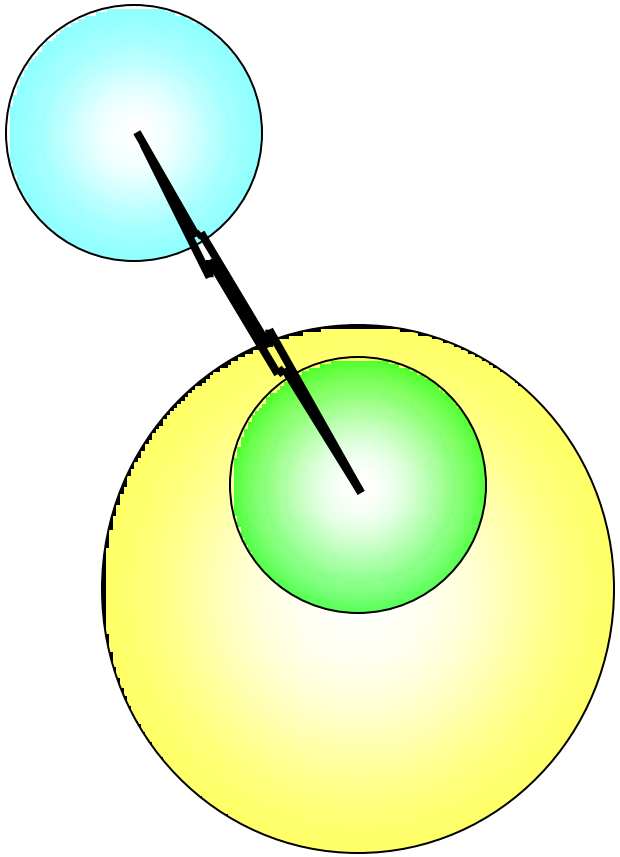

Knockout using Short Finite Range Repulsion

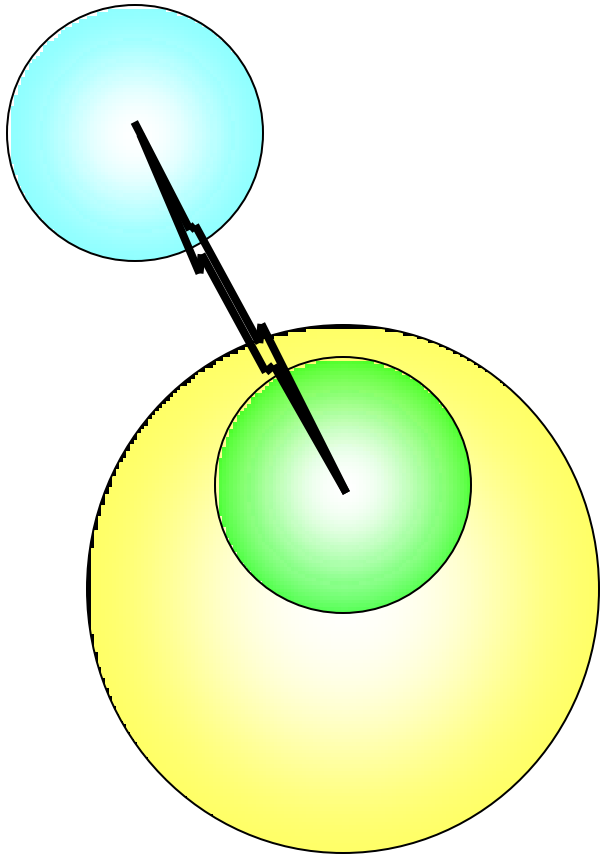

Knockout using Short Finite Range Repulsion

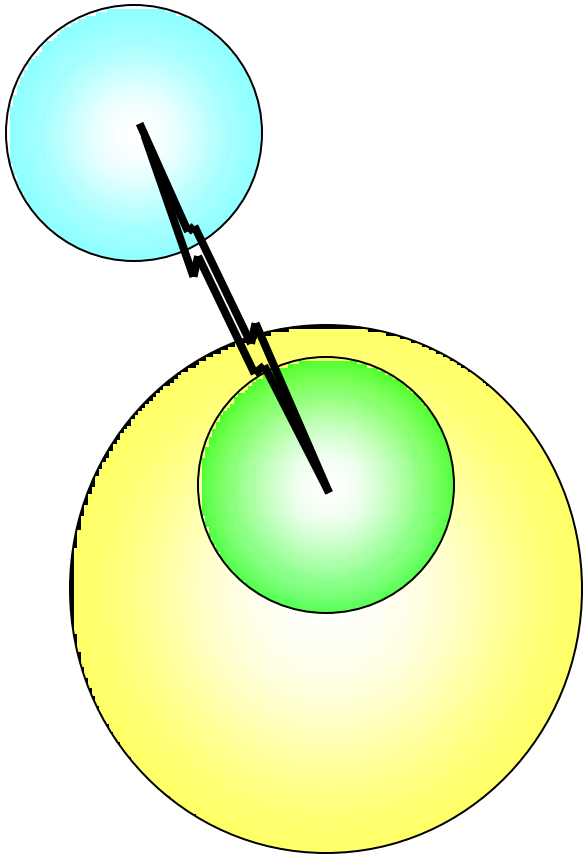

Knockout using Short Finite Range Repulsion

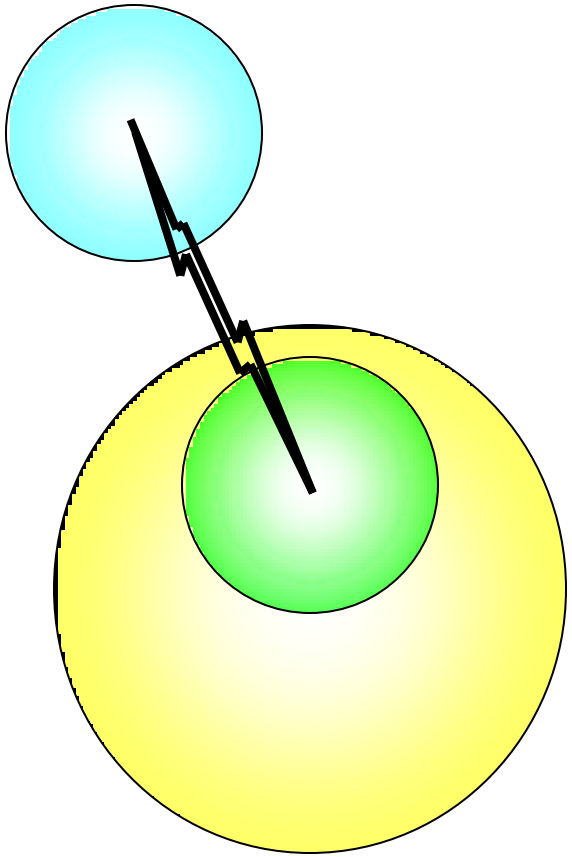

Knockout using Short Finite Range Repulsion

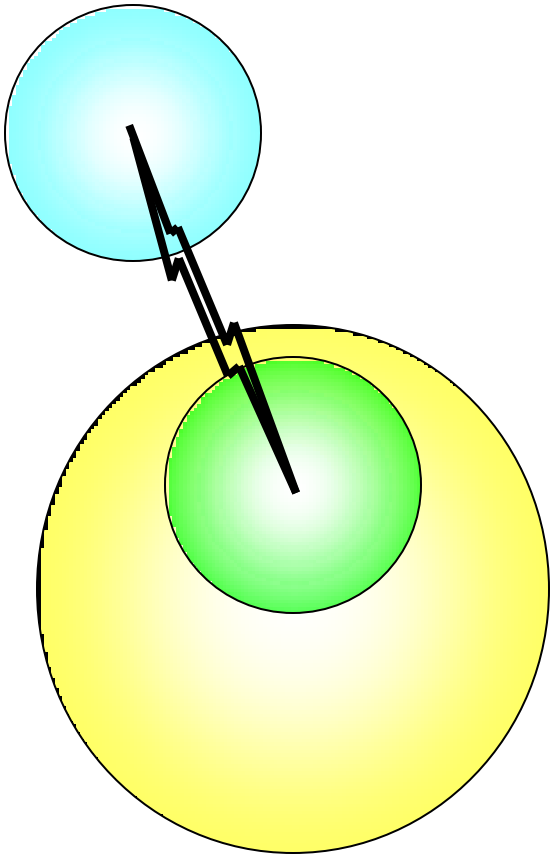

Knockout using Short Finite Range Repulsion

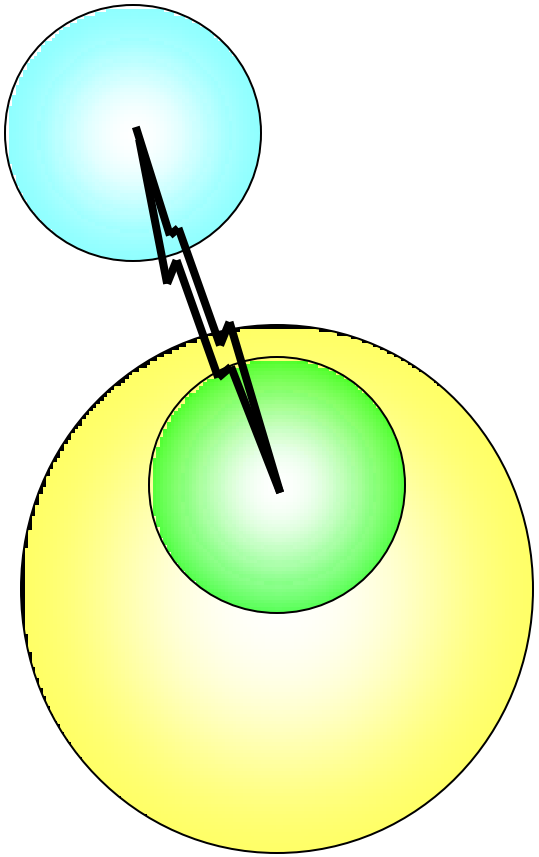

Knockout using Short Finite Range Repulsion

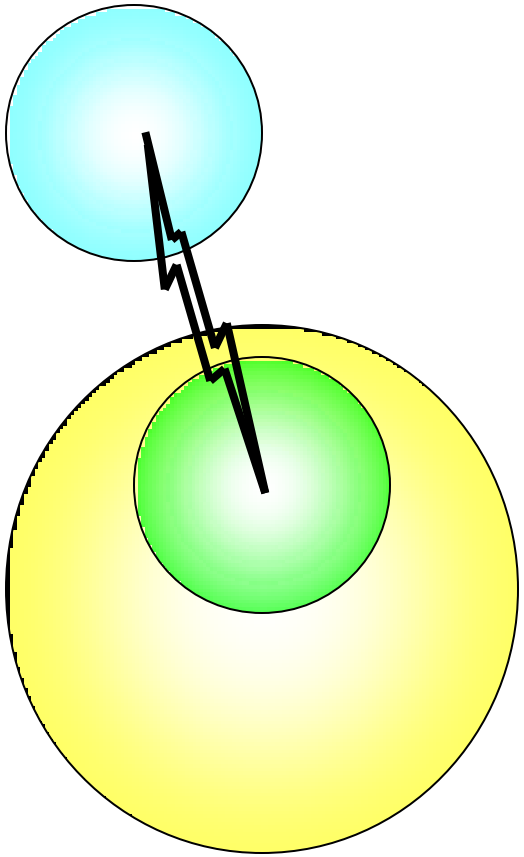

Knockout using Short Finite Range Repulsion

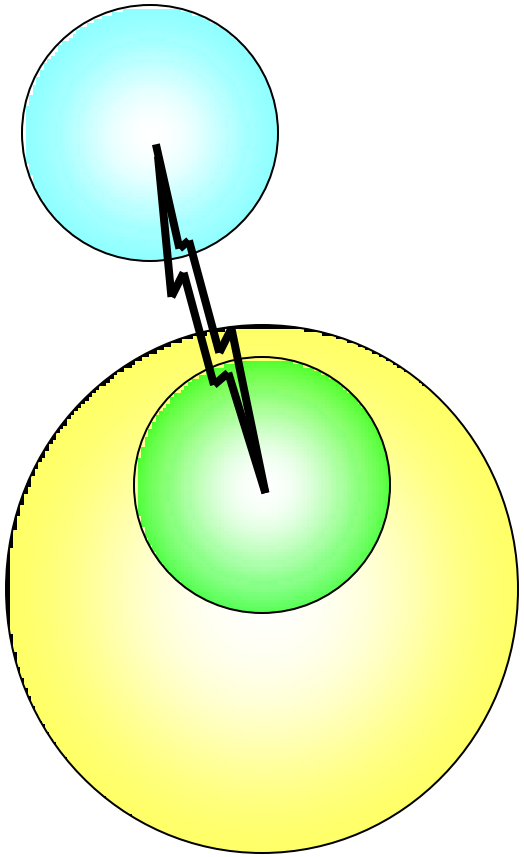

Knockout using Short Finite Range Repulsion

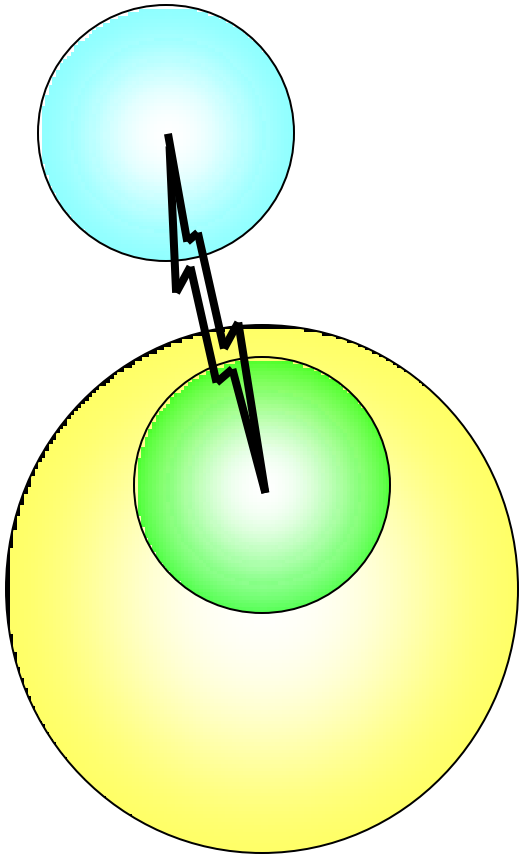

Knockout using Short Finite Range Repulsion

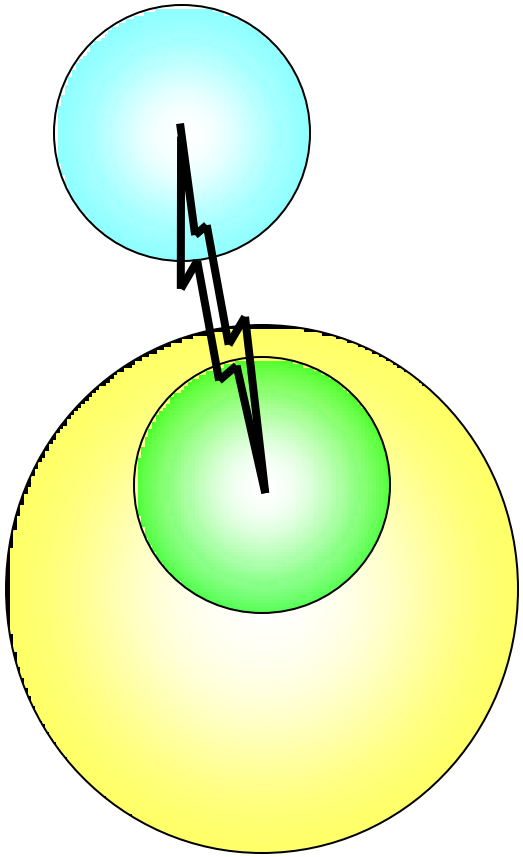

Knockout using Short Finite Range Repulsion

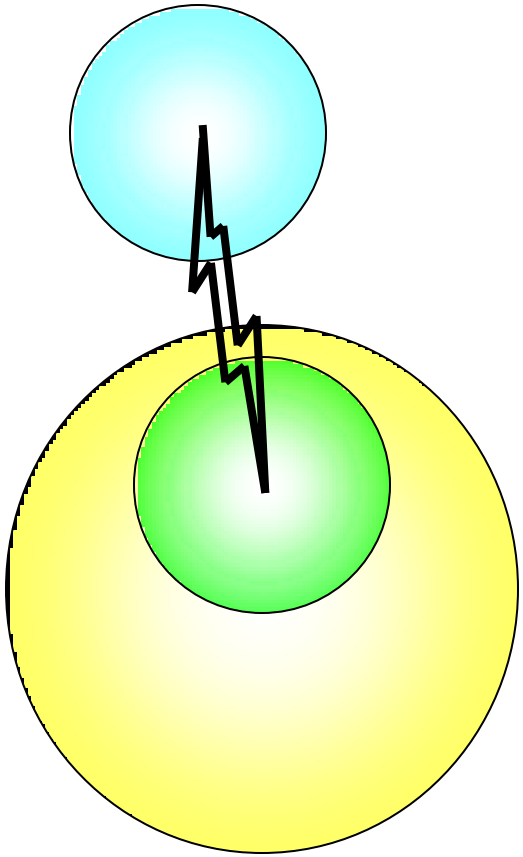

Knockout using Short Finite Range Repulsion

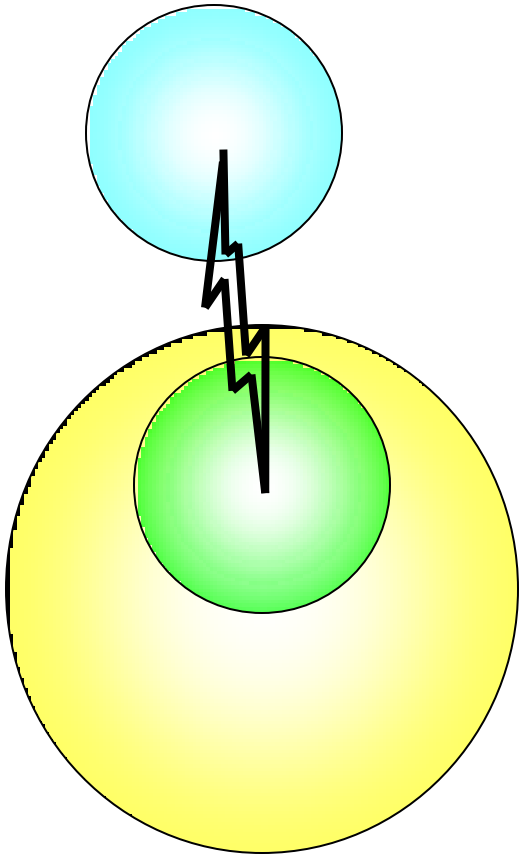

Knockout using Short Finite Range Repulsion

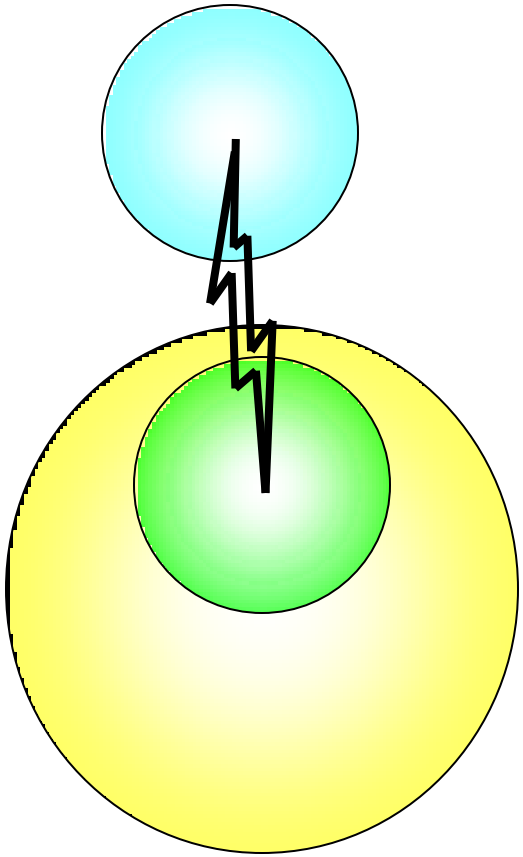

Knockout using Short Finite Range Repulsion

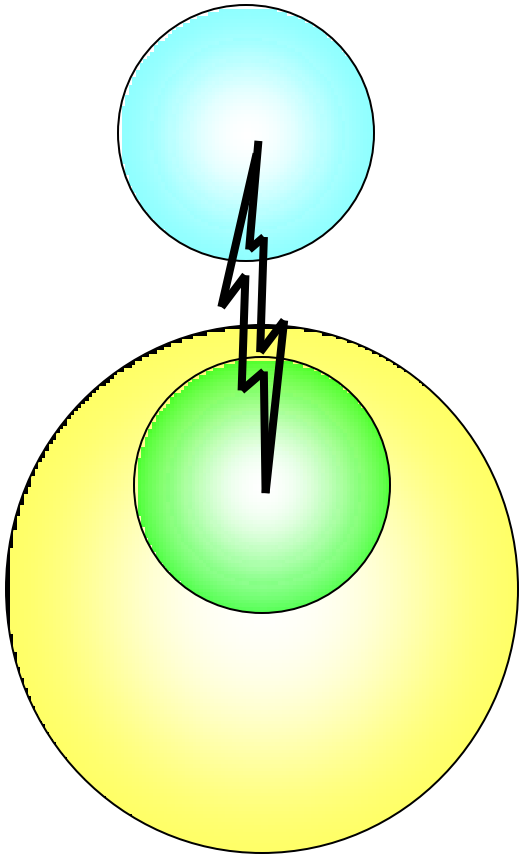

Knockout using Short Finite Range Repulsion

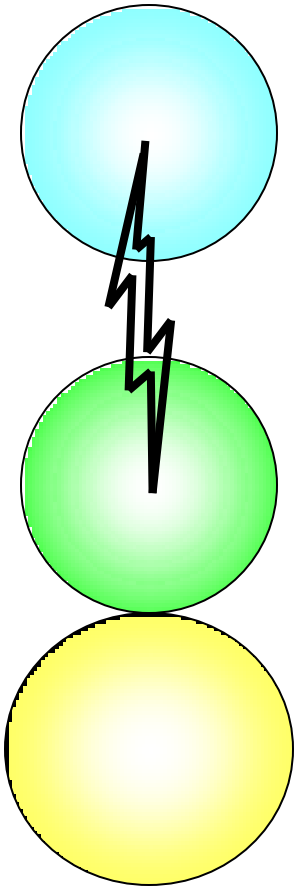

Knockout using Short Finite Range Repulsion

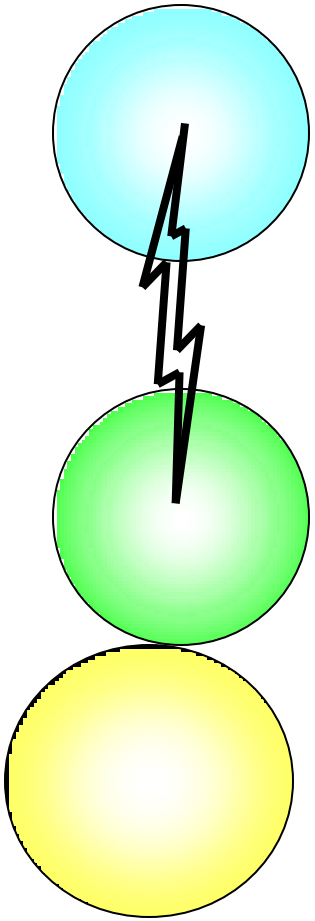

Knockout using Short Finite Range Repulsion

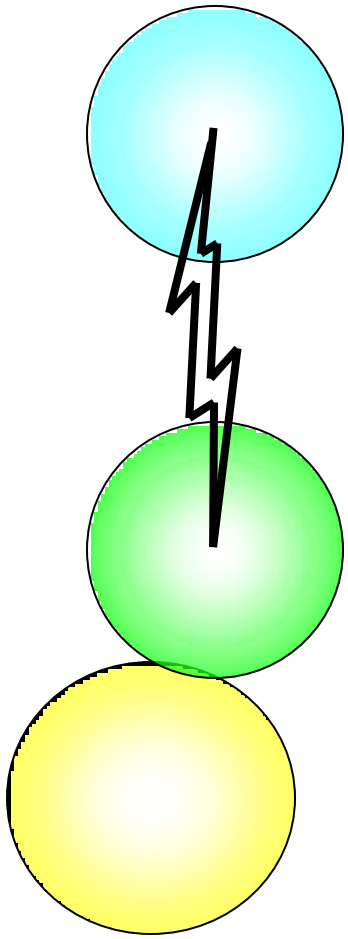

Knockout using Short Finite Range Repulsion

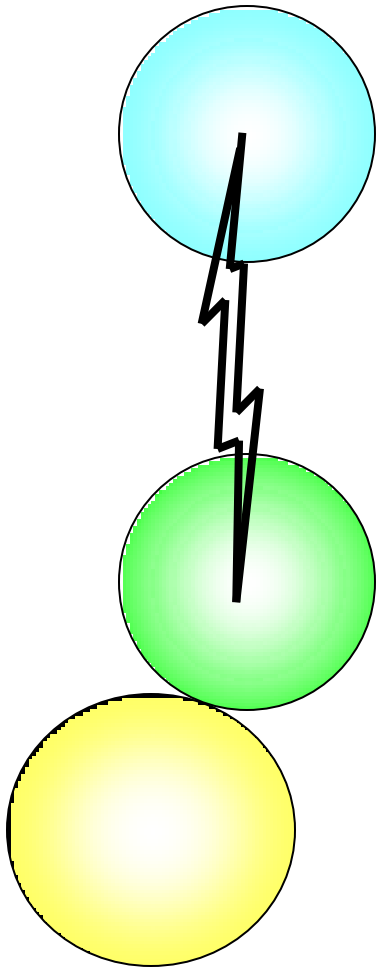

Knockout using Short Finite Range Repulsion

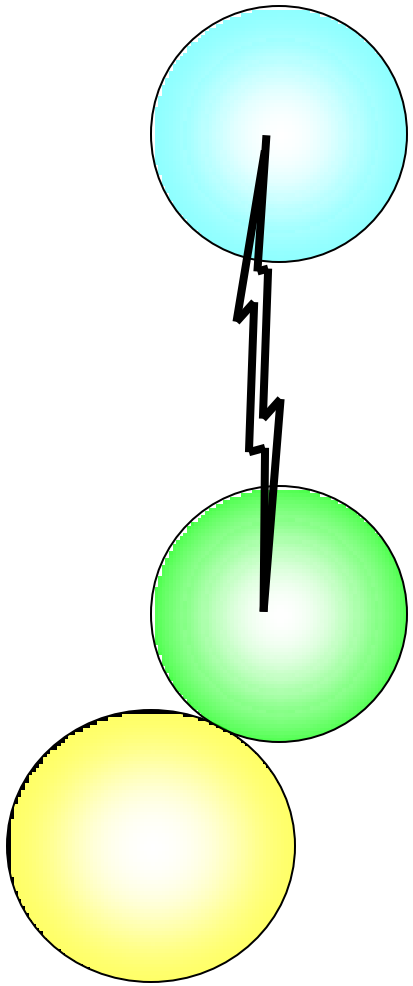

Knockout using Short Finite Range Repulsion

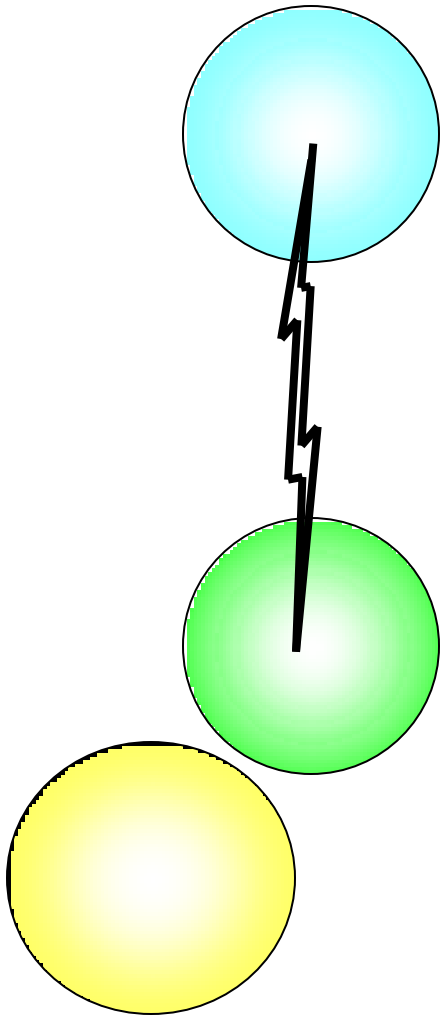

Knockout using Short Finite Range Repulsion

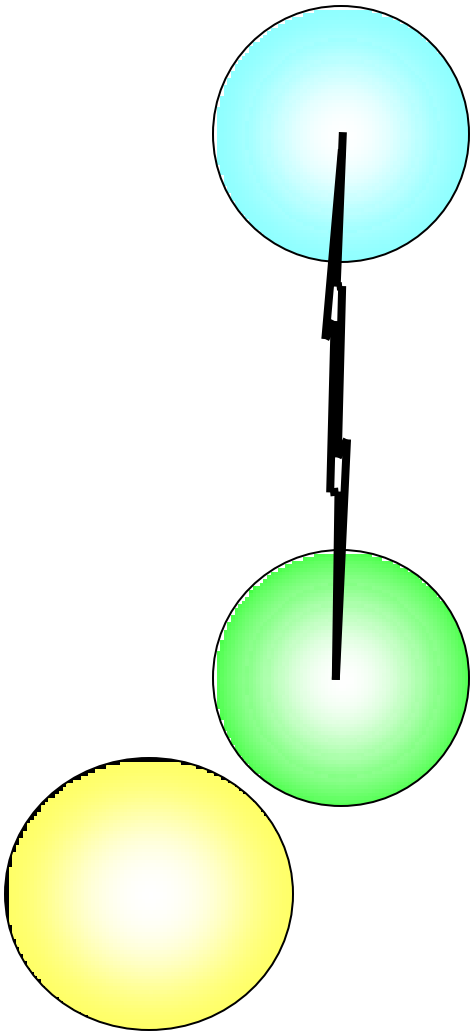

Knockout using Short Finite Range Repulsion

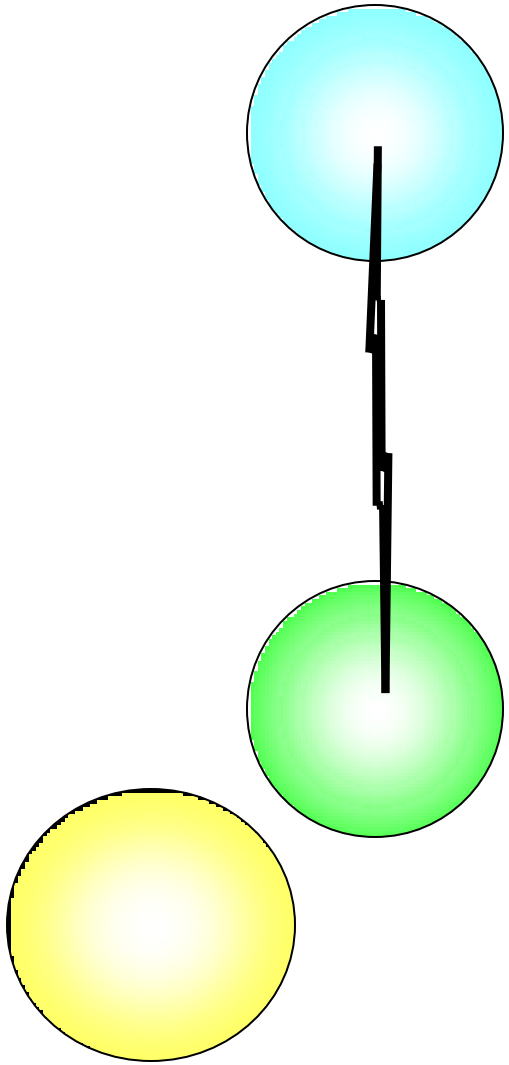

Knockout using Short Finite Range Repulsion

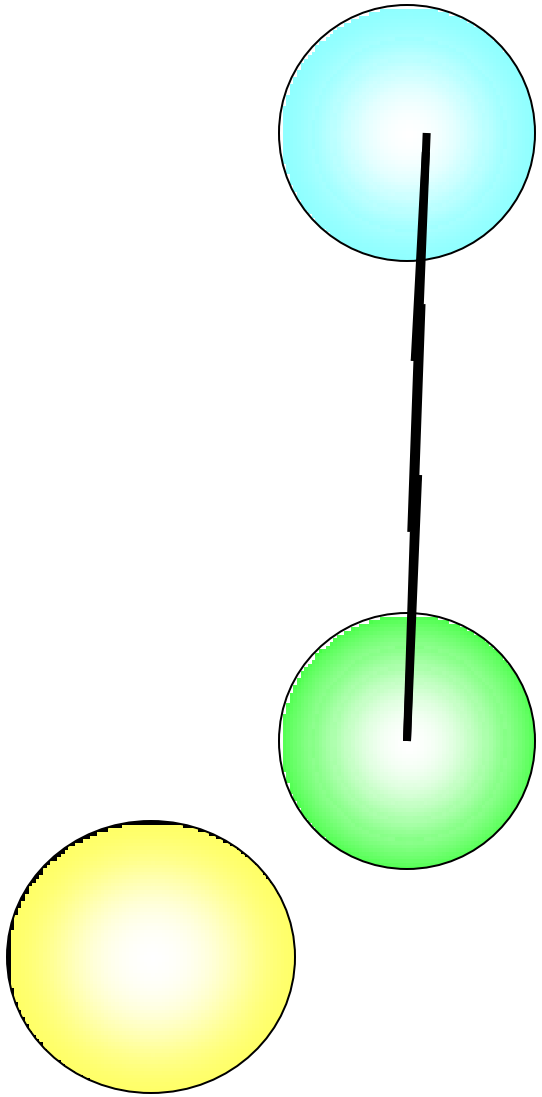

Knockout using Short Finite Range Repulsion

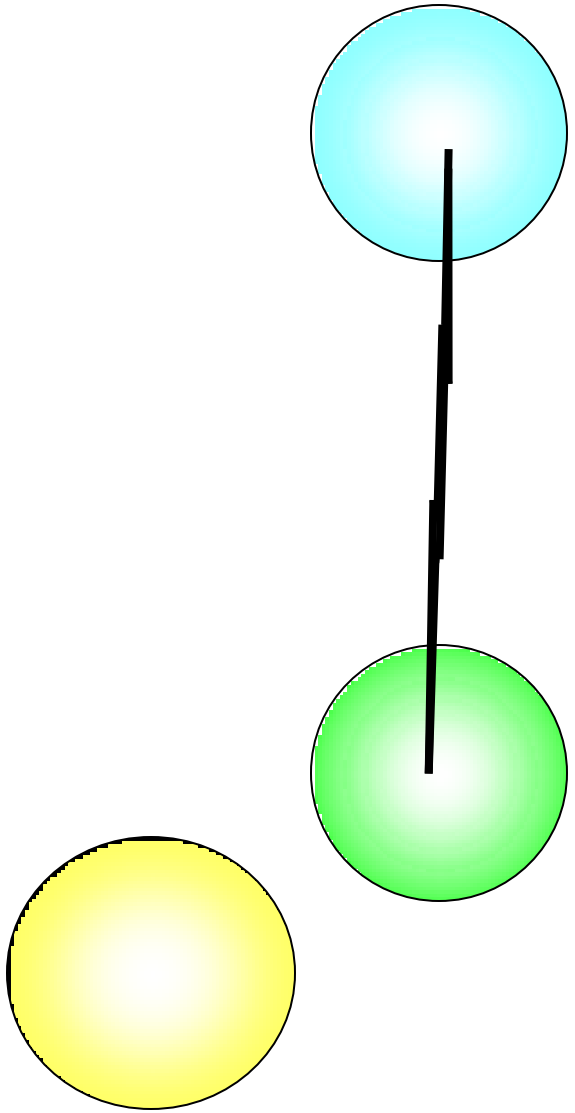

Knockout using Short Finite Range Repulsion

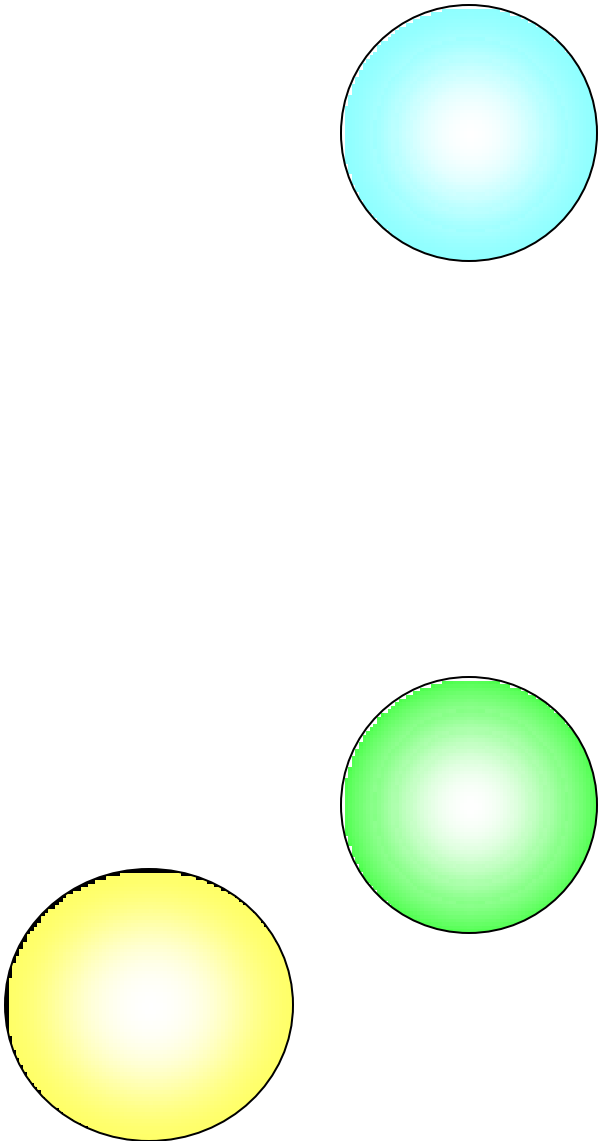

Knockout using Short Finite Range Repulsion

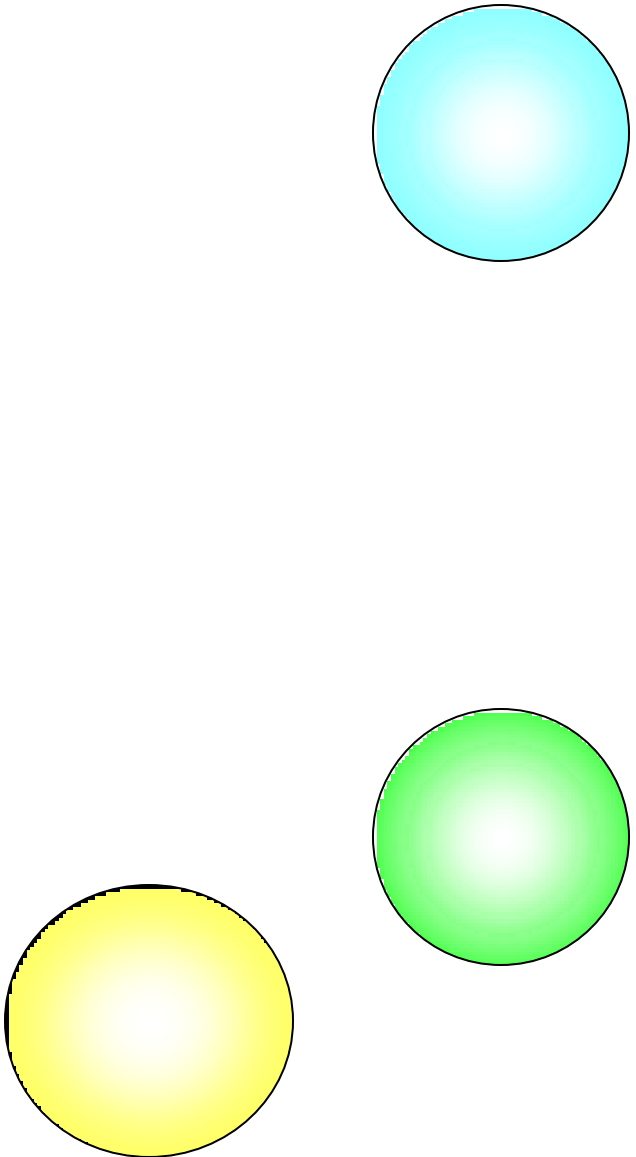

Knockout using Short Finite Range Repulsion

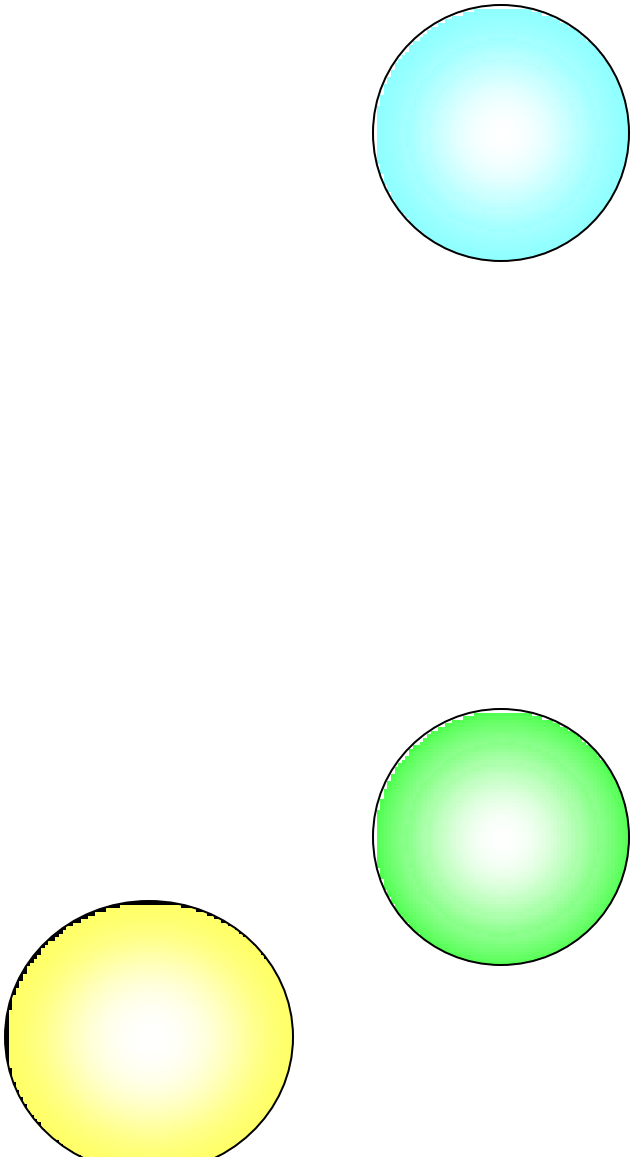

Knockout using Short Finite Range Repulsion

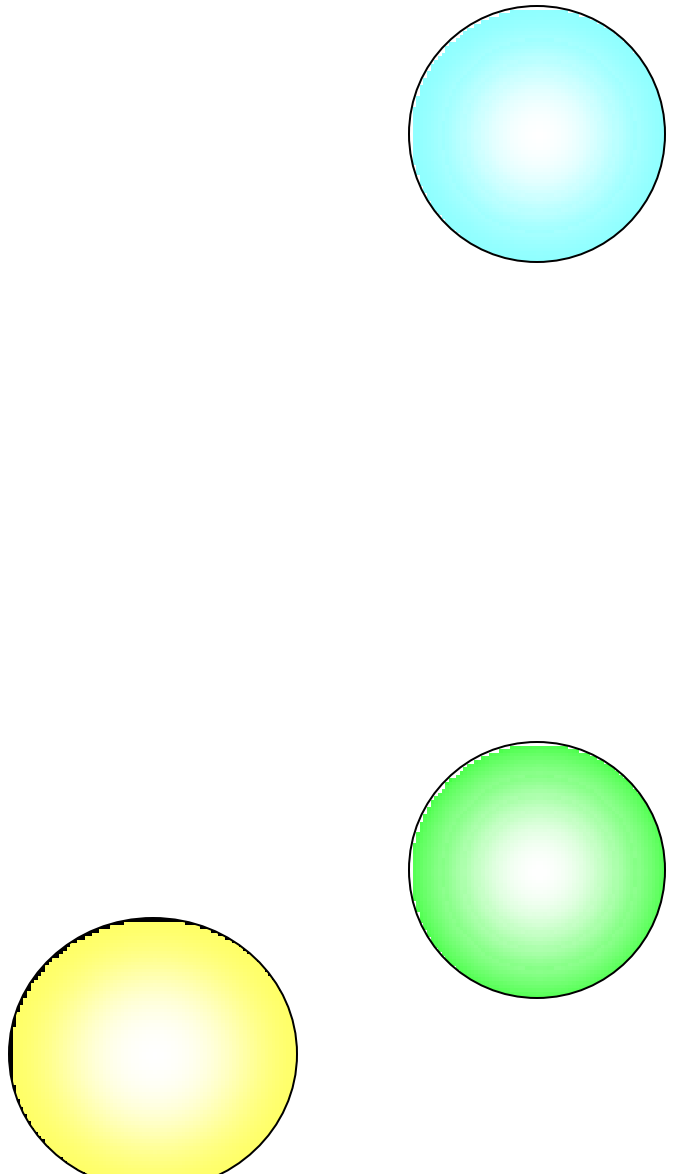

Knockout using Short Finite Range Repulsion

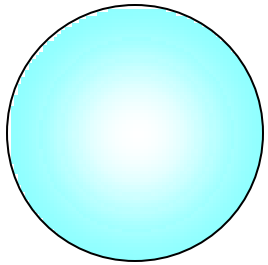

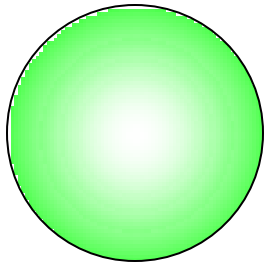

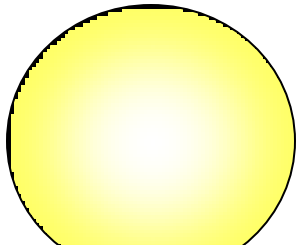

Knockout using Short Finite Range Repulsion

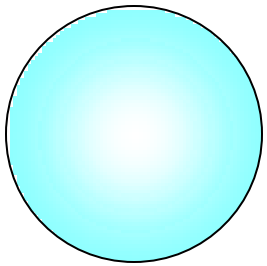

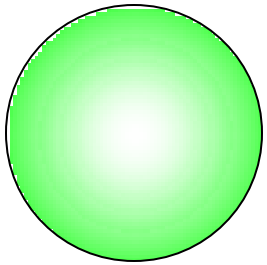

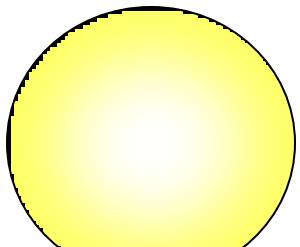

Knockout using Short Finite Range Repulsion

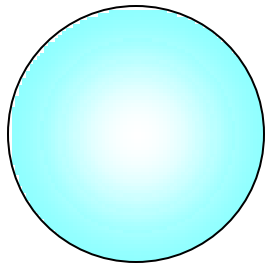

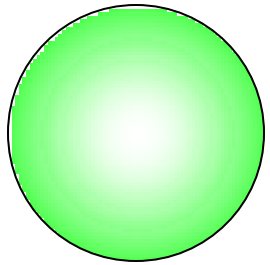

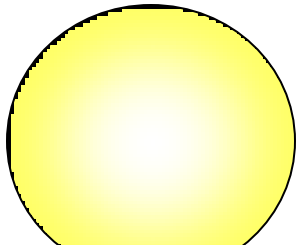

Knockout using Short Finite Range Repulsion

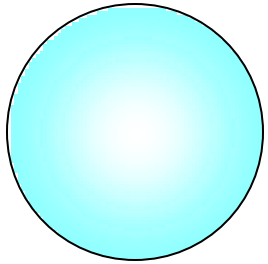

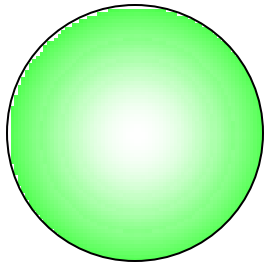

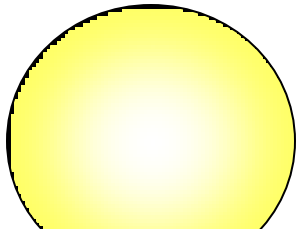

Knockout using Short Finite Range Repulsion

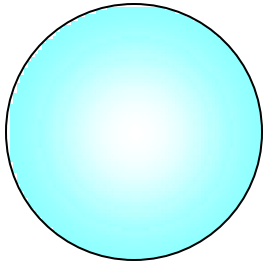

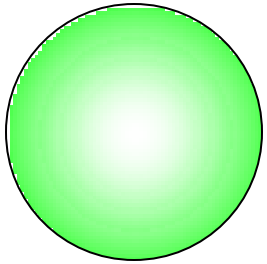

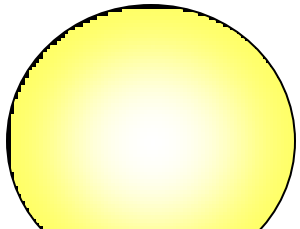

Knockout using Short Finite Range Repulsion

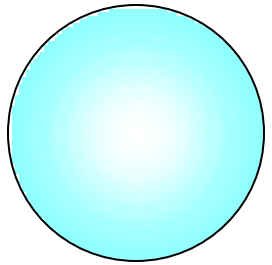

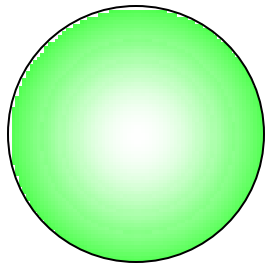

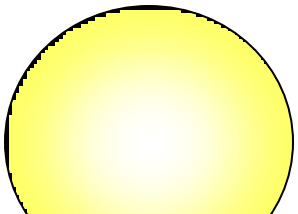

Knockout using Short Finite Range Repulsion

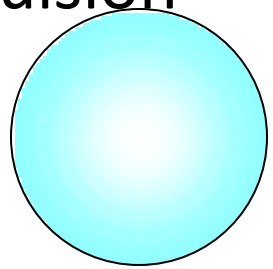

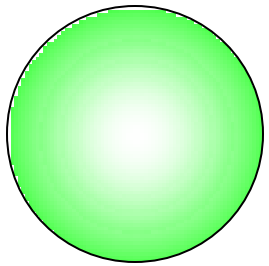

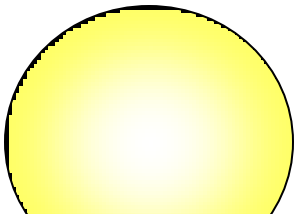

Knockout using Short Finite Range Repulsion

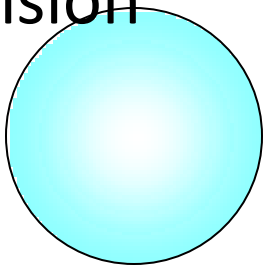

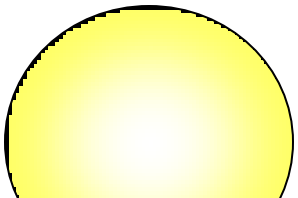

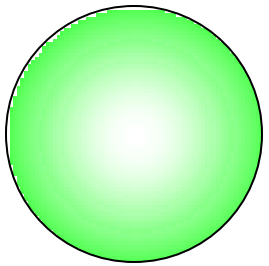

Knockout using Short Finite Range Repulsion

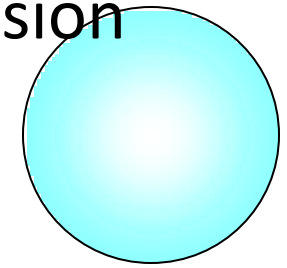

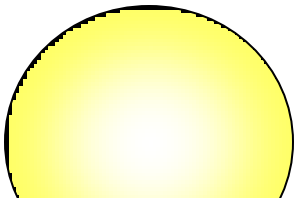

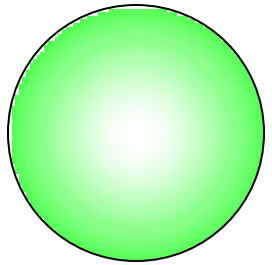

Knockout using Short Finite Range Repulsion

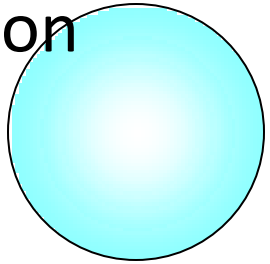

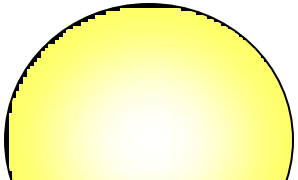

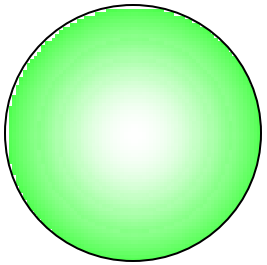

Knockout using Short Finite Range Repulsion

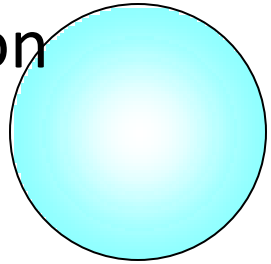

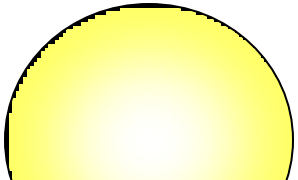

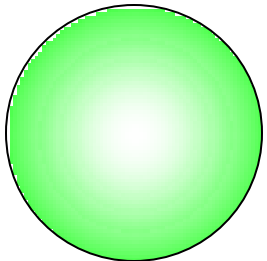

Zero Range Approximation for the knockout vertex is hidden in the conventional language of the factorization approximation of the knockout vertex matrix element.

Actually the transition matrix element and the double differential cross section are written as,

$$\frac{d^3\sigma^{L,J}}{d\Omega_1 d\Omega_2 dE_1} = F_{kin}.S_\alpha^{L\,J}.\sum_\Lambda \left|T_{fi}^{\alpha L\Lambda}(\vec{k}_f,\vec{k}_i)\right|^2$$

$$T_{fi}^{\alpha L\Lambda}(\vec{k}_f,\vec{k}_i) = \int g(r)dr$$

$$= \int \chi_1^{(-)*}(\vec{k}_{aB},\vec{r}_{aB})\chi_2^{(-)*}(\vec{k}_{2B},\vec{R}_{2B})t_{12}(\vec{r}_{12})\chi_0^{(+)}(\vec{k}_{1A},\vec{r}_{1A})\varphi_{L\Lambda}(\vec{R}_{2B})d\vec{r}_{12}d\vec{R}_{2B}$$

Which includes the finite range effects, which we have worked for the first time.

t- matrix effective Interaction

t-matrix:-

$$t^{\pm} = V\Omega^{\pm}$$

The Moller wave $\Omega^{\pm}$ operator is such that it transforms the plane wave states, Φ into scattering states, $\psi^{\pm}$ is defined in terms of radial scattering solutions $u_l(kr)$ as:

$$\psi^{\pm}_{\alpha\alpha}(\vec{r}) = \sum_{l=0,2,4} i^l (2l+1) \frac{u_l(kr)}{kr} e^{i\sigma_l} P_l(\hat{r})$$

$$t^{+}_{\alpha\alpha}(E,\vec{r}) = e^{-ikz} \sum_{l=0,2,4...} V_l(r) i^l (2l+1) \frac{u_l(kr)}{kr} e^{i\sigma_l} P_l(\hat{r})$$

$$t_L(E,r) = \frac{2L+1}{2} \sum_{l,m} V_l(r) i^l (2L+1) \frac{\mu_l(kr)}{kr} j_m(kr) (-i)^m (2m+1) e^{i\sigma_l} \int_{-1}^{+1} P_L^*(\cos\theta) P_l(\cos\theta) P_m(\cos\theta) d(\cos\theta)$$

Arun K Jain & Bhushan N. Joshi, Prog. Theor. Phys. 120 (2008) 1193

Repulsive core + Attractive α-α t-matrix, tψ=VΦ

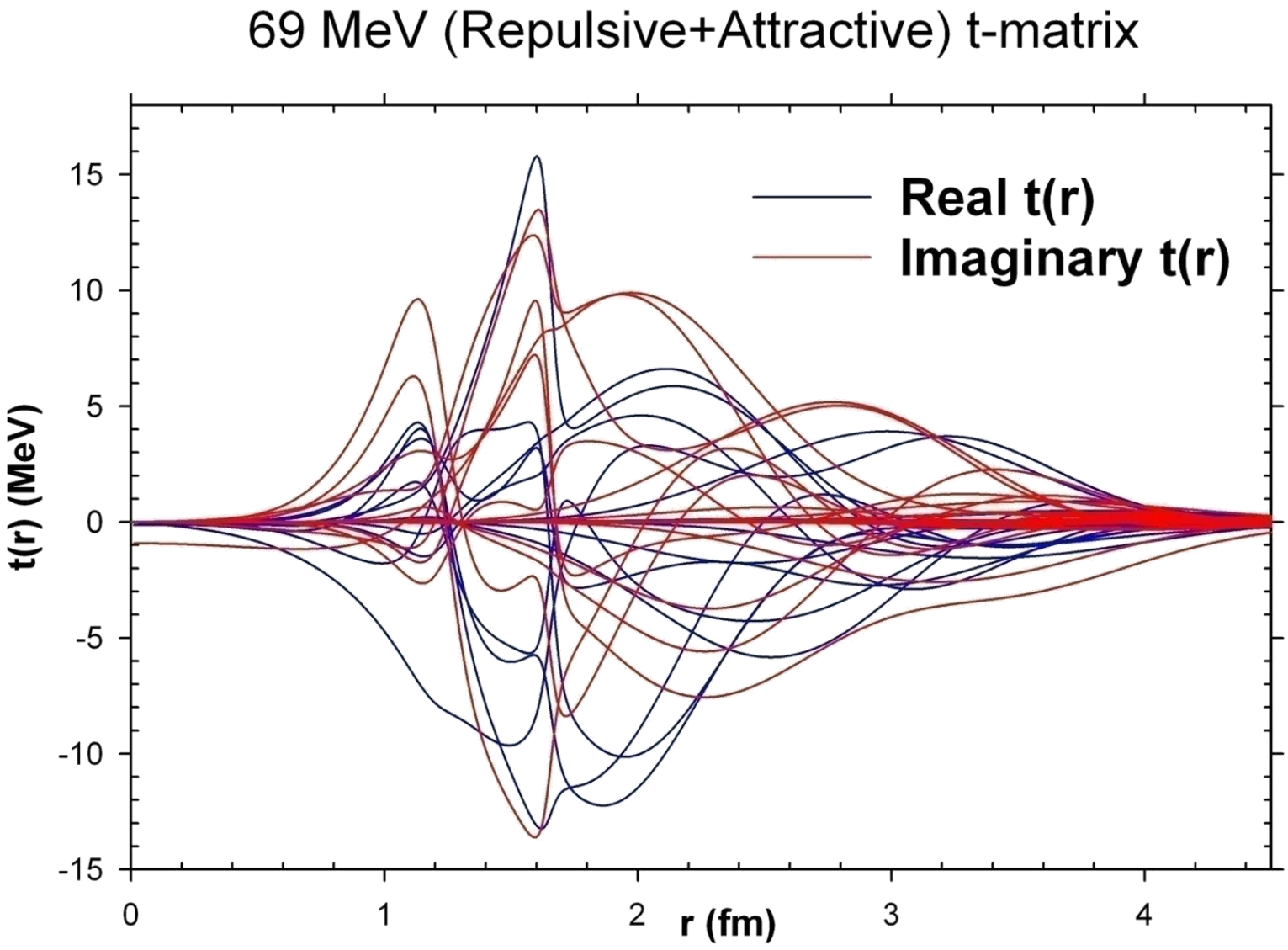

Arun K Jain & Bhushan N. Joshi, Prog. Theor. Phys. 120 (2008) 1193

Attractive α-α t-matrix, $t\psi = V\Phi$

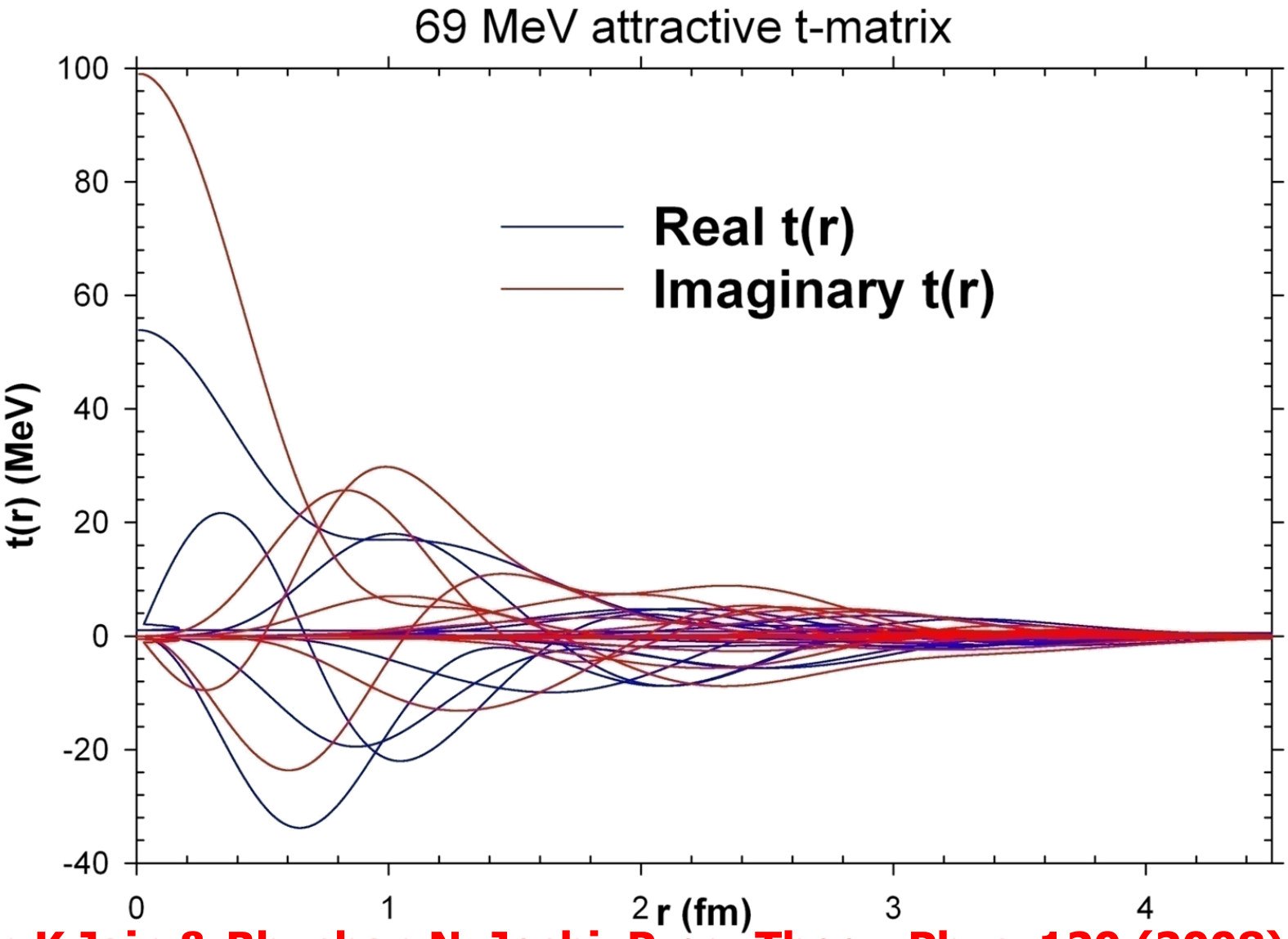

Arun K Jain & Bhushan N. Joshi, Prog. Theor. Phys. 120 (2008) 1193

dσ/dΩ from Attractive α-α potential

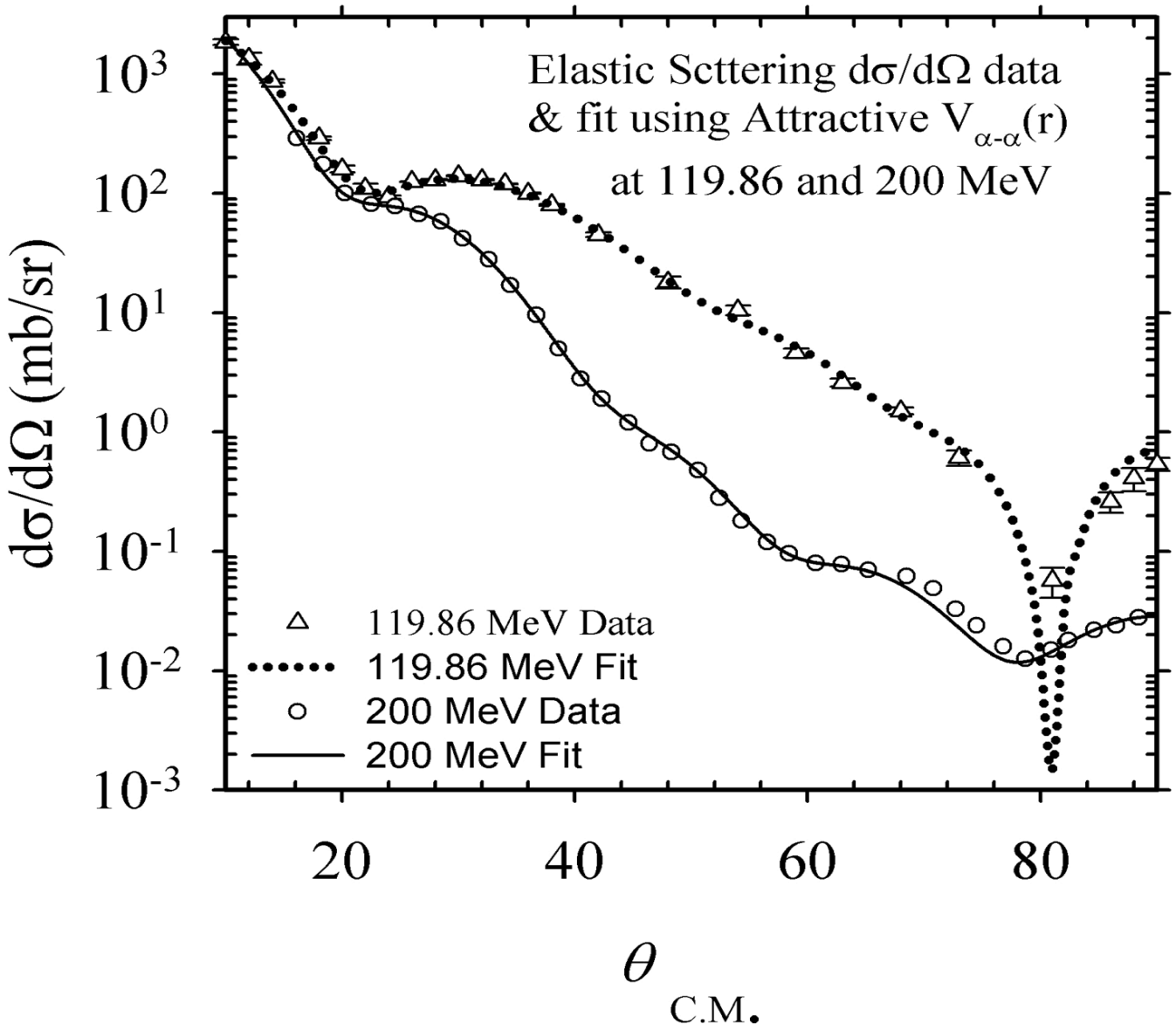

Arun K Jain & Bhushan N. Joshi, Prog. Theor. Phys. 120 (2008) 1193

dσ/dΩ from Attractive + Repulsive Core α-α Potential

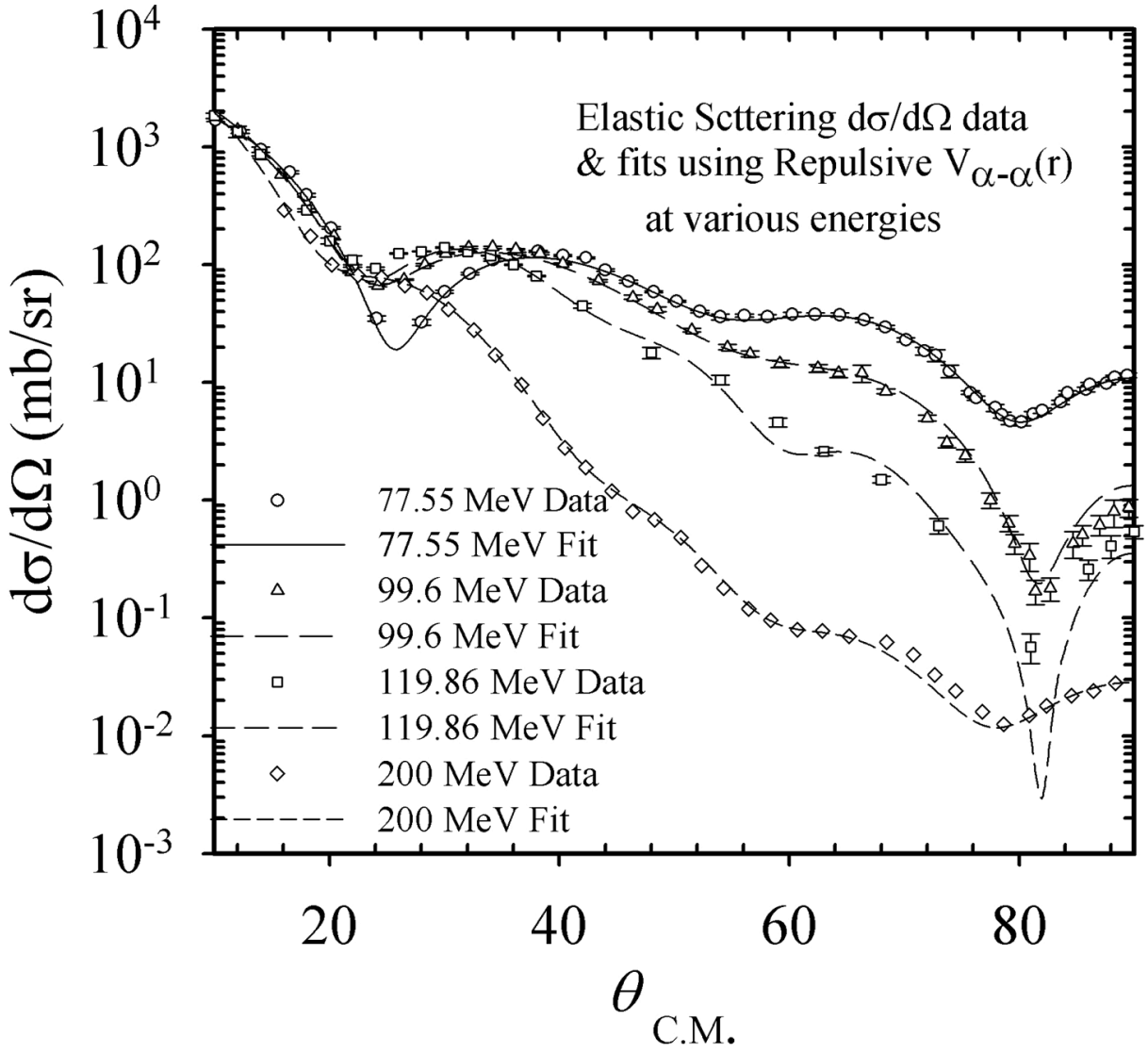

Arun K Jain & Bhushan N. Joshi, Prog. Theor. Phys. 120 (2008) 1193

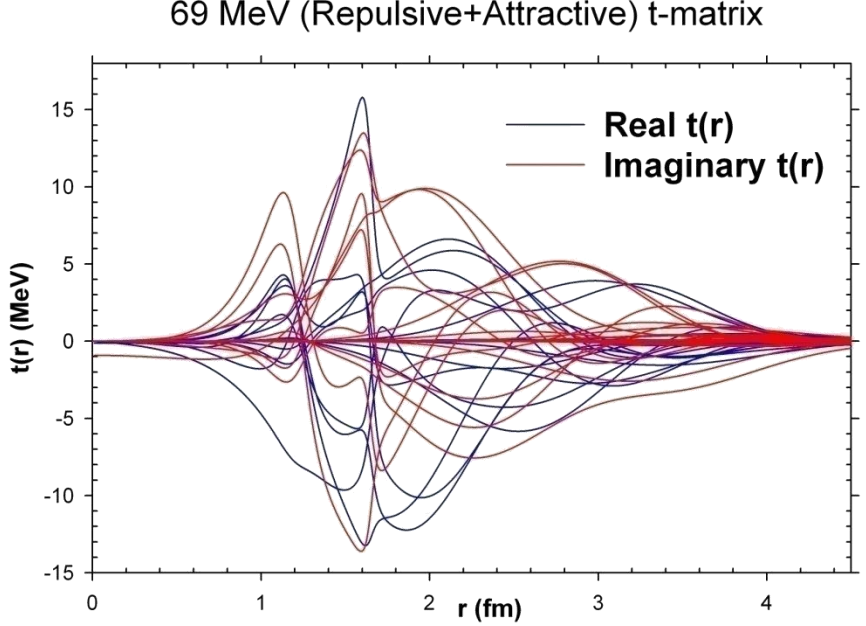
69 MeV (Repulsive+Attractive) t-matrix
Real t(r)
Imaginary t(r)
t(r) (MeV)
r (fm)

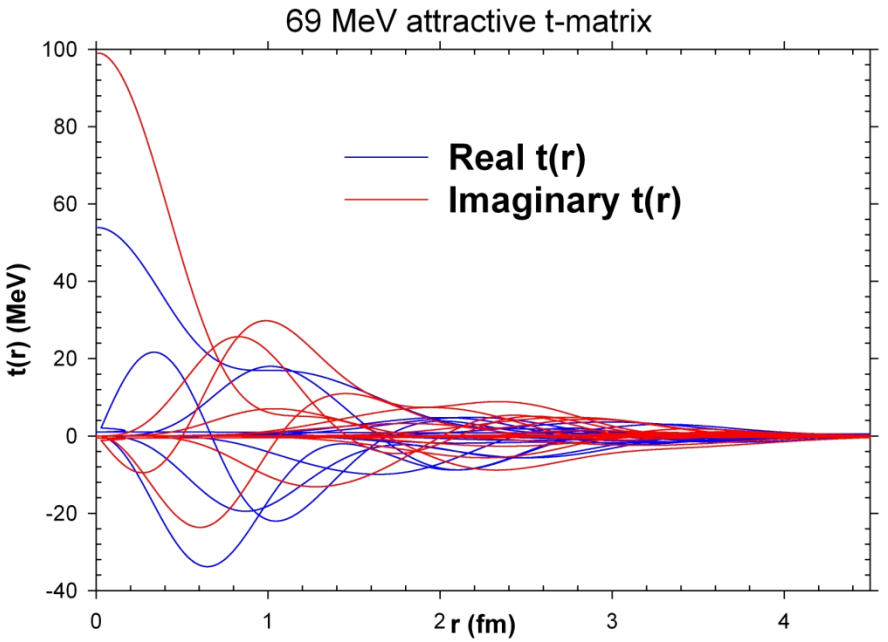
69 MeV attractive t-matrix
Real t(r)
Imaginary t(r)
t(r) (MeV)
r (fm)

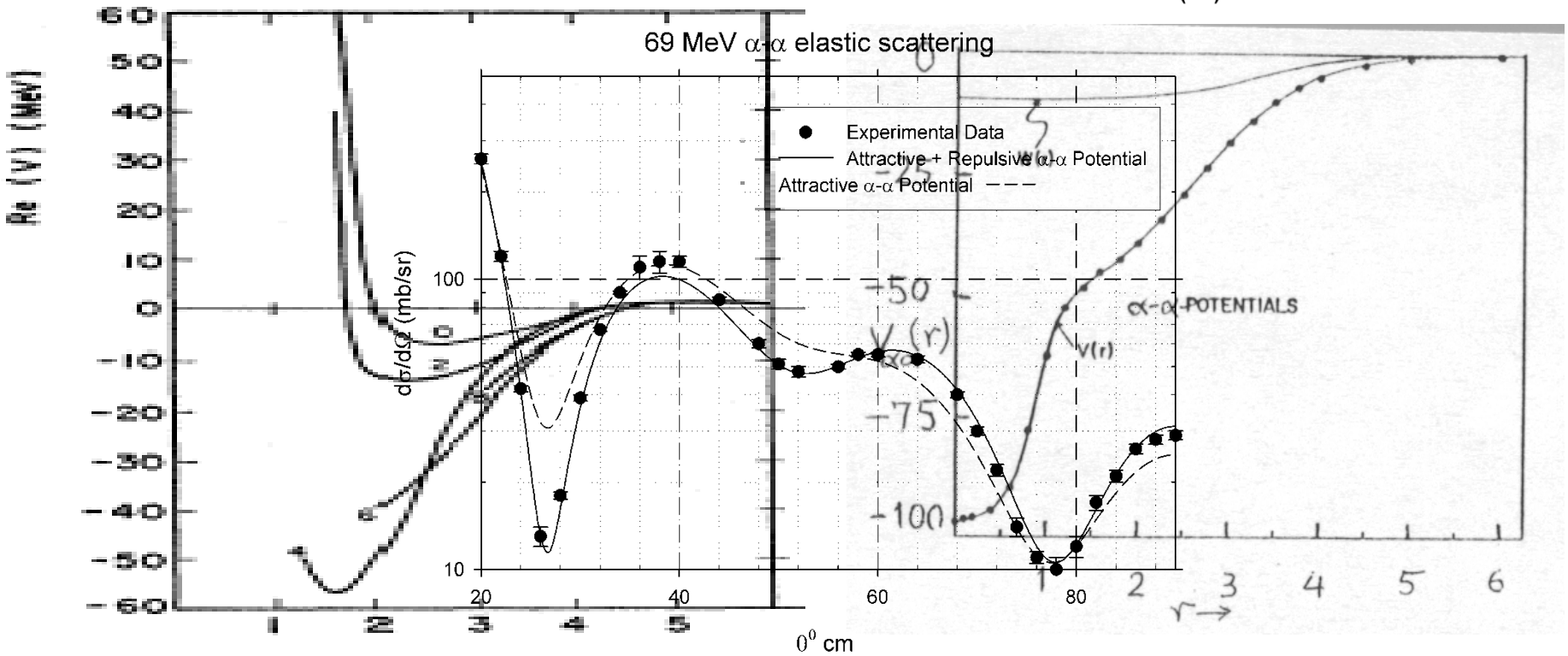
69 MeV α-α elastic scattering
Experimental Data
Attractive + Repulsive α-α Potential
Attractive α-α Potential
dσ/dΩ (mb/sr)
Re (V) (MeV)
α-α-POTENTIALS
V(r)
r →
0° cm

FR DWIA A2A CODE

$\chi_0 \longrightarrow \ell \qquad (r, \ \theta, \ \varphi, \ R, \ \Theta, \ \Phi)$

60 90, 64, 64, 22, 22, 22

$\chi_1 \longrightarrow \ell \ \ m \qquad (r, \ \theta, \ \varphi, \ R, \ \Theta, \ \Phi)$

60, 121 90, 64, 64, 22, 22, 22

$\chi_2 \longrightarrow \ell \ \ m \qquad (R, \ \Theta, \ \Phi)$

60, 121 22, 22, 22

$\Psi(\boldsymbol{R}) \longrightarrow \qquad (R, \ \Theta, \ \Phi)$

22, 22, 22

$t_\ell(r) \longrightarrow \ell \qquad (r, \ \theta, \ \varphi)$

60 90, 64, 64

$D_{\ell m}(\beta) \longrightarrow \ell \ \ m$

60, 121

$64*64*90*22*22*22 = 3.9*10^9$ Multiplications

$60*60*121*60*121*60*60*121 = 1.38*10^{15}$ Sums

(α, 2α) results

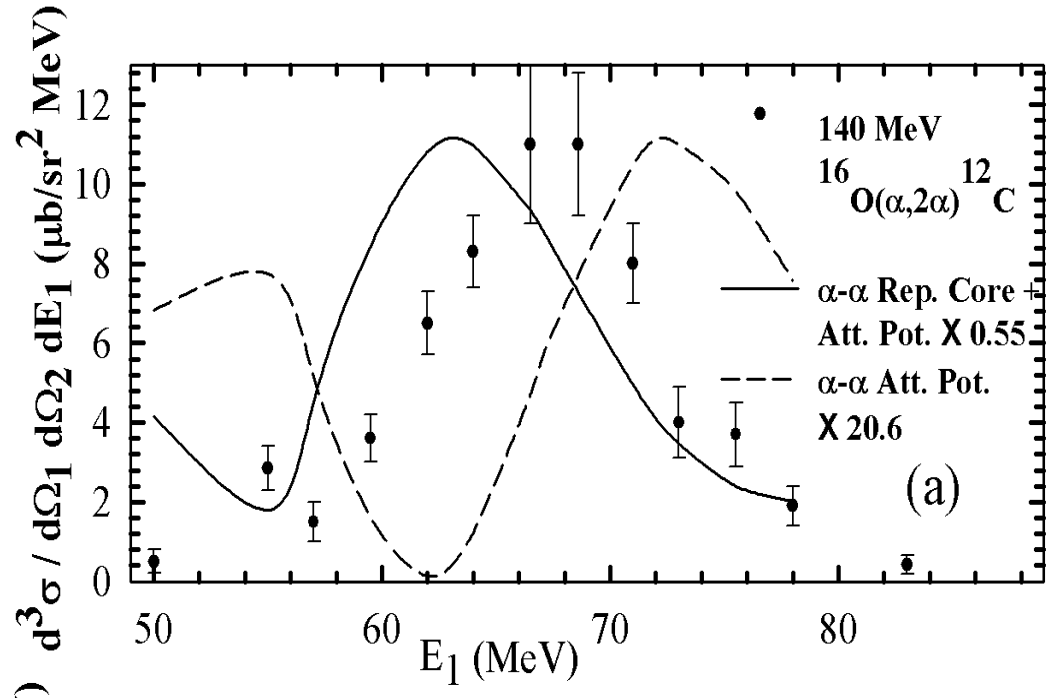

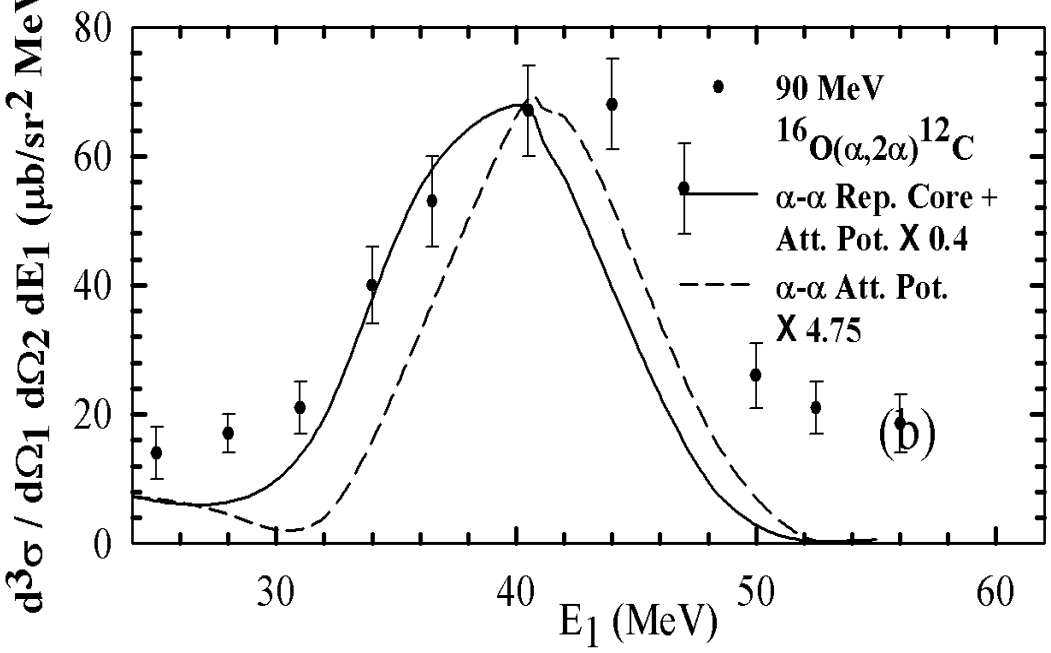

Arun Jain & Bhushan Joshi

P R L, 103 (2009)132503

140 MeV $^{16}O(\alpha, 2\alpha)^{12}C$ Repulsive α-α potential explains the spectroscopic factor

90 MeV $^{16}O(\alpha, 2\alpha)^{12}C$ Repulsive α-α potential explains the spectroscopic factor

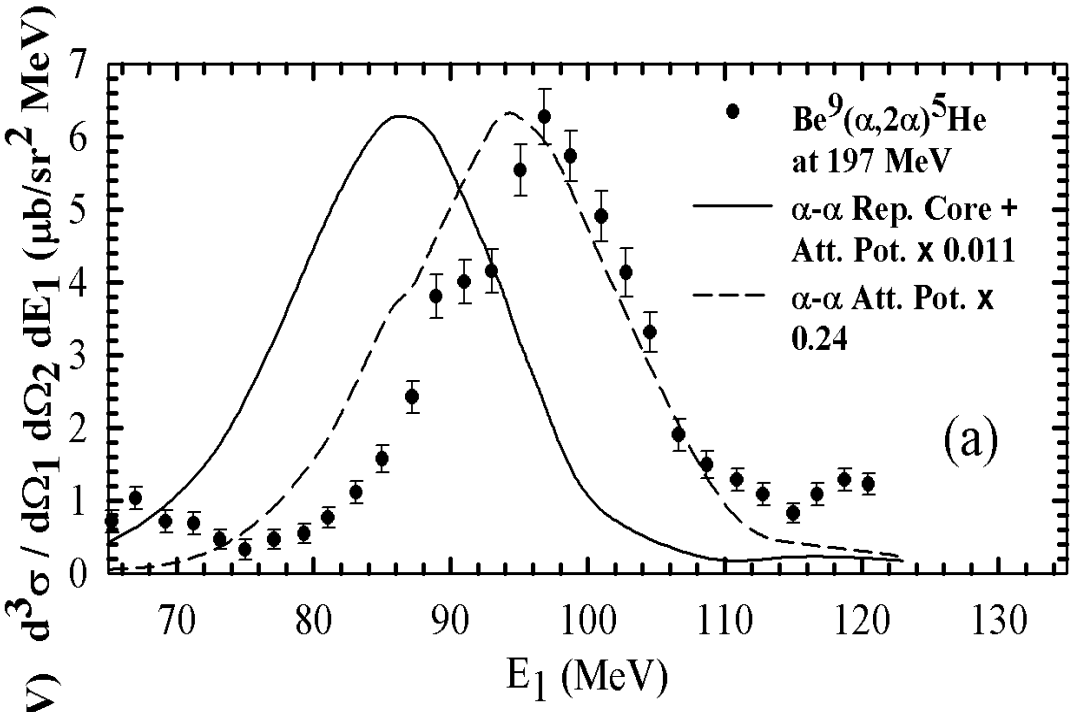

Arun Jain & Bhushan Joshi

P R L, 103 (2009)132503

197 MeV ^{9}Be(α, 2α)^{5}He
Attractive α-α potential
explains the spectroscopic factor

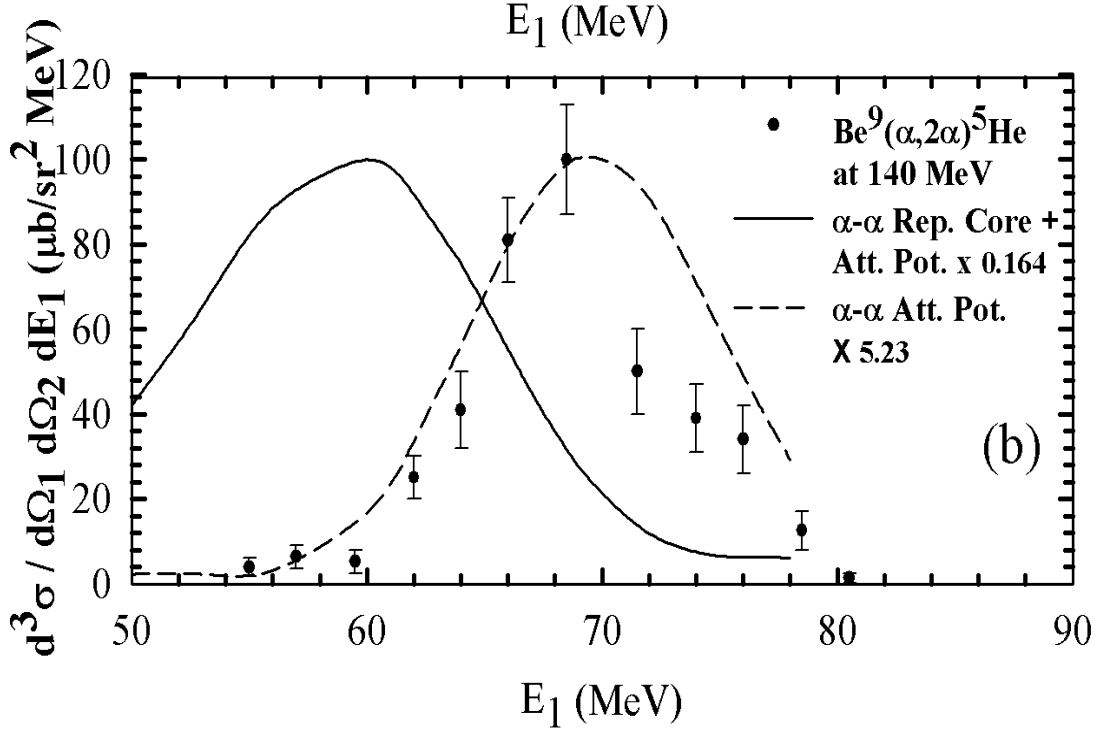

90 MeV ^{9}Be(α, 2α)^{5}He
Repulsive α-α potential
explains the spectroscopic factor

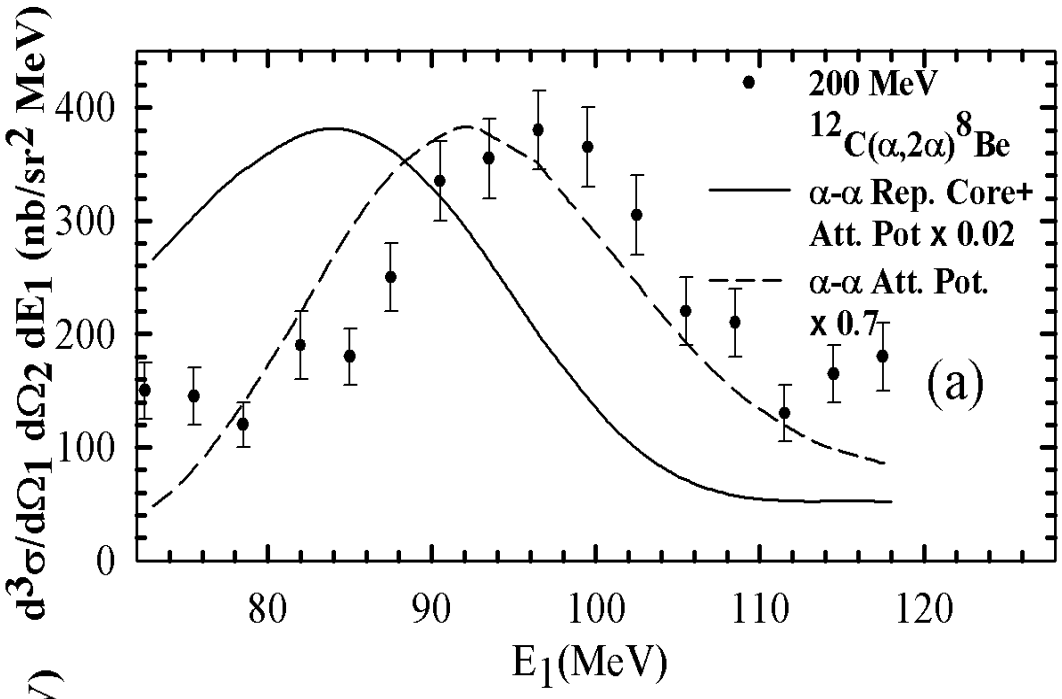

Arun Jain & Bhushan Joshi

P R L, 103 (2009)132503

200 MeV $^{12}C(\alpha, 2\alpha)^{8}Be$ Attractive α-α potential explains the spectroscopic factor

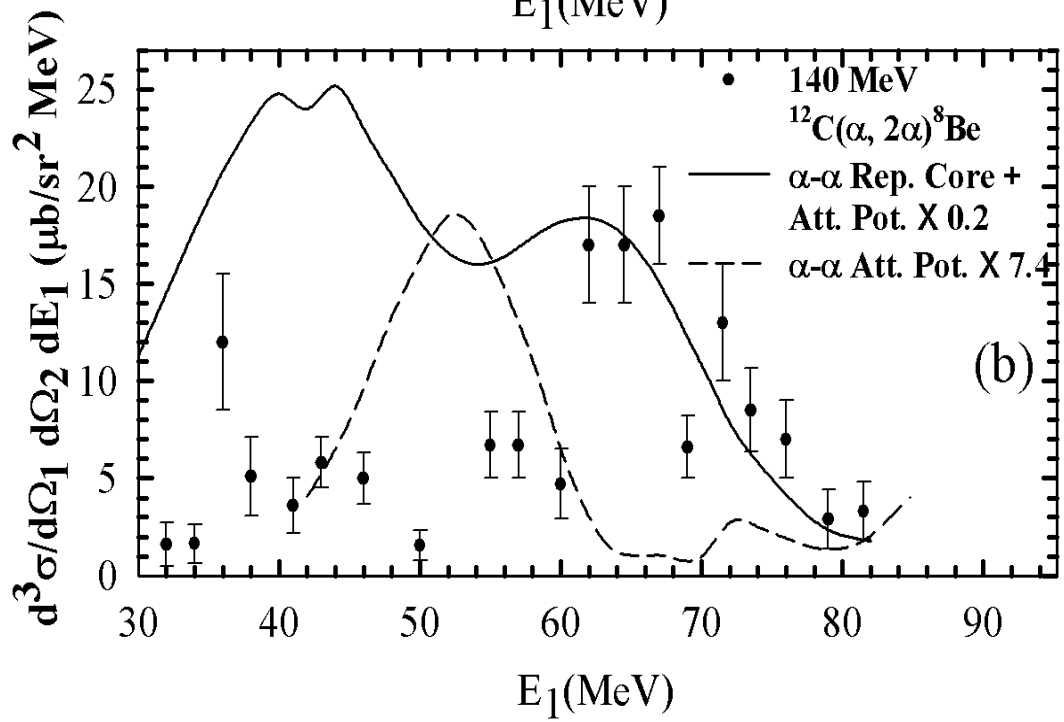

140 MeV $^{12}C(\alpha, 2\alpha)^{8}Be$ Repulsive α-α potential explains the spectroscopic factor

Comparison of (α, 2α) Spectroscopic factors from FR-DWIA calculations on ^{9}Be, ^{12}C, ^{16}O nuclei at various energies

Reaction	Eα (*MeV*)	Sα		
		(R+A)	(A)	Theory
^{9}Be(α,2α)^{5}He	197	0.011	0.24	0.57
	140	0.164	5.23	
^{12}C(α,2α)^{8}Be	200	0.02	0.7	0.55, 0.29
	140	0.2	7.4	
^{16}O(α,2α)^{12}C	140	0.55	20.6	0.23, 0.3
	90	0.4	4.75	

Arun Jain & Bhushan Joshi, P R L, 103 (2009) 132503

Understanding:-

In the shell model picture the two α's can not physically overlap unless their nucleonic wave functions satisfy Pauli Principle.

Which means that their shell model single particle orbitals are to be occupied by the second set of 2-neutrons and 2-protons with their single particle 1s -1p energy gap. Which can be seen in the excitation of α -particle at ~20 MeV.

4-particles of the other alpha to be promoted to this level require an excitation of ~80 MeV.

In the α - α lab system it will be ~160 MeV.

Thus the two α's repel each other below this lab energy.

- ***Thus we have achieved an explanation of most of the puzzling features of the Direct Nuclear Reactions.***

Explanation of α-α potential in RGM - Shell Model picture

α-α Repulsive Core + Attractive Potential

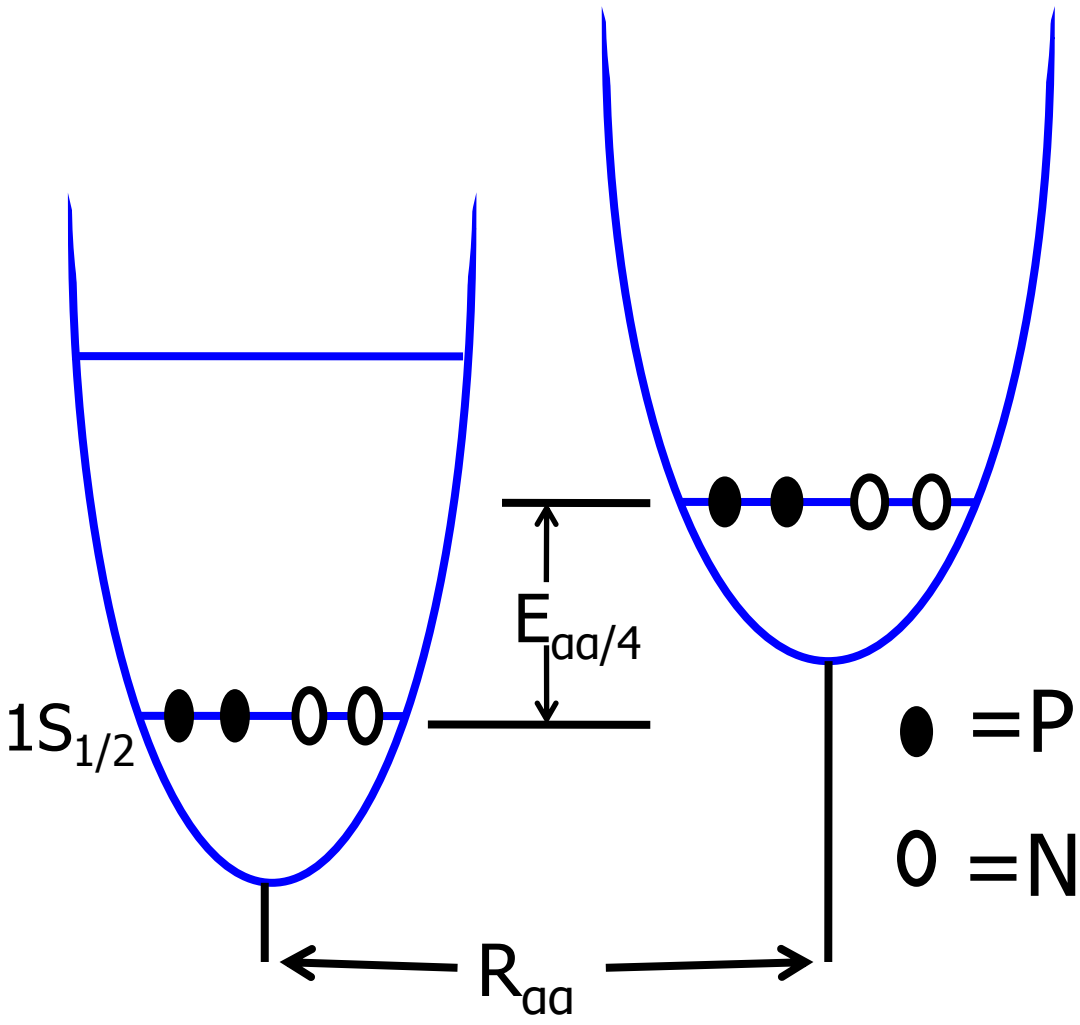

α-α Attractive Potential

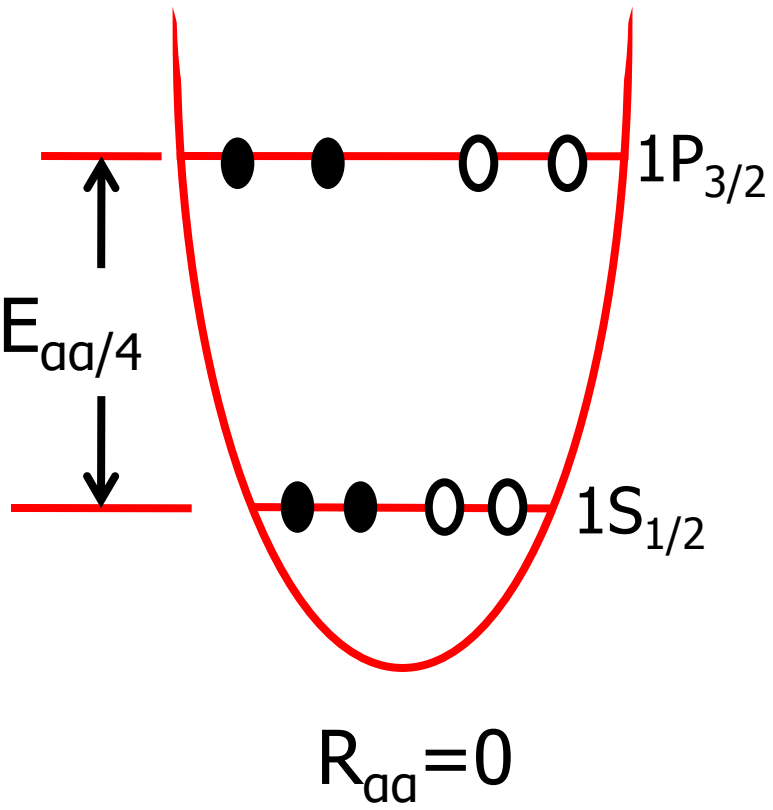

● =Proton

0 =Neuron

Heavy Cluster Knockout

$(\alpha, 2\alpha)$

$(C, 2C)$

Comparison of

$^{16}O\ (\alpha,2\alpha)\ ^{12}C$ and $^{16}O\ (^{12}C,\ 2^{12}C)\ ^{4}He$

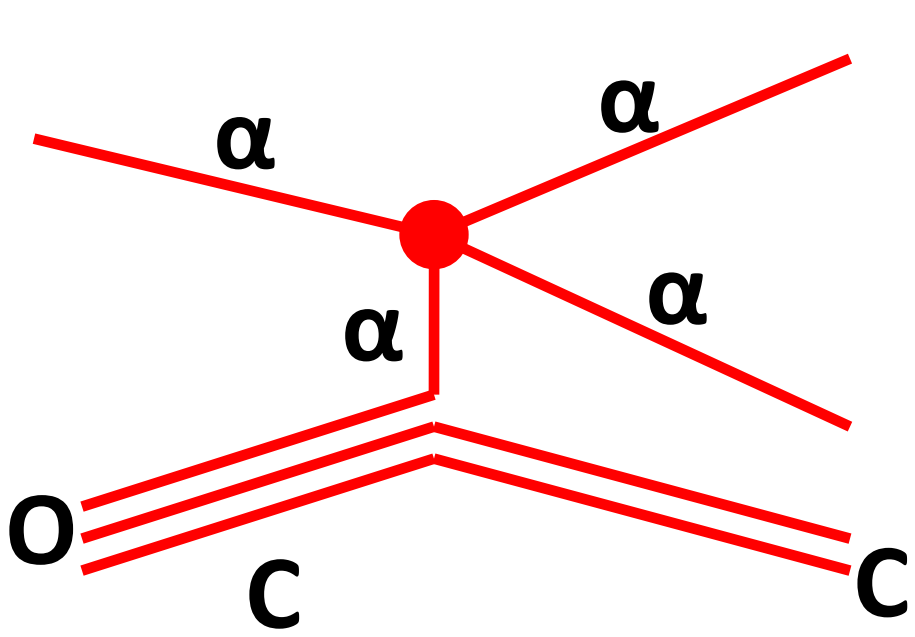

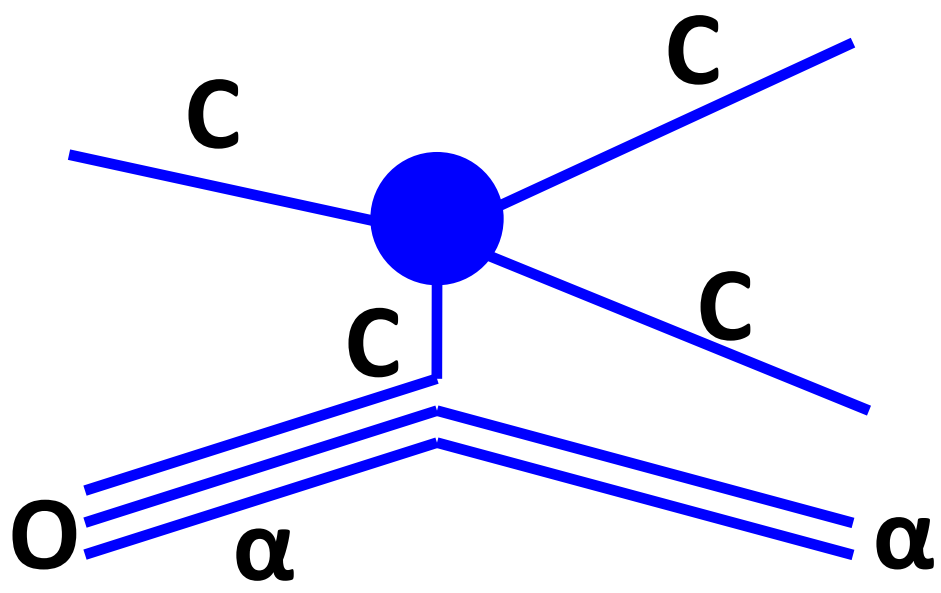

$^{16}O(C,2C)\alpha$ was performed at Mumbai LINAC-Pelletron at E_C=119 MeV

Summed energy spectrum for the $^{16}O(^{12}C, 2^{12}C)^{4}He$ Reaction

Bhushan Joshi *et al*, P R L 106 (2011) 022501

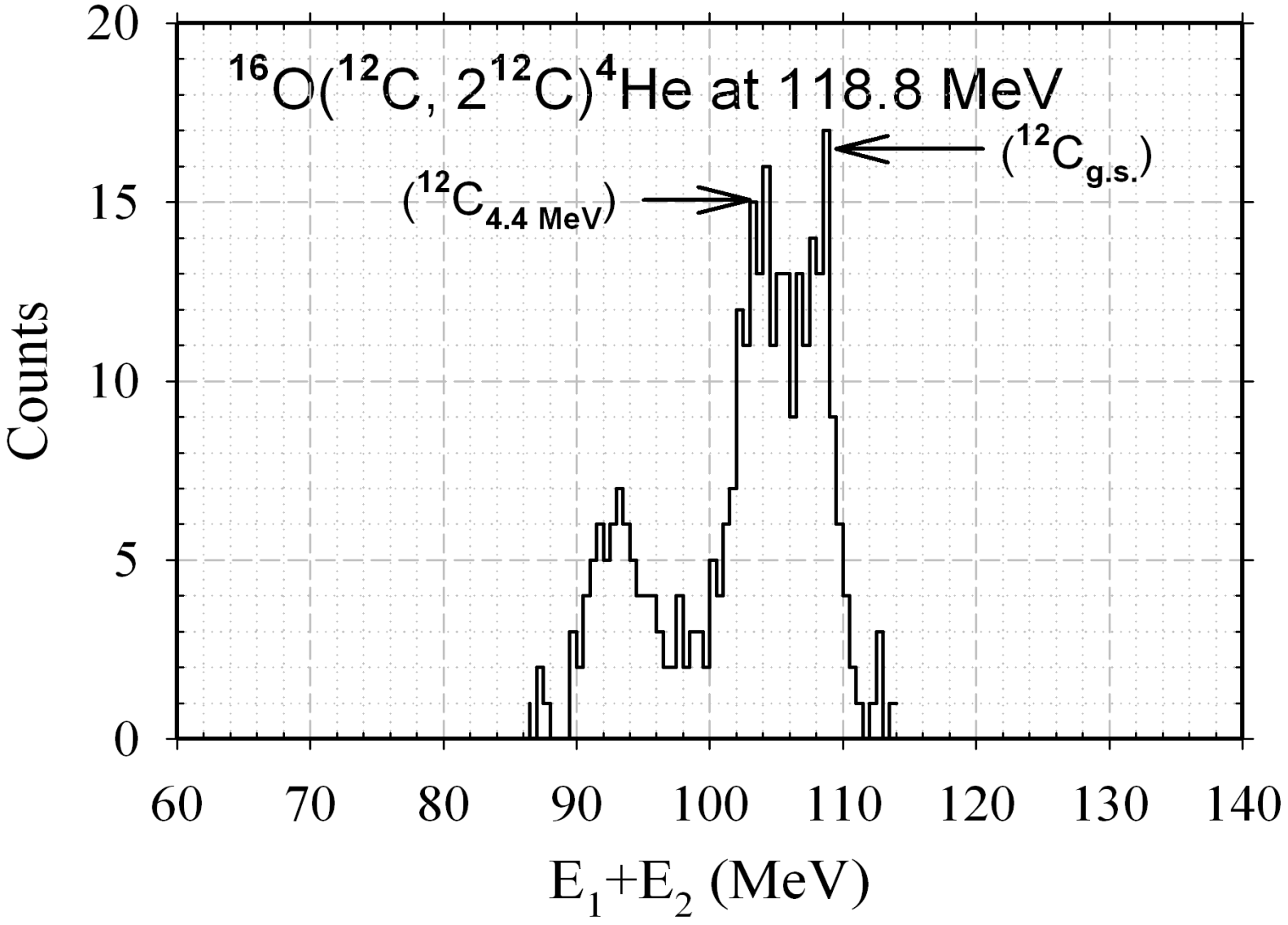

Comparison of Theory and Experiment: energy sharing distribution for 119 MeV $^{16}O(C, 2C)^{4}He$ Reaction:-

ZR-DWIA

FR-DWIA

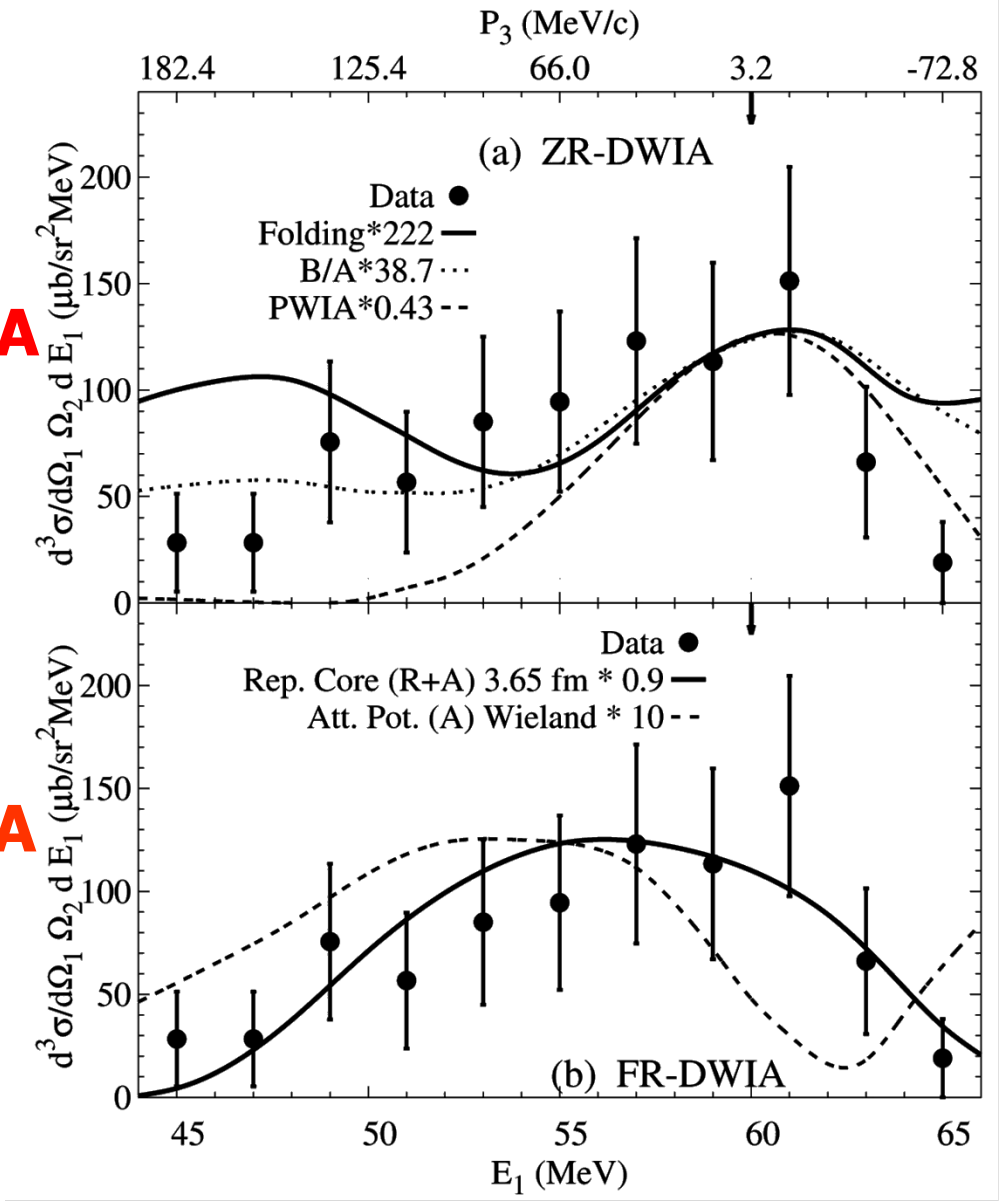

Bhushan Joshi,

Arun Jain, Y. K. Gupta,

D. C. Biswas, A. Saxena

B. V. John, L. S. Danu,

R. P. Vind and

R. K. Choudhury

P R L 106 (2011) 022501

Comparison of the (α, 2α) and (C, 2C) reactions on ^{16}O

Proje-ctile Energy (MeV)	Reaction	Exptl. X-Section μb/sr^2 MeV	ZR-DWIA X-Section μb/sr^2 MeV	S_α ZR-DWIA	FR-DWIA X-Section μb/sr^2 MeV		S_α FR-DWIA		Theory
					A	R+A	A	R+A	
140	^{16}O(α,2α)^{12}C	10.5	0.96	11	0.51	19.1	20.6	0.55	0.23
119	^{16}O(C,2C)α	125±50	0.56	222	12.5	138	10	0.9	0.23

Comparison of S_α (ZR-DWIA) indicates an enhancement of

20 times more in (C, 2C) case as compared to (α, 2α) case

A comparison of S_α (ZR-DWIA) with theory indicates an enhancement of **965** times in the (C, 2C) case

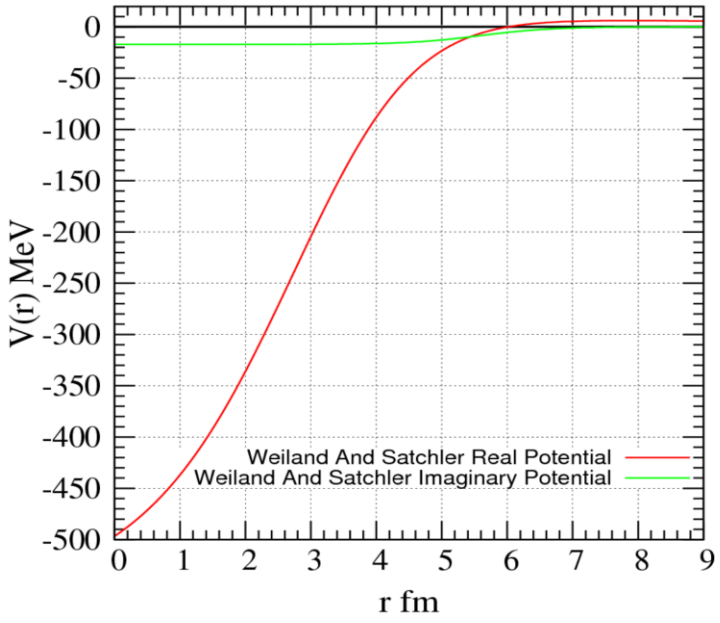
V(r) MeV
r fm
Weiland And Satchler Real Potential
Weiland And Satchler Imaginary Potential

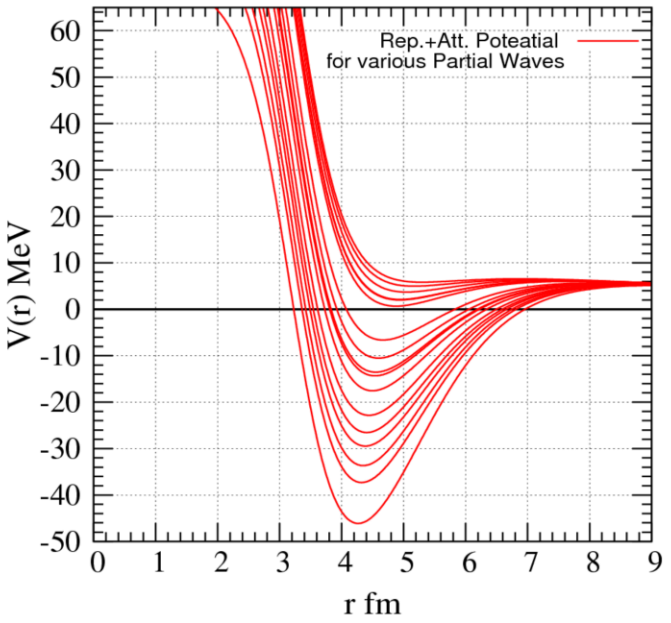
V(r) MeV
r fm
Rep.+Att. Poteatial
for various Partial Waves

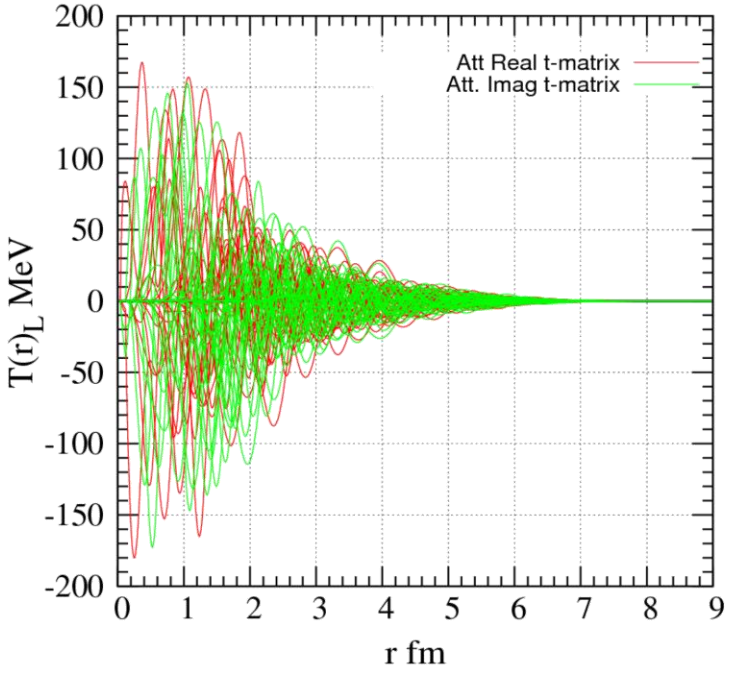
T(r)L MeV
r fm
Att Real t-matrix
Att. Imag t-matrix

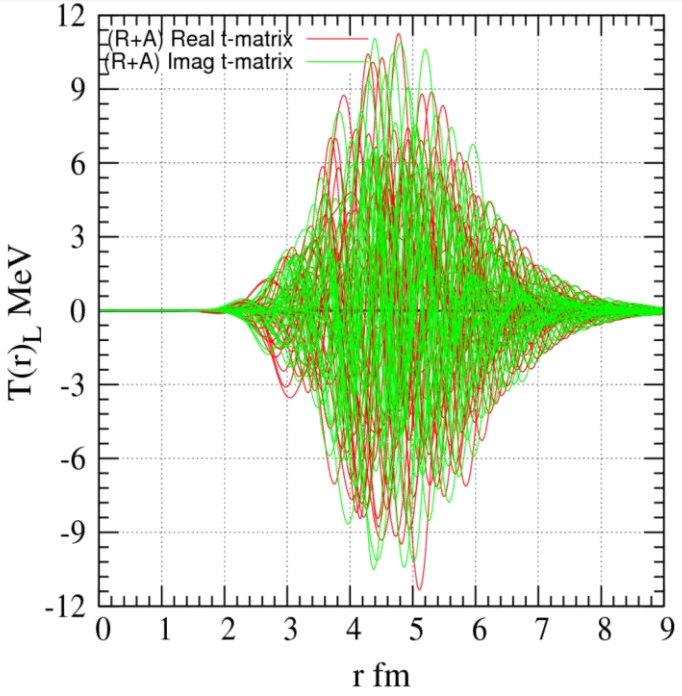
T(r)L MeV
r fm
(R+A) Real t-matrix
(R+A) Imag t-matrix

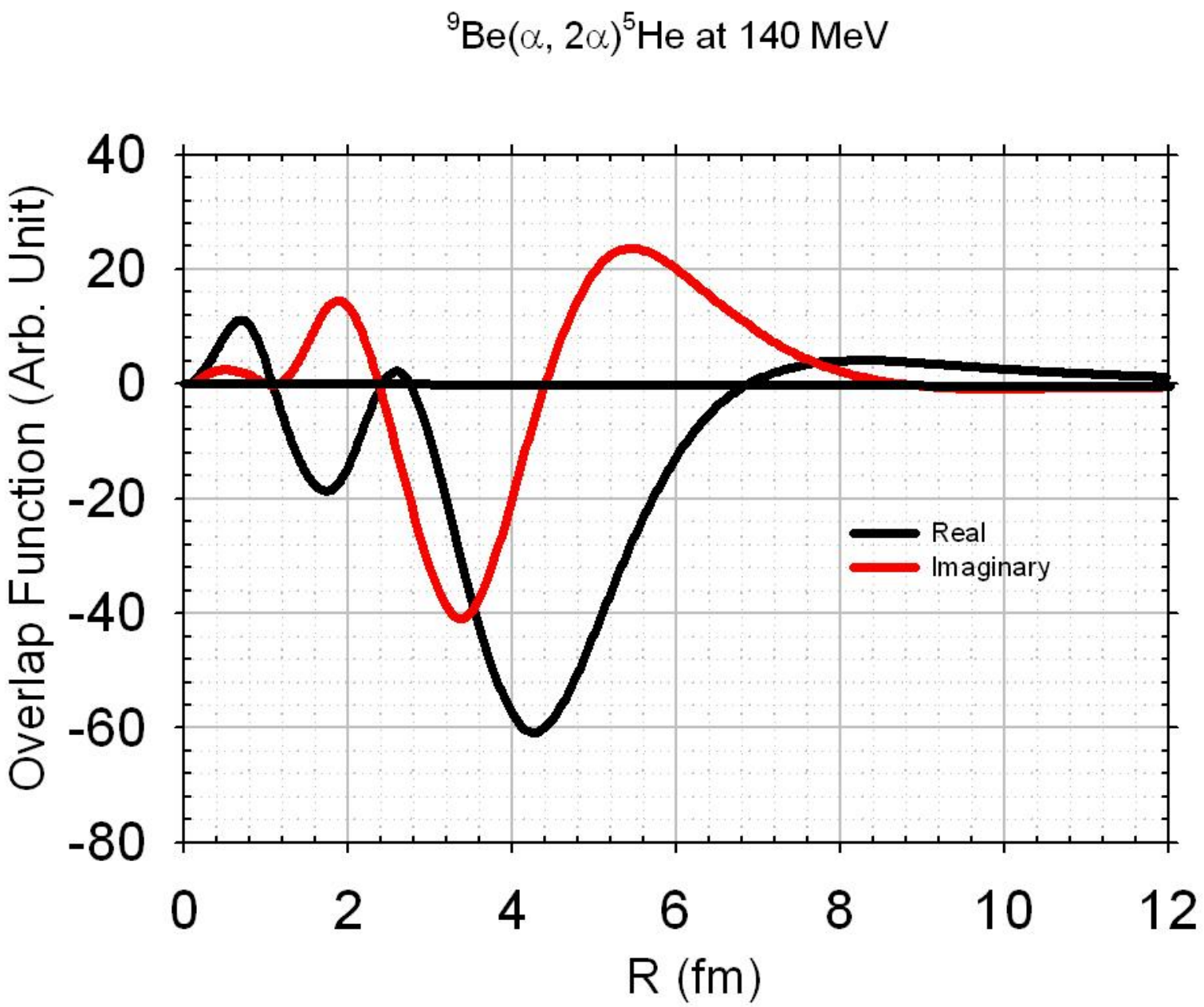
^{9}Be(α, 2α)^{5}He at 140 MeV
Overlap Function (Arb. Unit)
40
20
0
-20
-40
-60
-80
0
2
4
6
8
10
12
R (fm)
Real
Imaginary

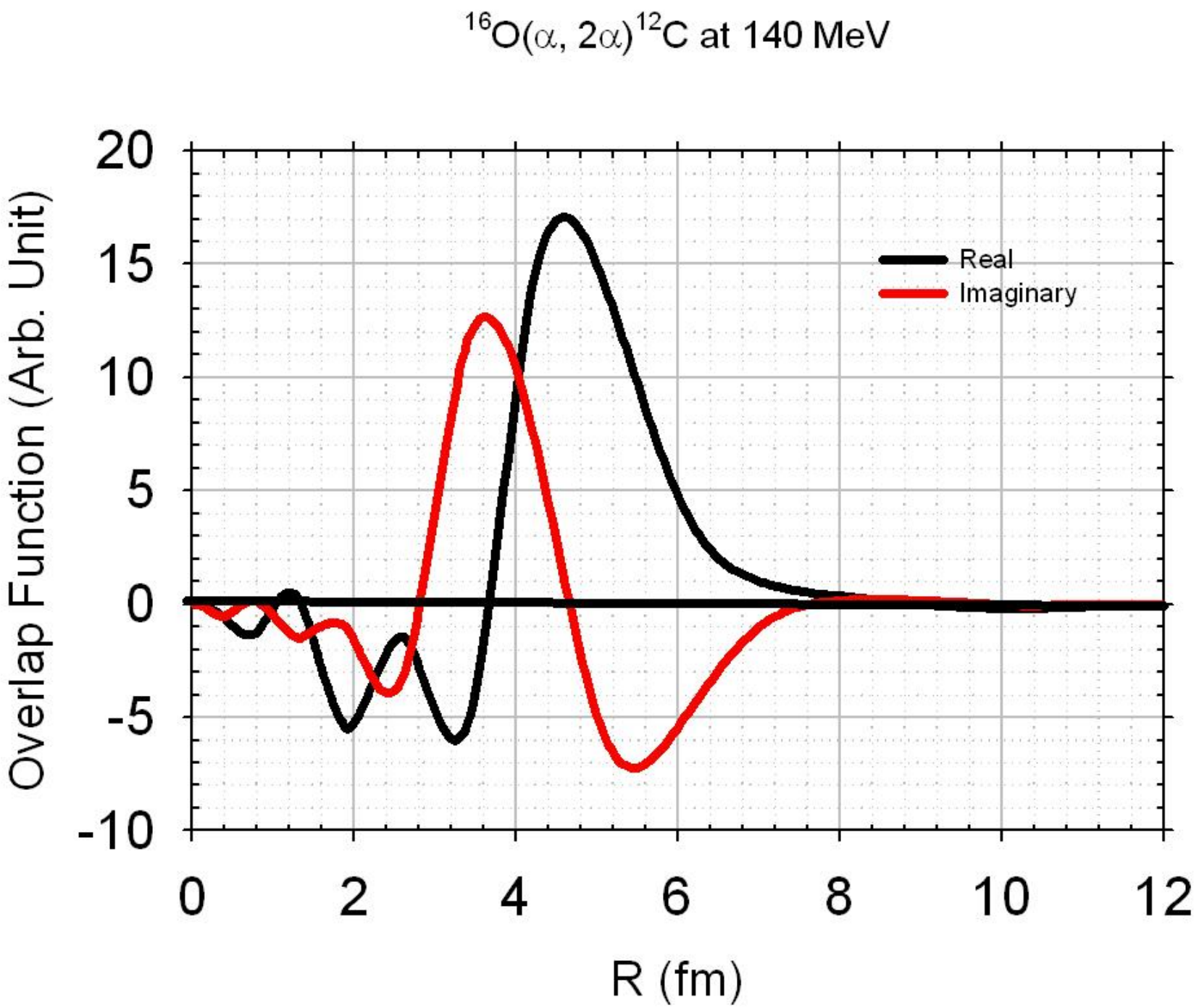
$^{16}O(\alpha, 2\alpha)^{12}C$ at 140 MeV
Overlap Function (Arb. Unit)
R (fm)
Real
Imaginary
20
15
10
5
0
-5
-10
0
2
4
6
8
10
12

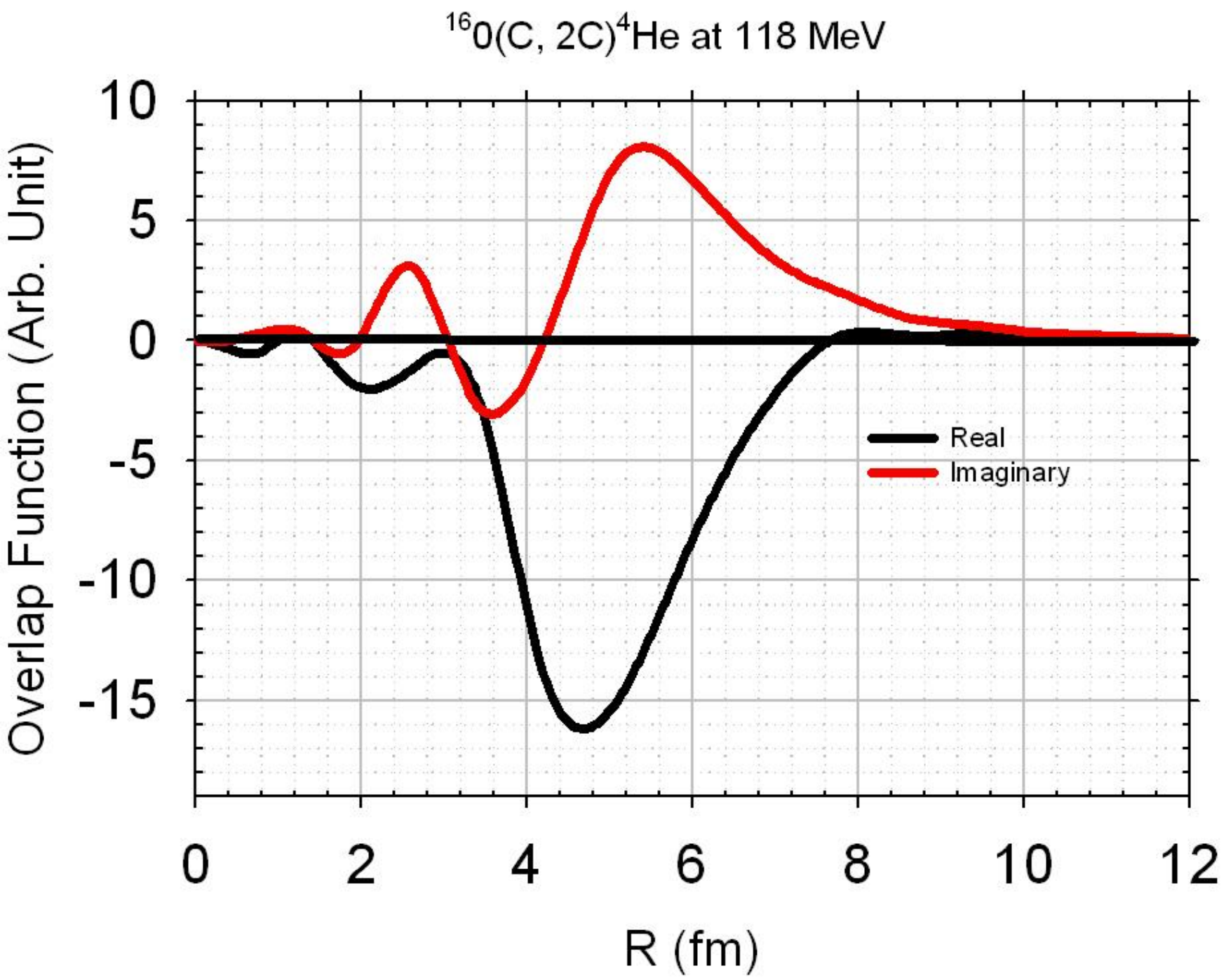
^{16}0(C, 2C)^{4}He at 118 MeV
Overlap Function (Arb. Unit)
10
5
0
-5
-10
-15
0
2
4
6
8
10
12
R (fm)
Real
Imaginary

$$T_{fi}^{\alpha L\Lambda}(\vec{k}_f,\vec{k}_i)=\int g(r)dr$$

$$=\int \chi_1^{(-)*}(\vec{k}_{aB},\vec{r}_{aB})\chi_2^{(-)*}(\vec{k}_{2B},\vec{R}_{2B})t_{12}(\vec{r}_{12})\chi_0^{(+)}(\vec{k}_{1A},\vec{r}_{1A})\varphi_{L\Lambda}(\vec{R}_{2B})d\vec{r}_{12}d\vec{R}_{2B}$$

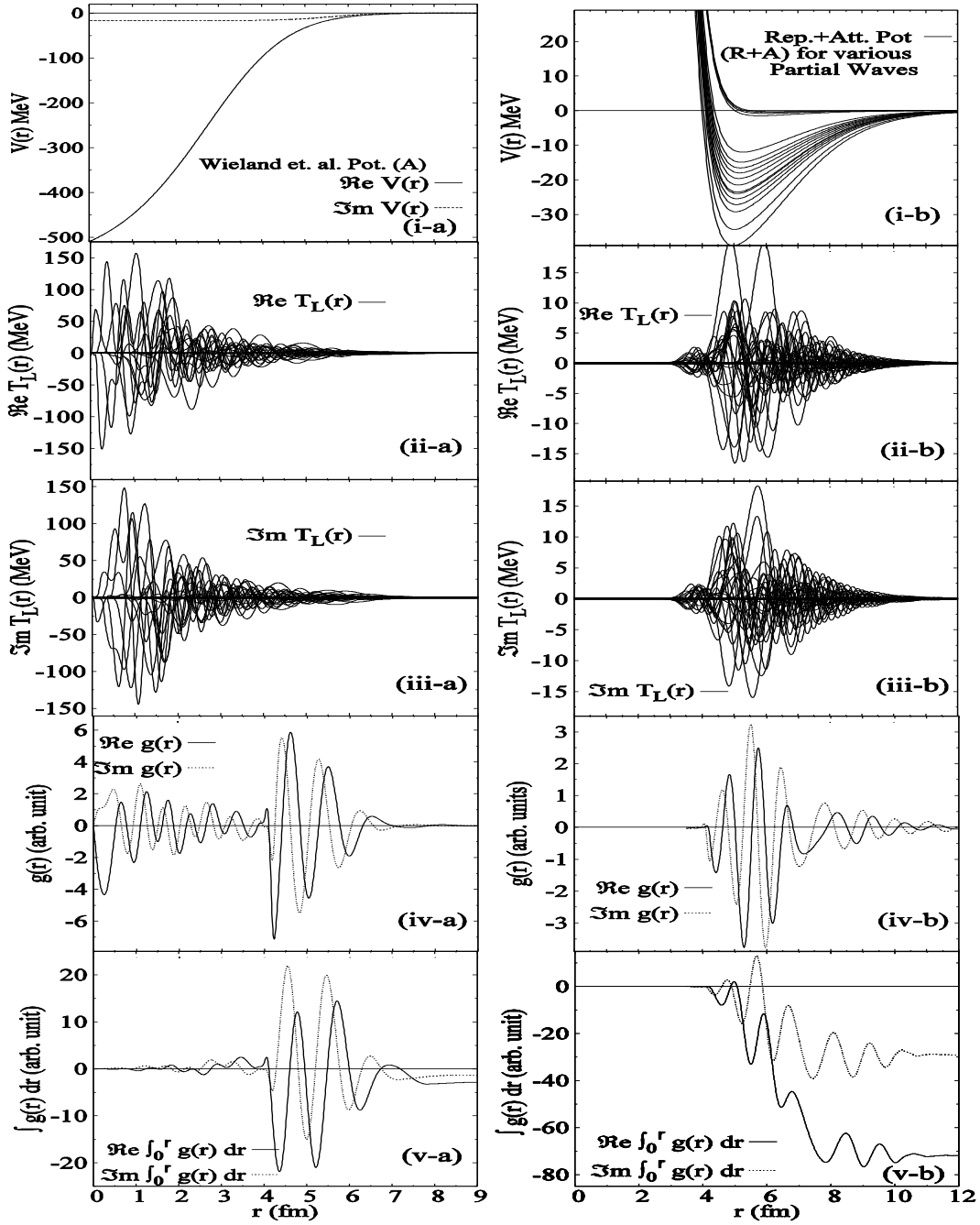
Wieland et. al. Pot. (A)
Re V(r)
Im V(r)
(i-a)
V(r) MeV
Rep.+Att. Pot
(R+A) for various
Partial Waves
(i-b)
Re T_L(r)
(ii-a)
Re T_L(r) (MeV)
(ii-b)
Im T_L(r)
(iii-a)
Im T_L(r) (MeV)
(iii-b)
Re g(r)
Im g(r)
(iv-a)
g(r) (arb. unit)
g(r) (arb. units)
(iv-b)
Re ∫0r g(r) dr
Im ∫0r g(r) dr
(v-a)
∫ g(r) dr (arb. unit)
(v-b)
r (fm)

Summed Energy Spectrum of $^{24}Mg(^{12}C, 2^{12}C)^{12}C$ at 104 MeV. Q=13.9 MeV at coplanar symmetric angle of 40.5^0

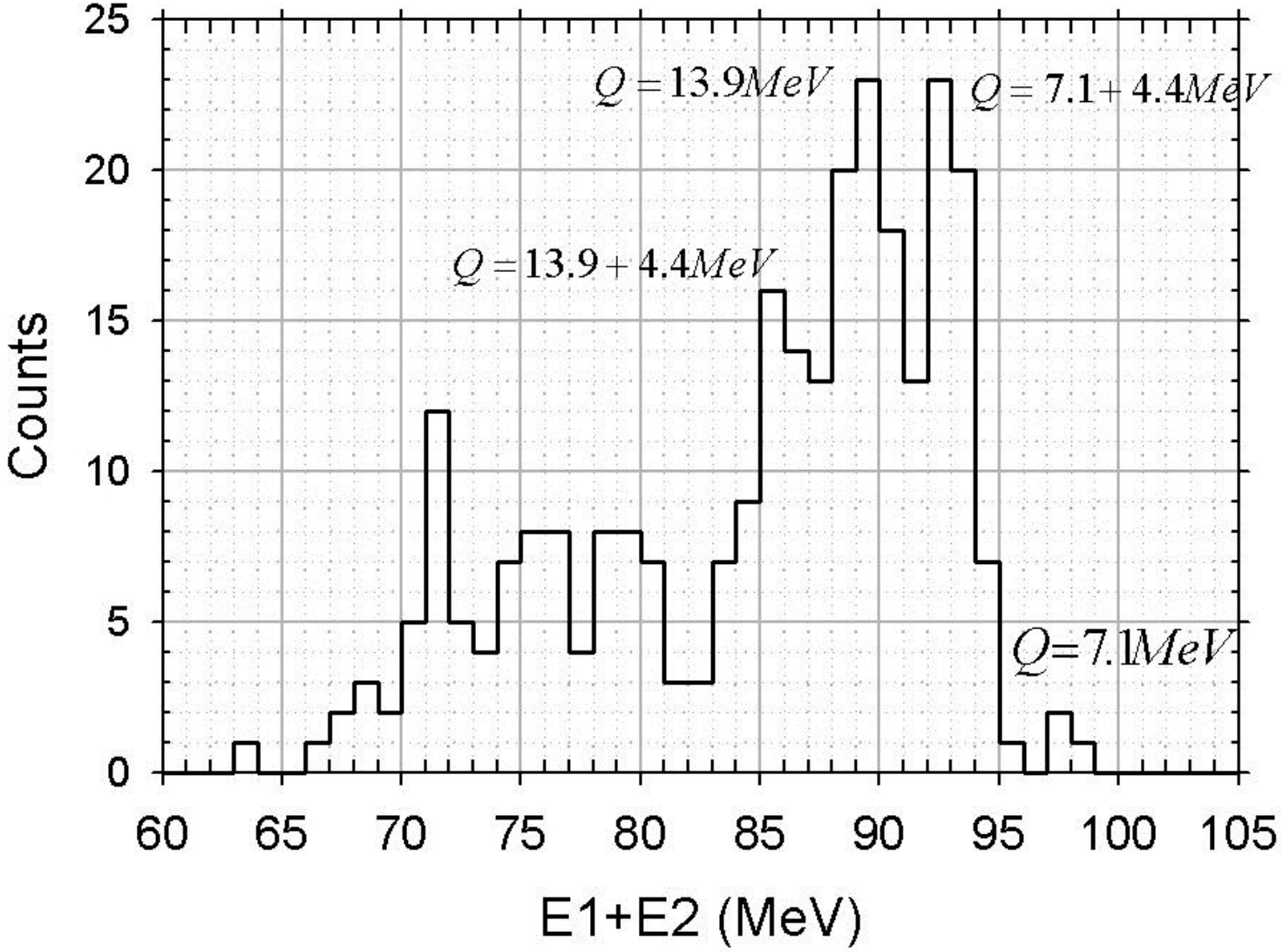

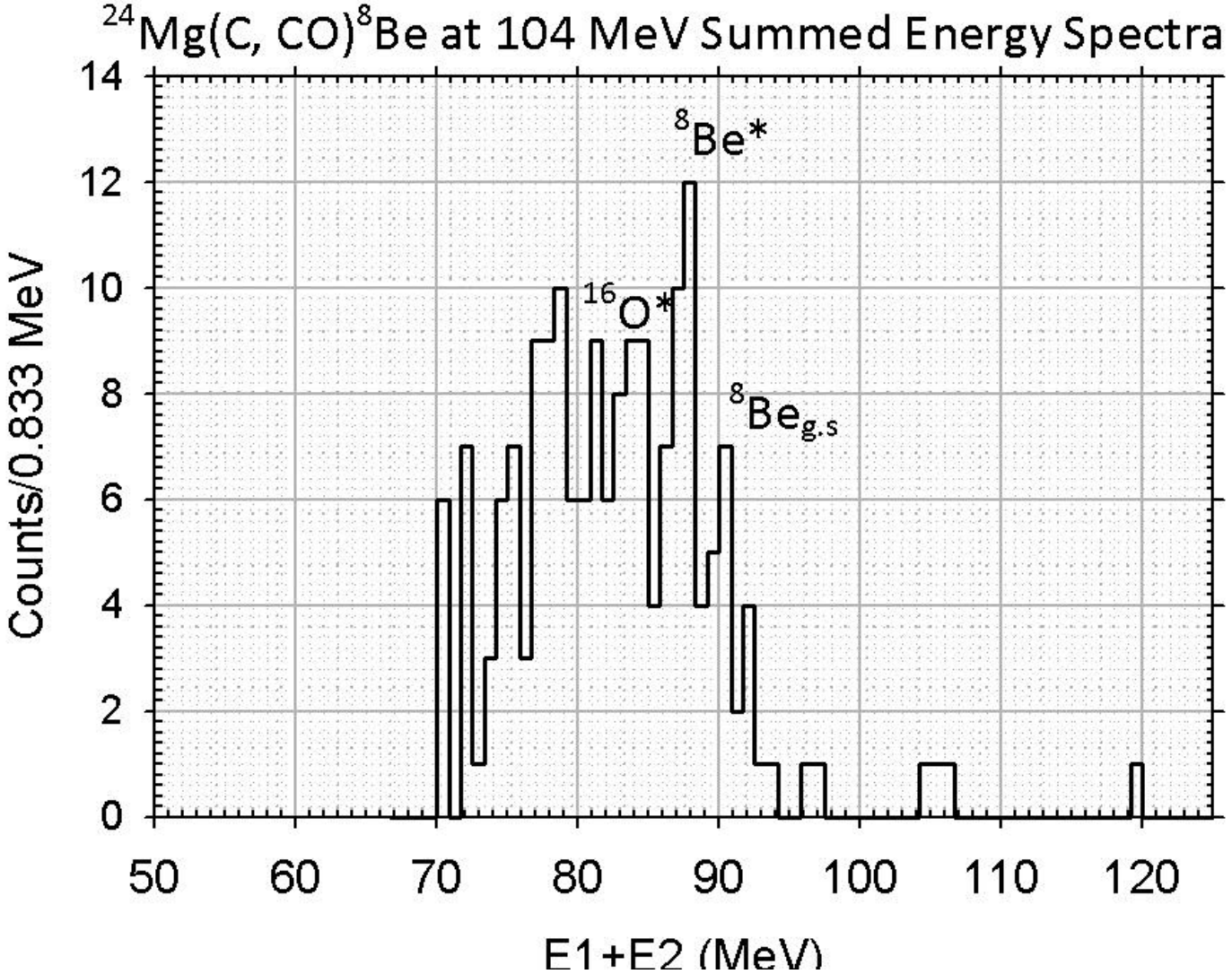
^{24}Mg(C, CO)^{8}Be at 104 MeV Summed Energy Spectra
Counts/0.833 MeV
E1+E2 (MeV)
^{8}Be*
^{16}O*
^{8}Be$_{g.s}$
0
2
4
6
8
10
12
14
50
60
70
80
90
100
110
120

Energy sharing spectra of $^{24}Mg(^{12}C, 2^{12}C)^{12}C$ at 104 MeV with Q=13.9 MeV at coplanar symmetric angle of 40.5^0

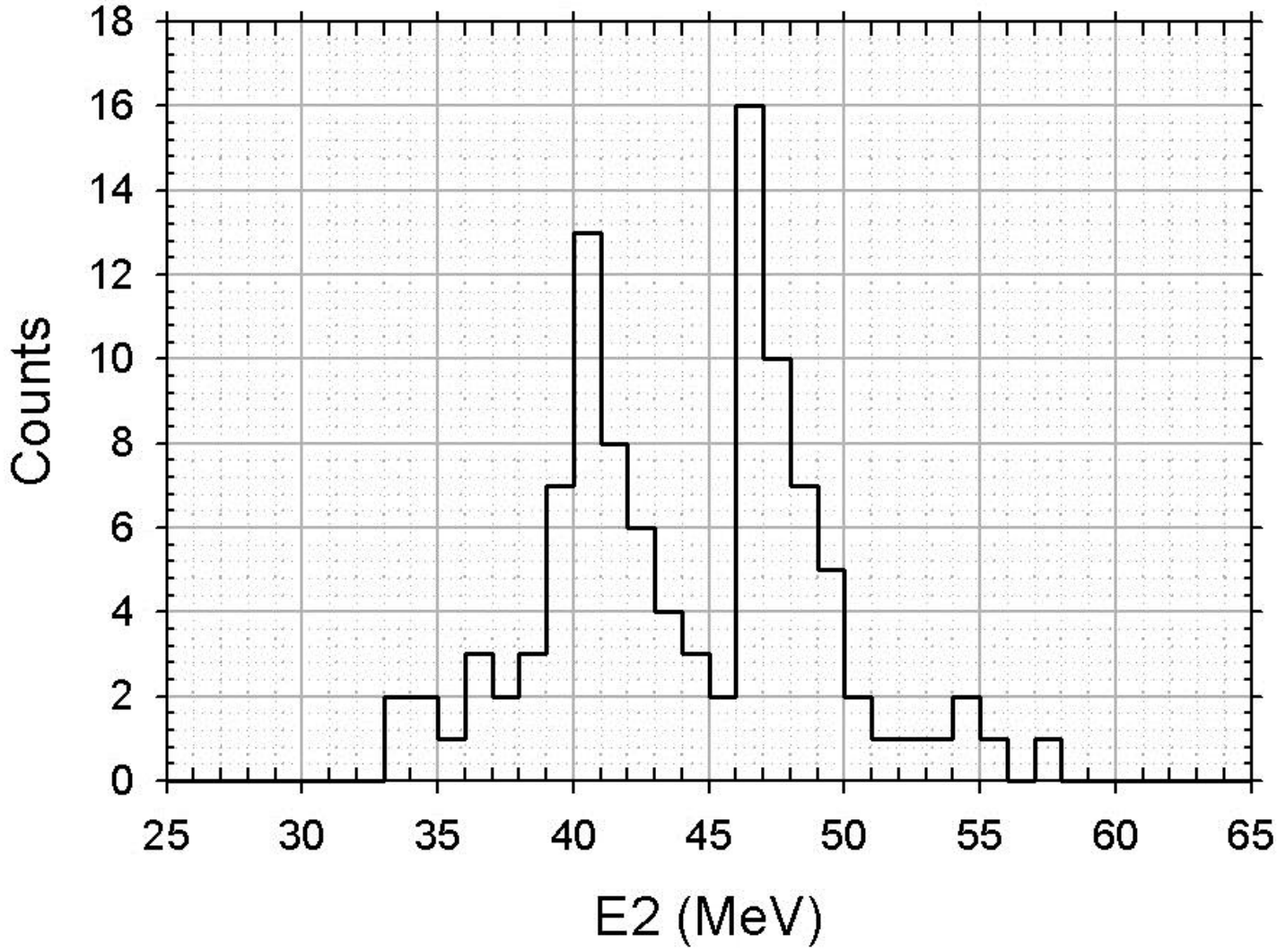

Summed Energy Spectrum of $^{24}Mg(^{12}C, 2^{12}C)^{12}C$ at 104 MeV.
Q=13.9 MeV at coplanar symmetric angle of 36.7^0

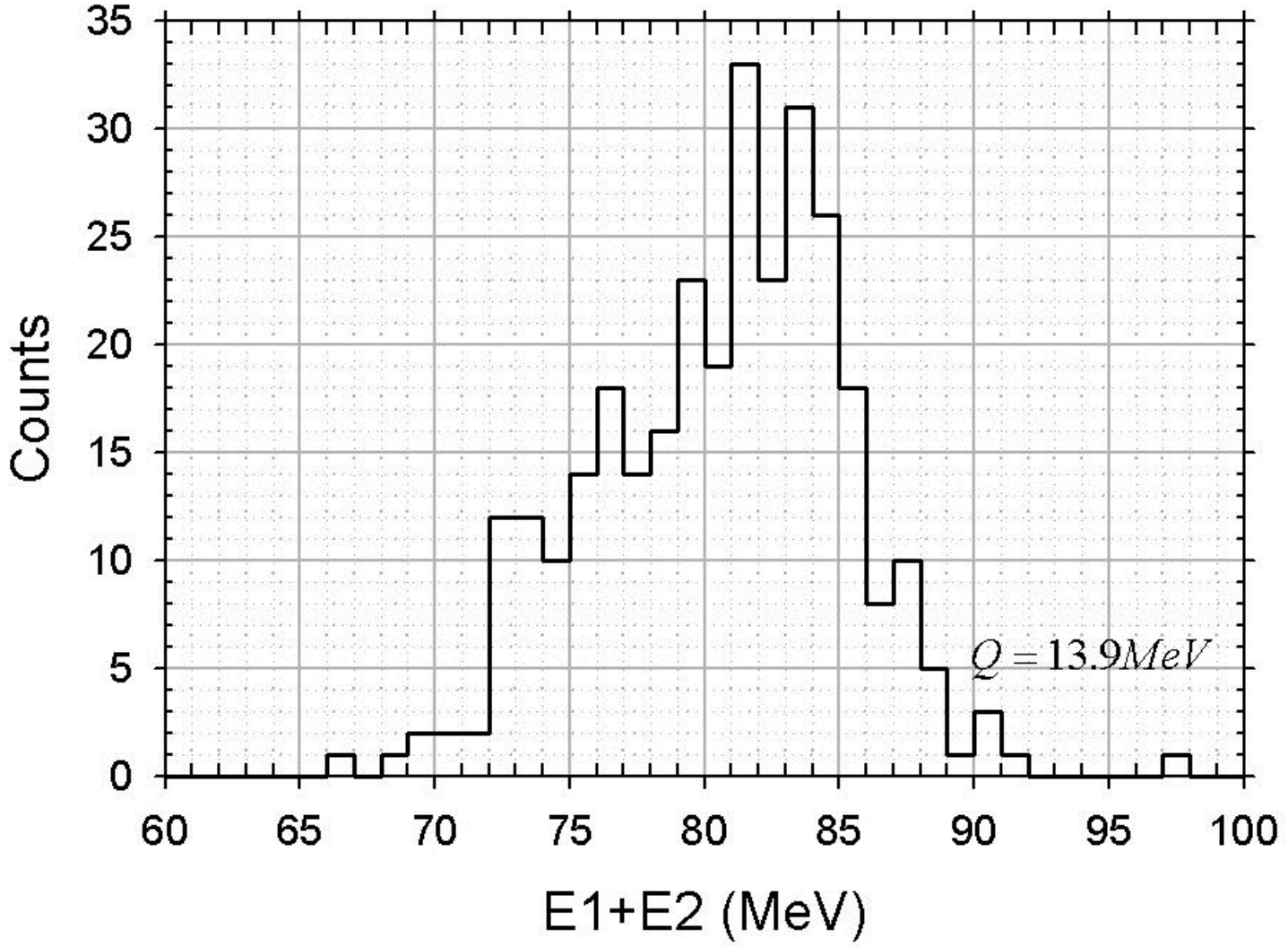

Summed Energy Spectrum of $^{24}Mg(^{12}C, 2^{12}C)^{12}C$ at 104 MeV.
Q=13.9 MeV at coplanar symmetric angle of 33.9^0

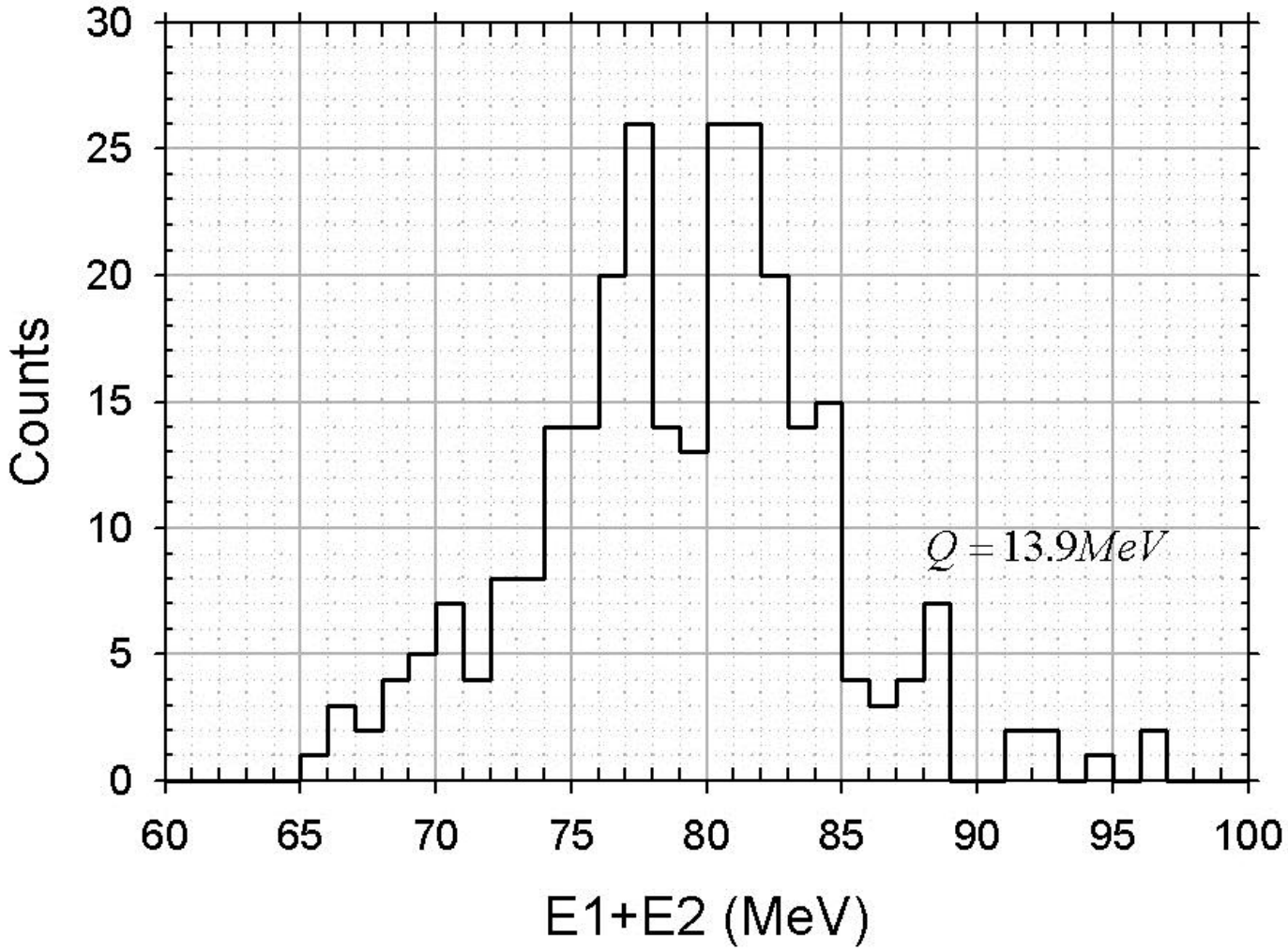

- Finite Range with distortions explain elastic as well as knockout data.
- One can do heavy cluster knockout similar to (C,2C) reaction to study the short distance behaviour of the heavy clusters vertex (Repulsive core radius).
- The repulsion arises from the antisymmetrization of the many fermions system.
- Distortions due to the residual nucleus can be used as an observer (not just a spectator) of the knockout vertex.
- Knockout reactions are very sensitive to the interaction at the knockout vertex. Which has never been imagined by earlier workers.
- Heavy cluster knockout is possible to analyze because of our Finite Range Formalism and program.

Shrinkage of Deuteron in ^{6}Li

Surface Clustering in Light Nuclei

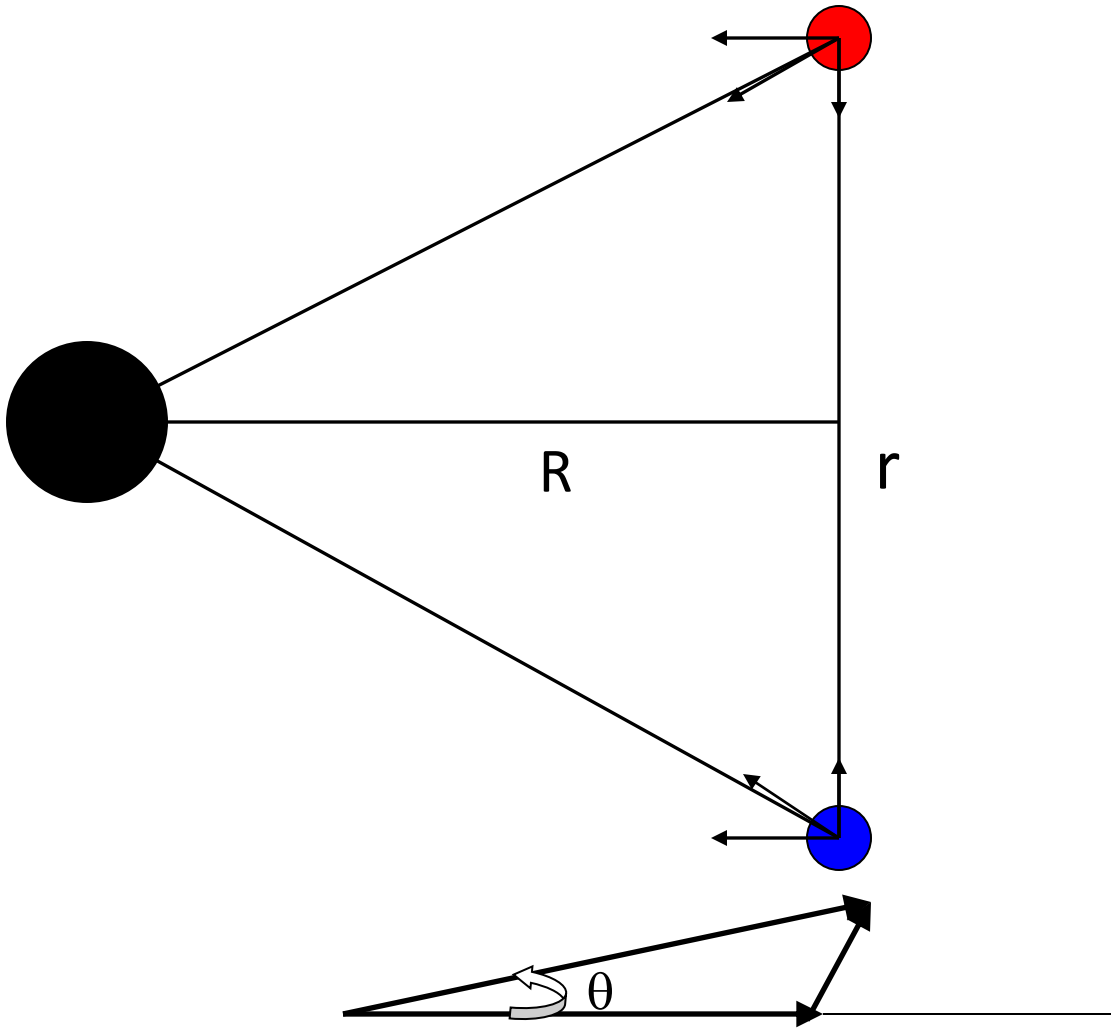

Surface Clustering in Light Nuclei

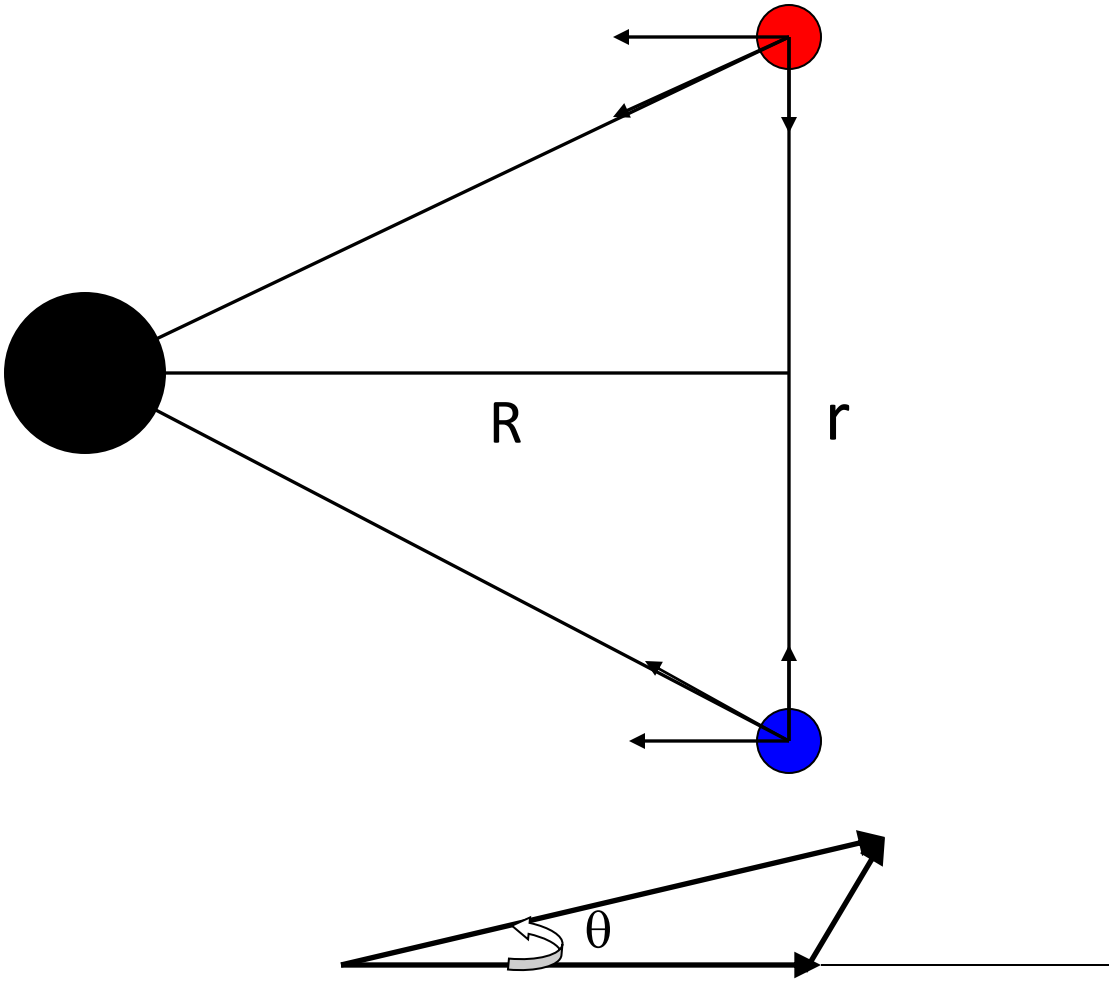

Surface Clustering in Light Nuclei

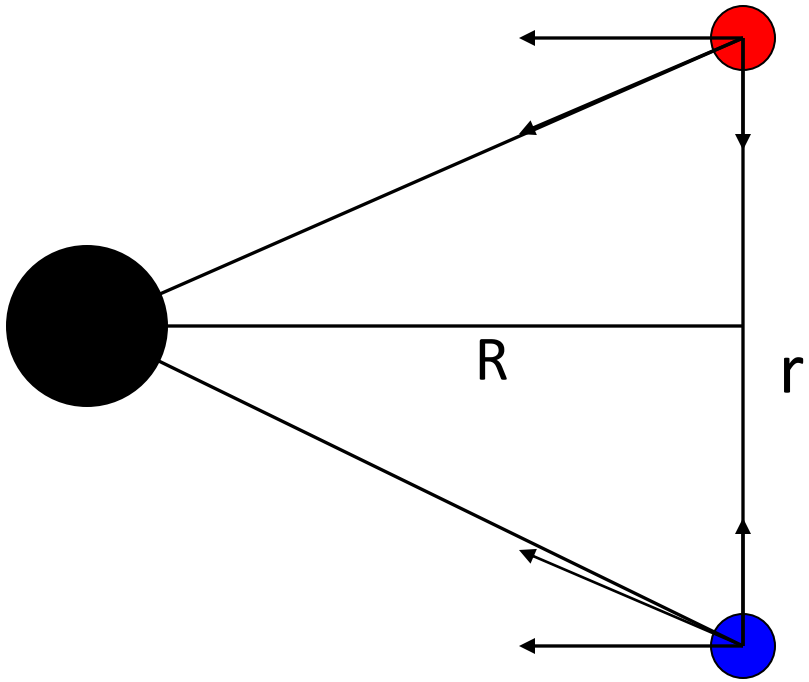

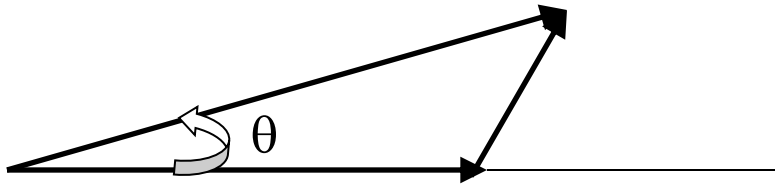

Surface Clustering in Light Nuclei

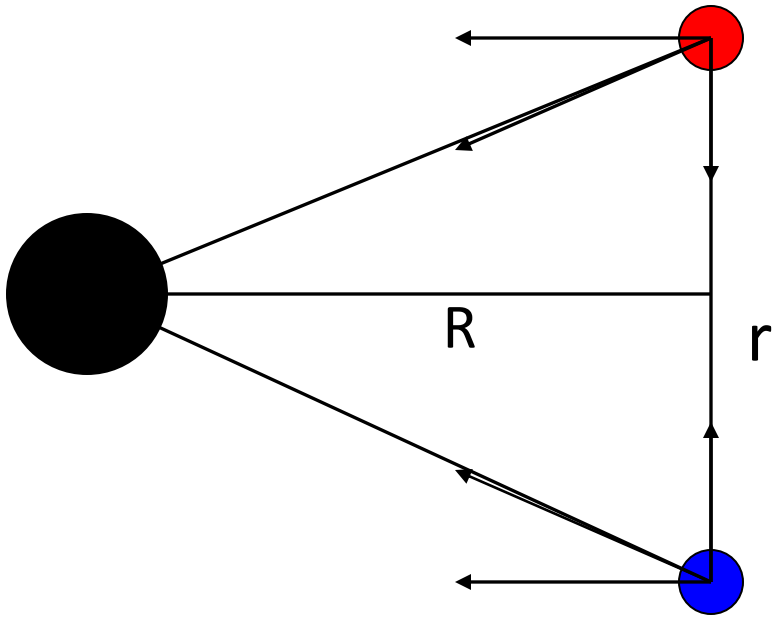

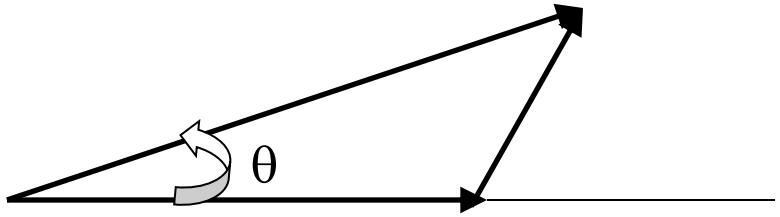

Surface Clustering in Light Nuclei

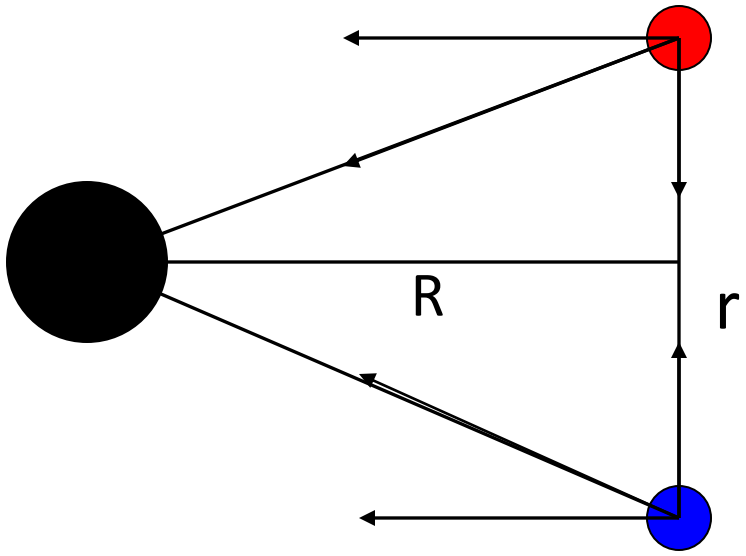

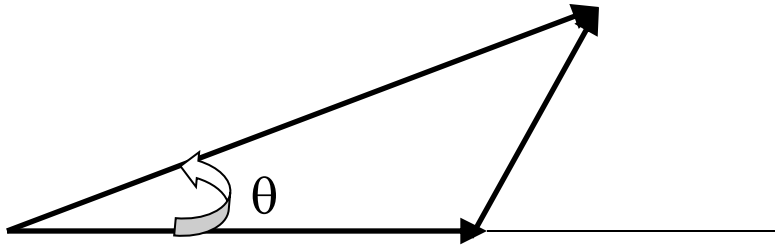

Surface Clustering in Light Nuclei

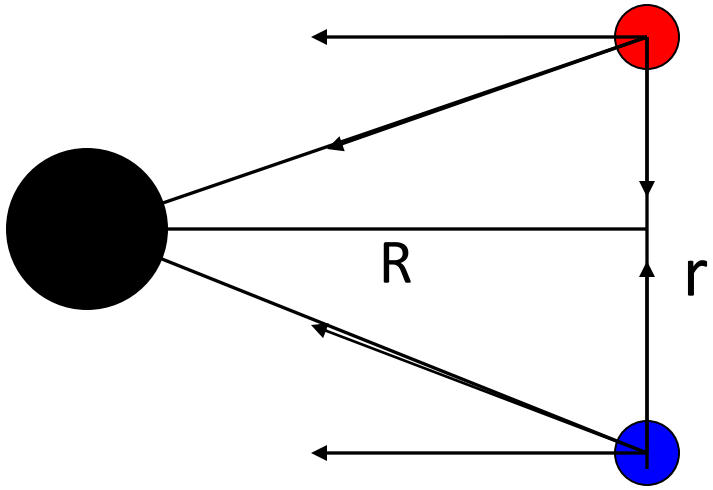

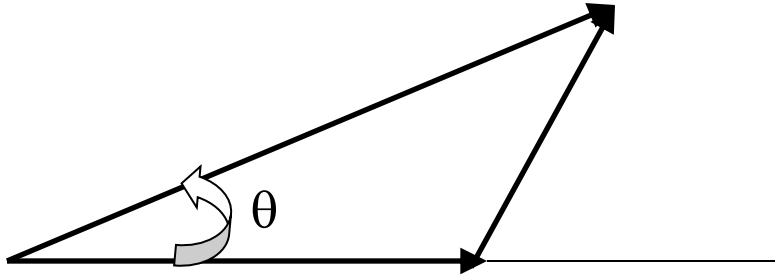

Surface Clustering in Light Nuclei

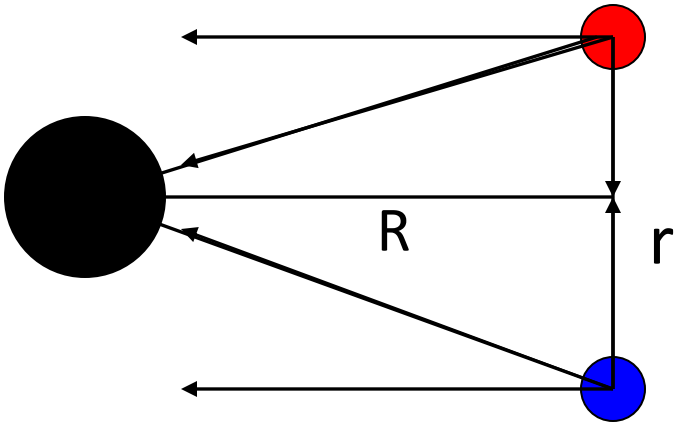

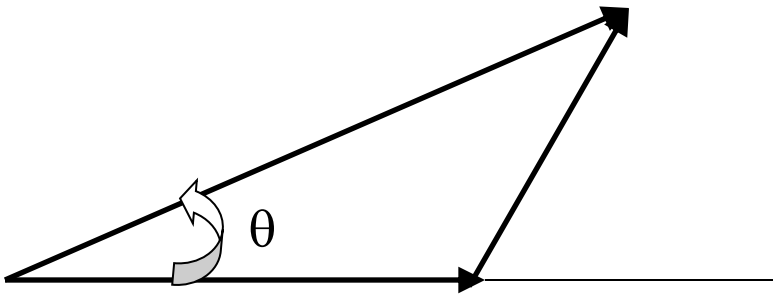

Surface Clustering in Light Nuclei

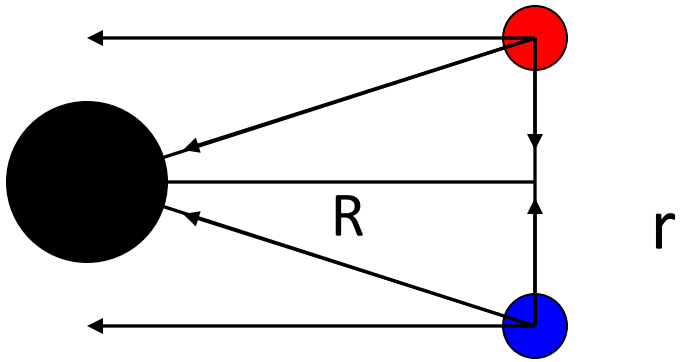

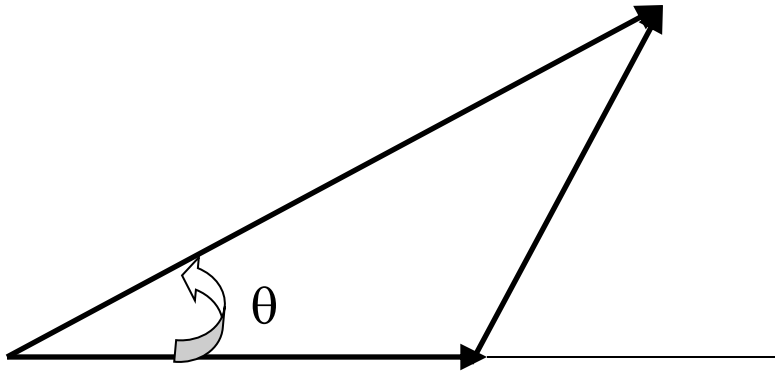

Surface Clustering in Light Nuclei

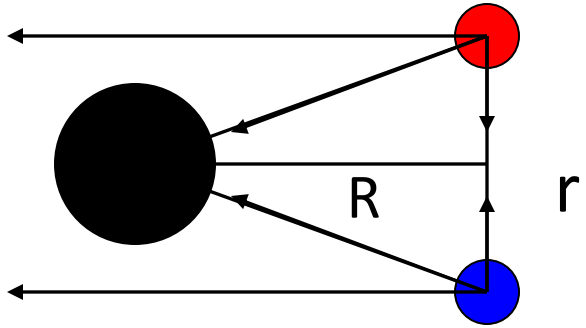

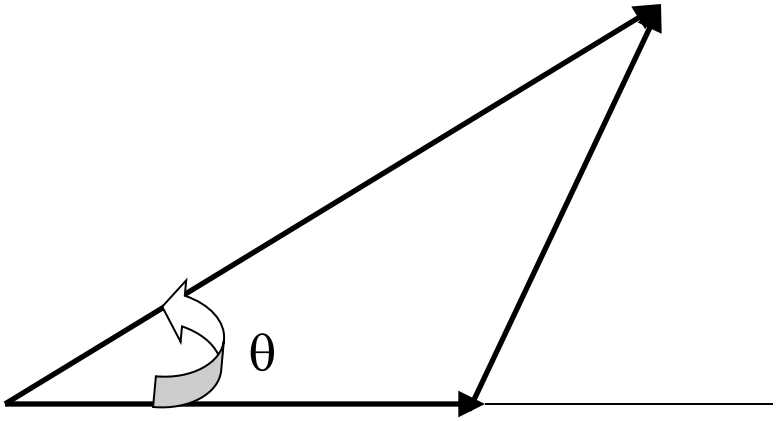

Surface Clustering in Light Nuclei

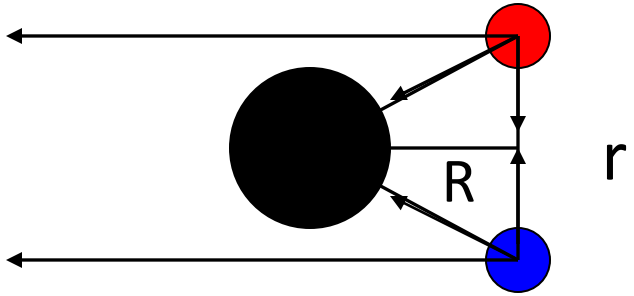

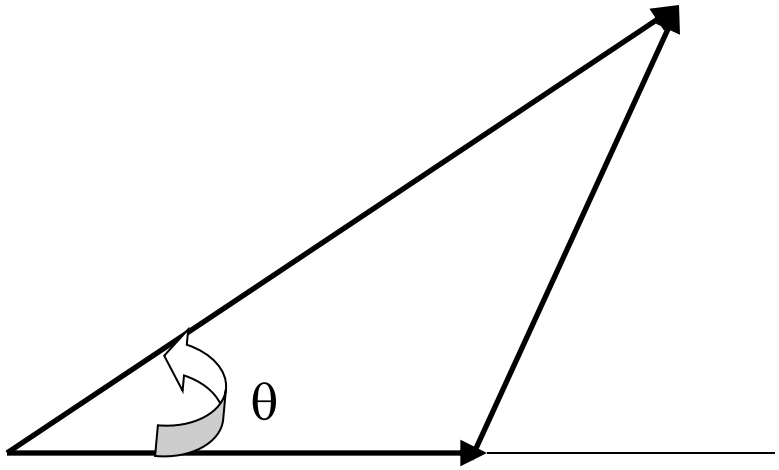

Surface Clustering in Light Nuclei

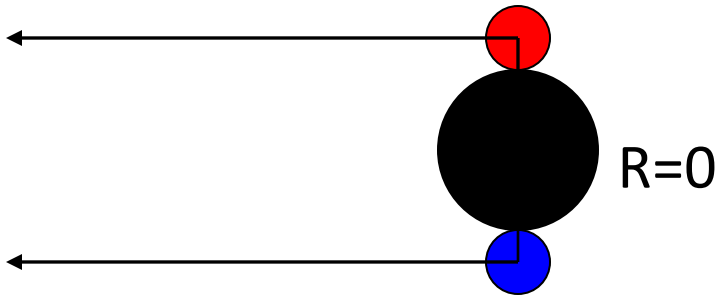

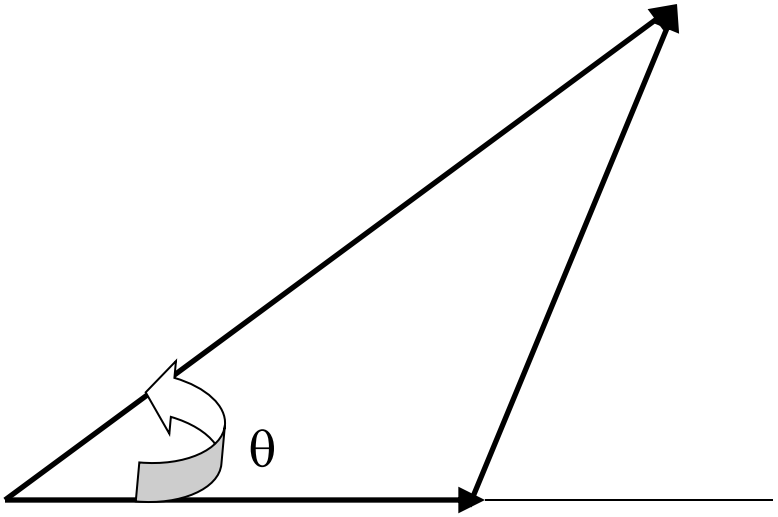

Surface Clustering in Light Nuclei

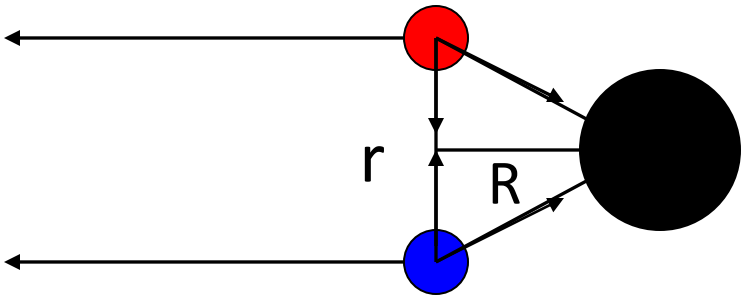

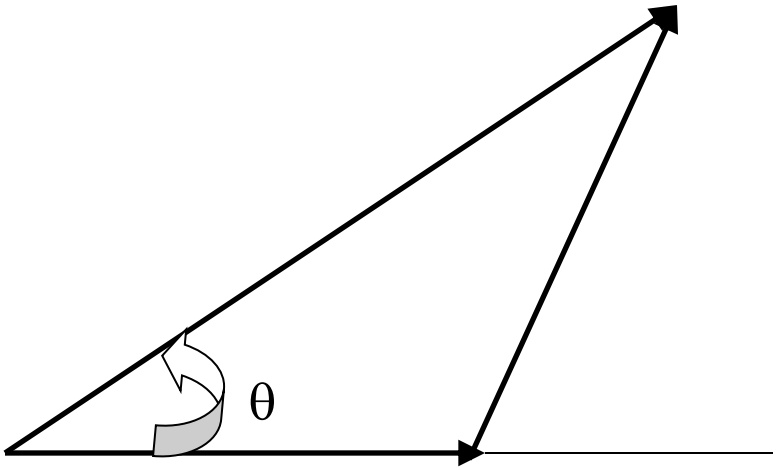

Surface Clustering in Light Nuclei

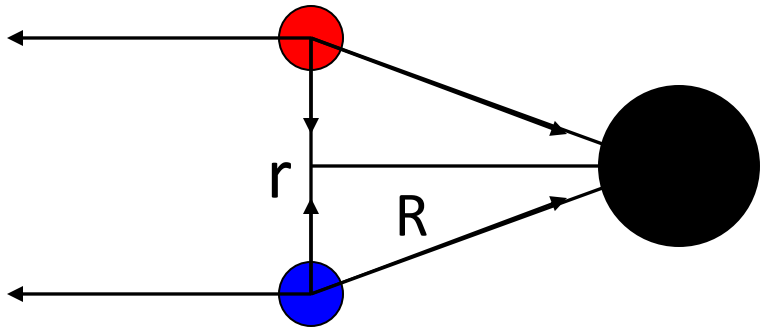

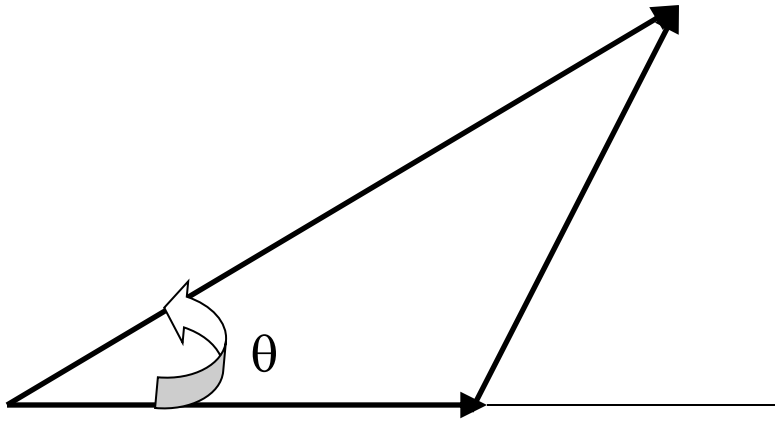

Surface Clustering in Light Nuclei

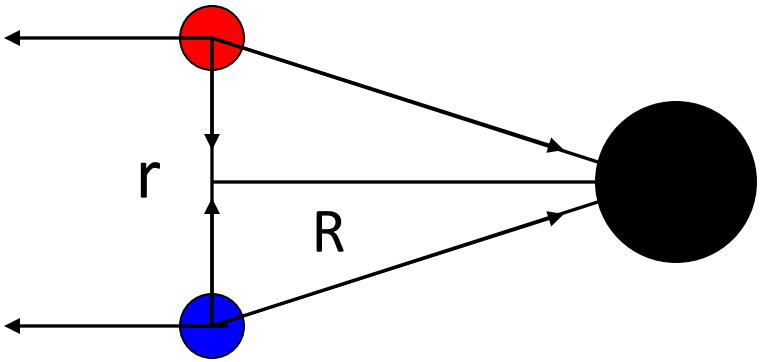

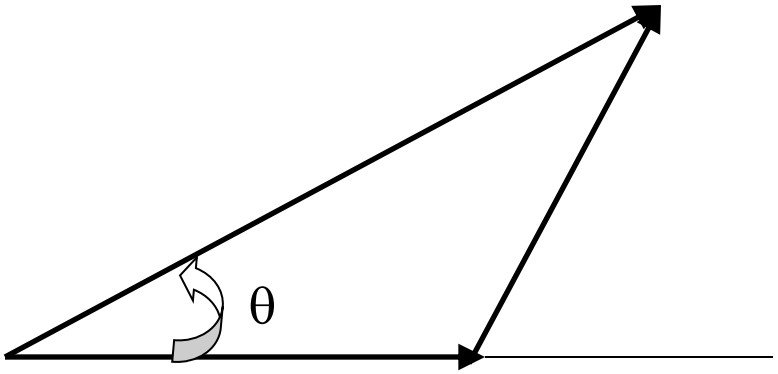

Surface Clustering in Light Nuclei

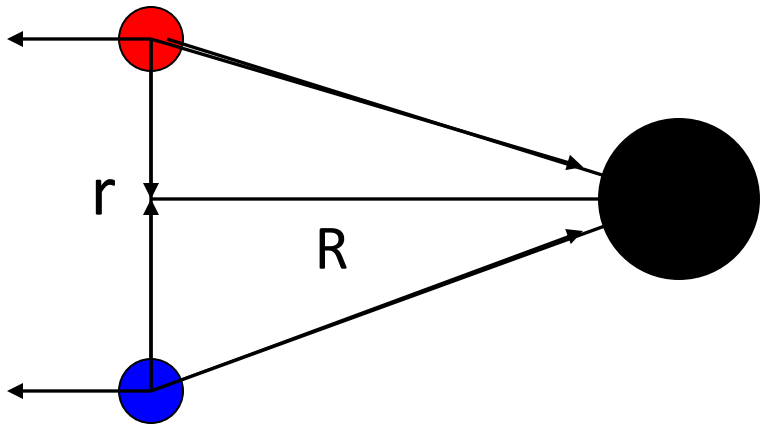

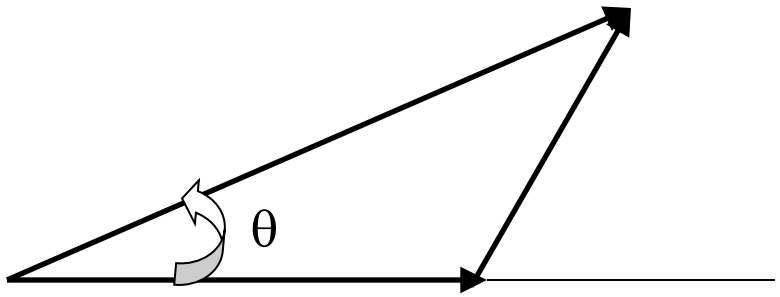

Surface Clustering in Light Nuclei

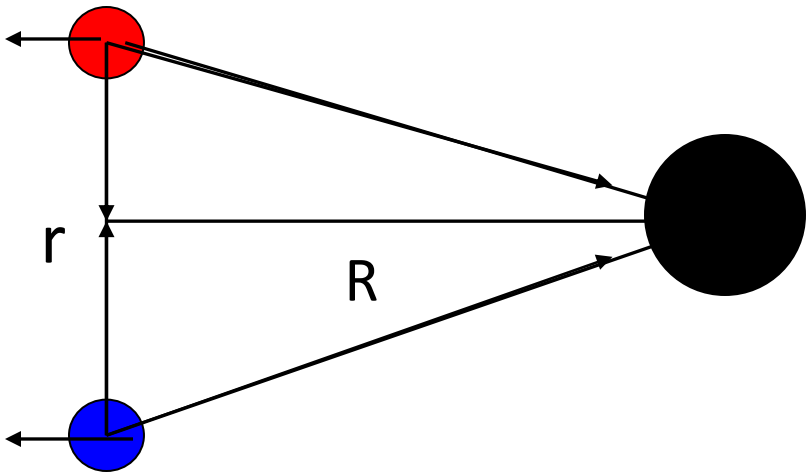

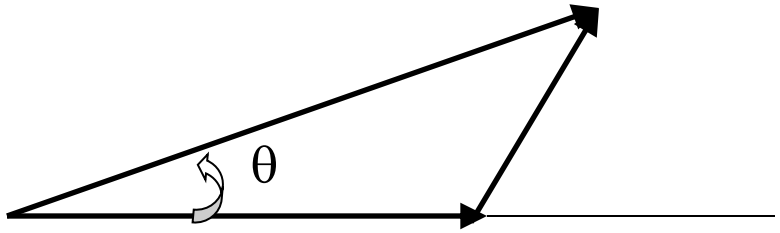

Surface Clustering in Light Nuclei

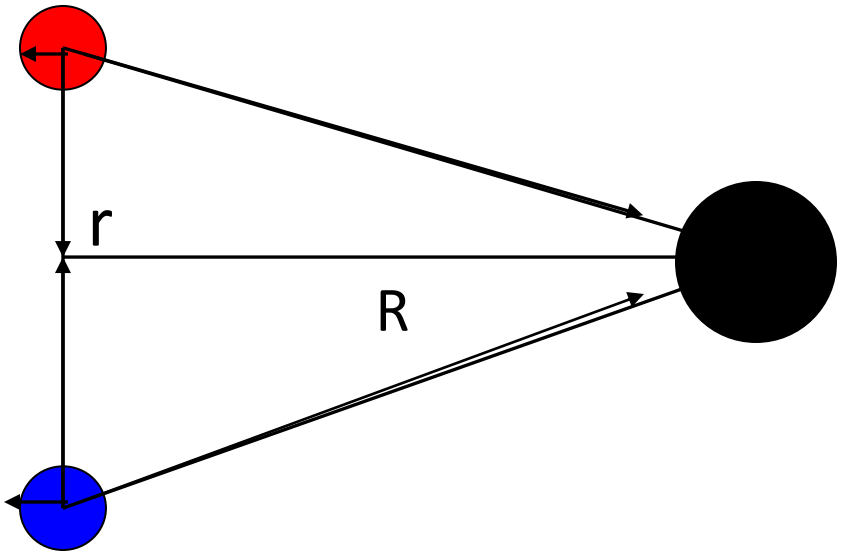

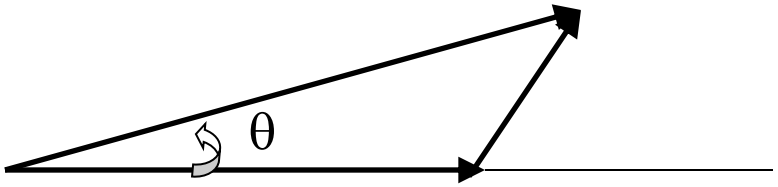

Surface Clustering in Light Nuclei

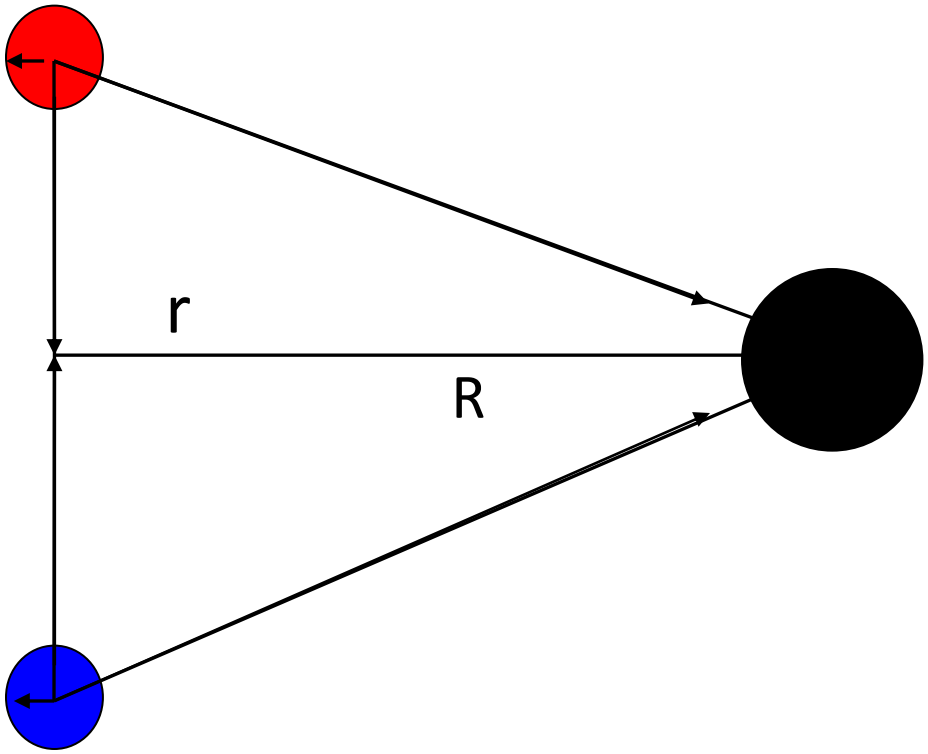

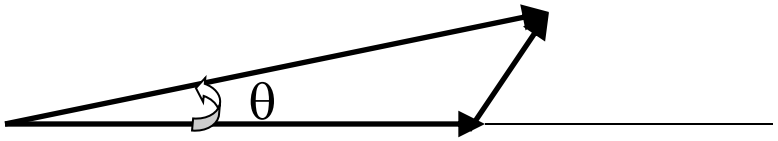

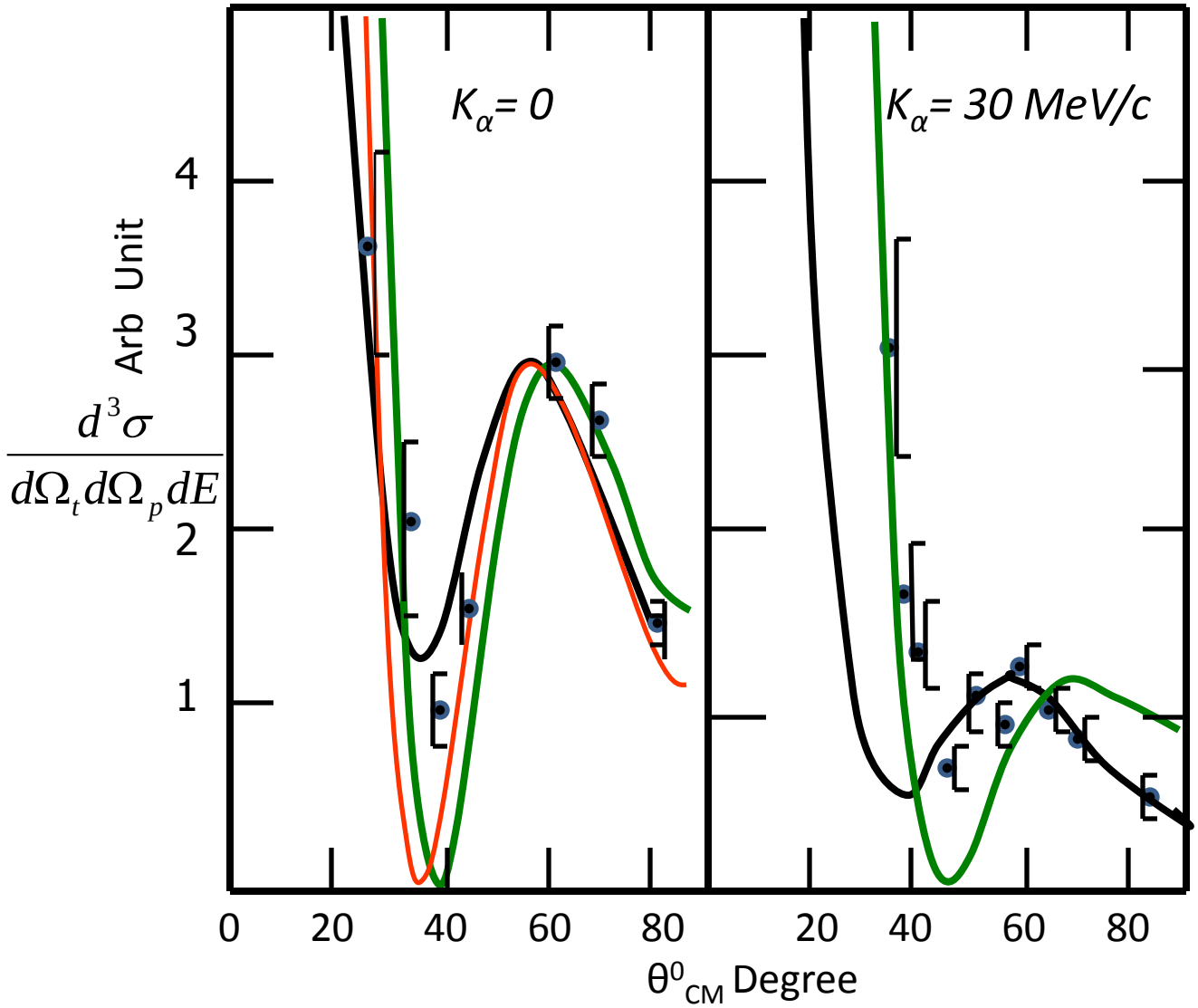

Shift of the Angular distribution of $Li^6(d, tp)He^4$ reaction to larger angles for k_α *= 30 MeV/c* exhibiting shrinkage of d - cluster in ^6Li as it approaches α - cluster

Plane wave overlap function for $Li^6(d, tp)He^4$ Reaction ~28 MeV

PRL. ***32*** *(1974) 173*

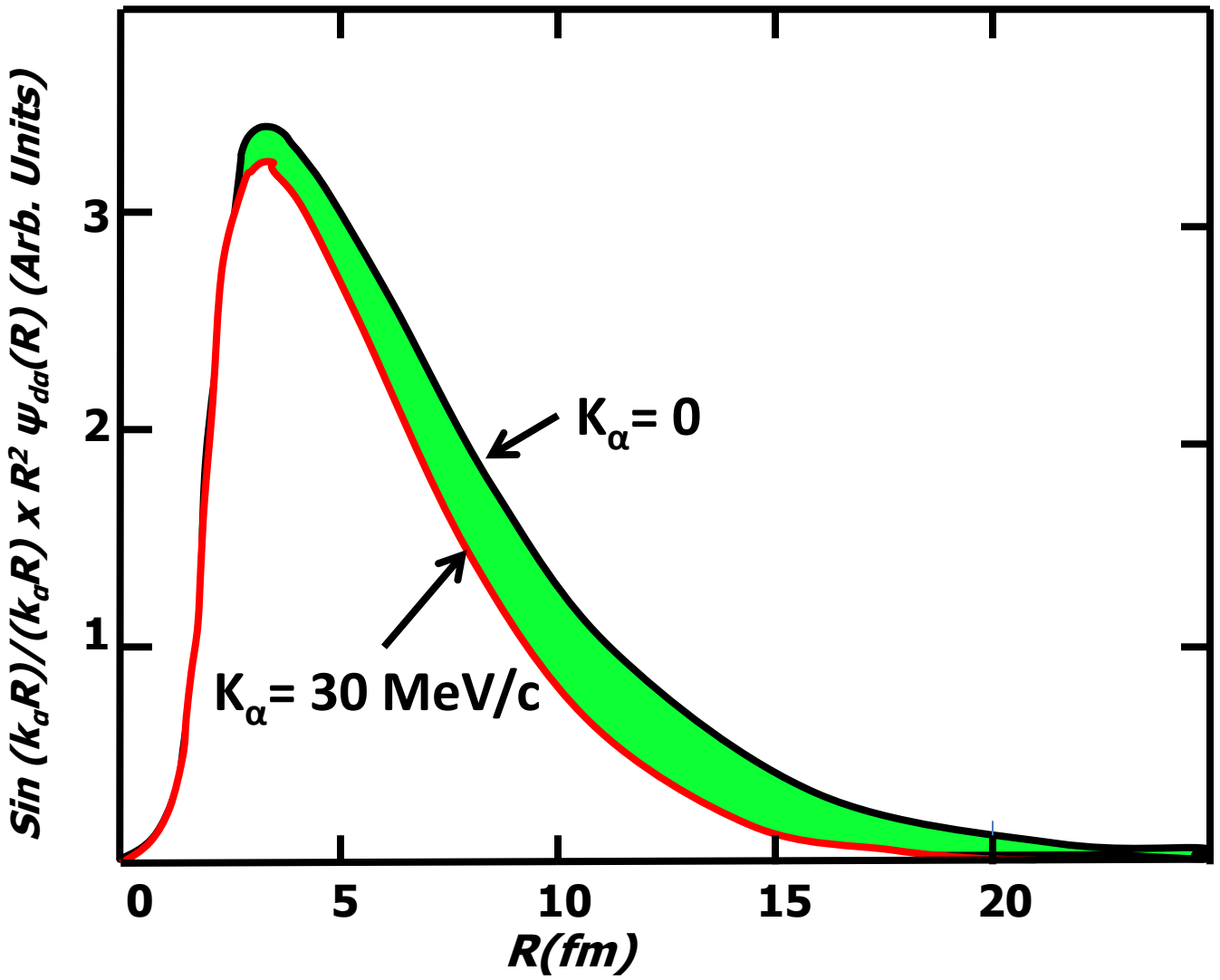

- As seen in the previous figure, when the Deuteron cluster goes farther away from the α cluster (when $K\alpha$= 0 MeV/c) the transition amplitude has relatively more contribution from larger $R_{d-\alpha}$.

- Otherwise, corresponding to K_{α}= -30MeV/c the ^{6}Li(d, t p)^{4}He is expected to display more contribution from the distorted deuteron and if the *n-p* residual interaction in Deuteron cluster is long range type then we will see shrinkage.

- It is clear from next slide; as compared to the free d(d, t)p distribution (free Deuteron cluster), the c.m. *t-p* angular distribution of the ^{6}Li(d, t p)^{4}He reaction shifts outwards. Which means that the relative momentum between *the n – p of the deuteron cluster* in ^{6}Li increased.

from **Halo** to **Hollow**!!!

Halo to Hollow !!

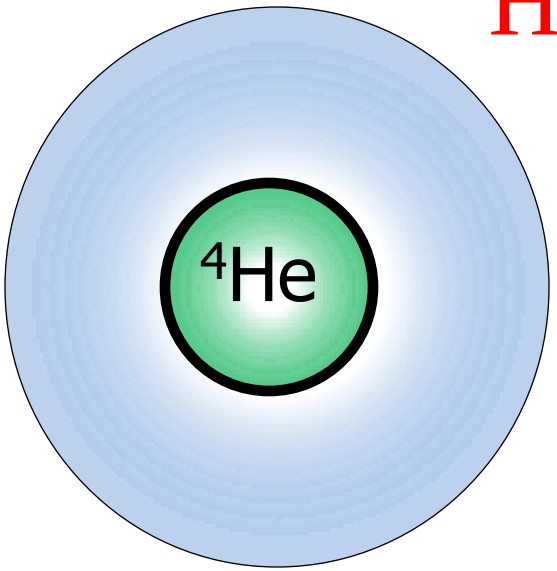

$^{11}Li \rightarrow {}^{4}He + {}^{7}H$

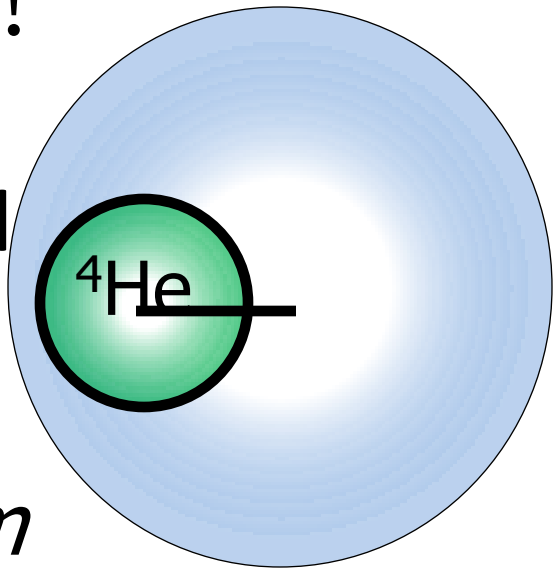

R=1-2 *fm*

R=0

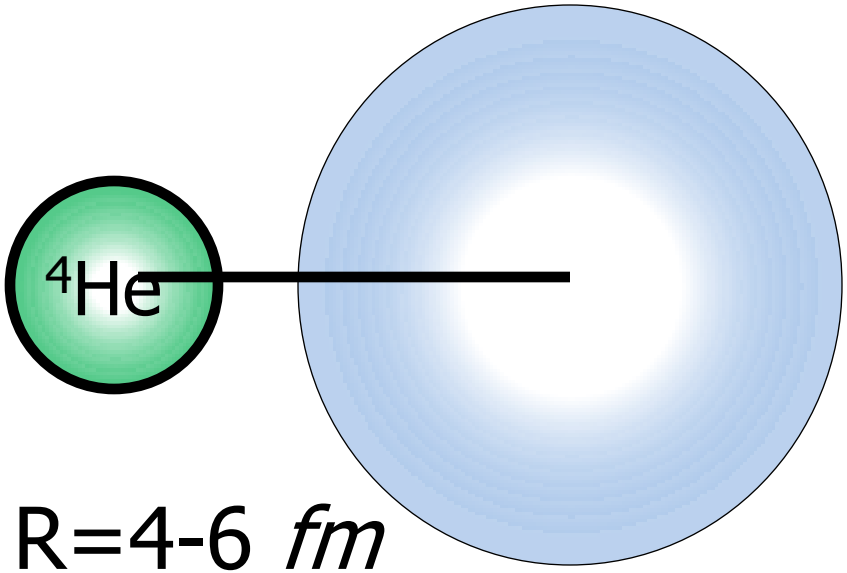

R=4-6 *fm*

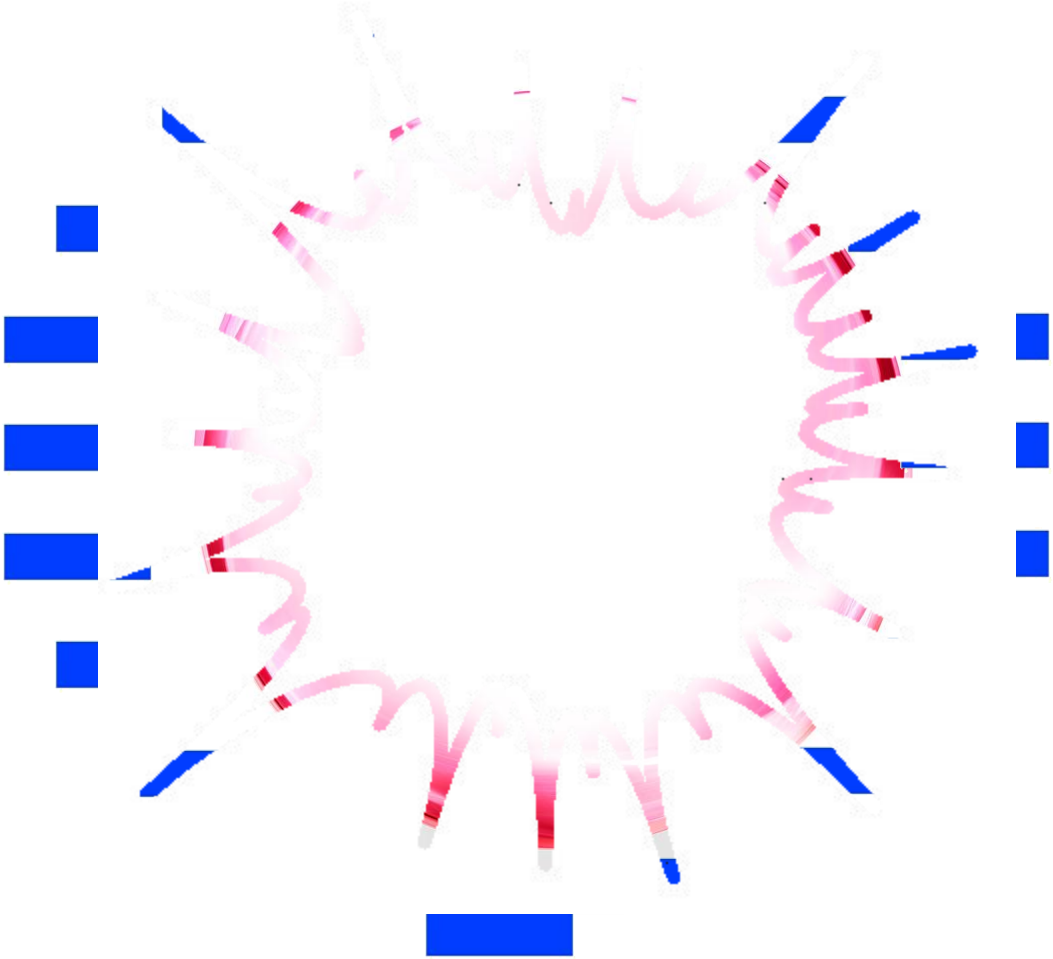

Otherwise

Deflation of a balloon when the surface tension is larger that the pressure inside the balloon.

It nicely represent the decay of a cluster to a compact shape when the long range *N-N* residual interaction is strong.

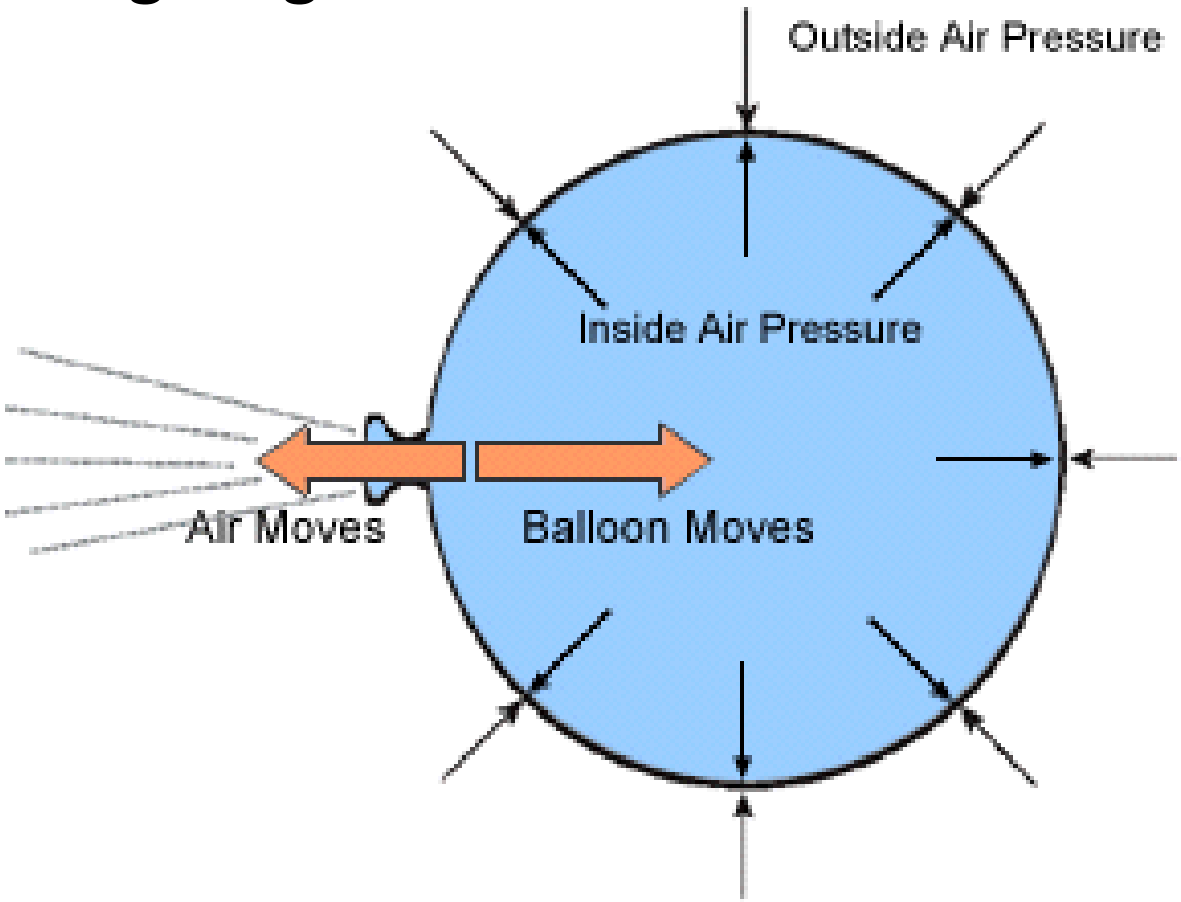

Core Knockout Reaction of a Halo Nuclues:-

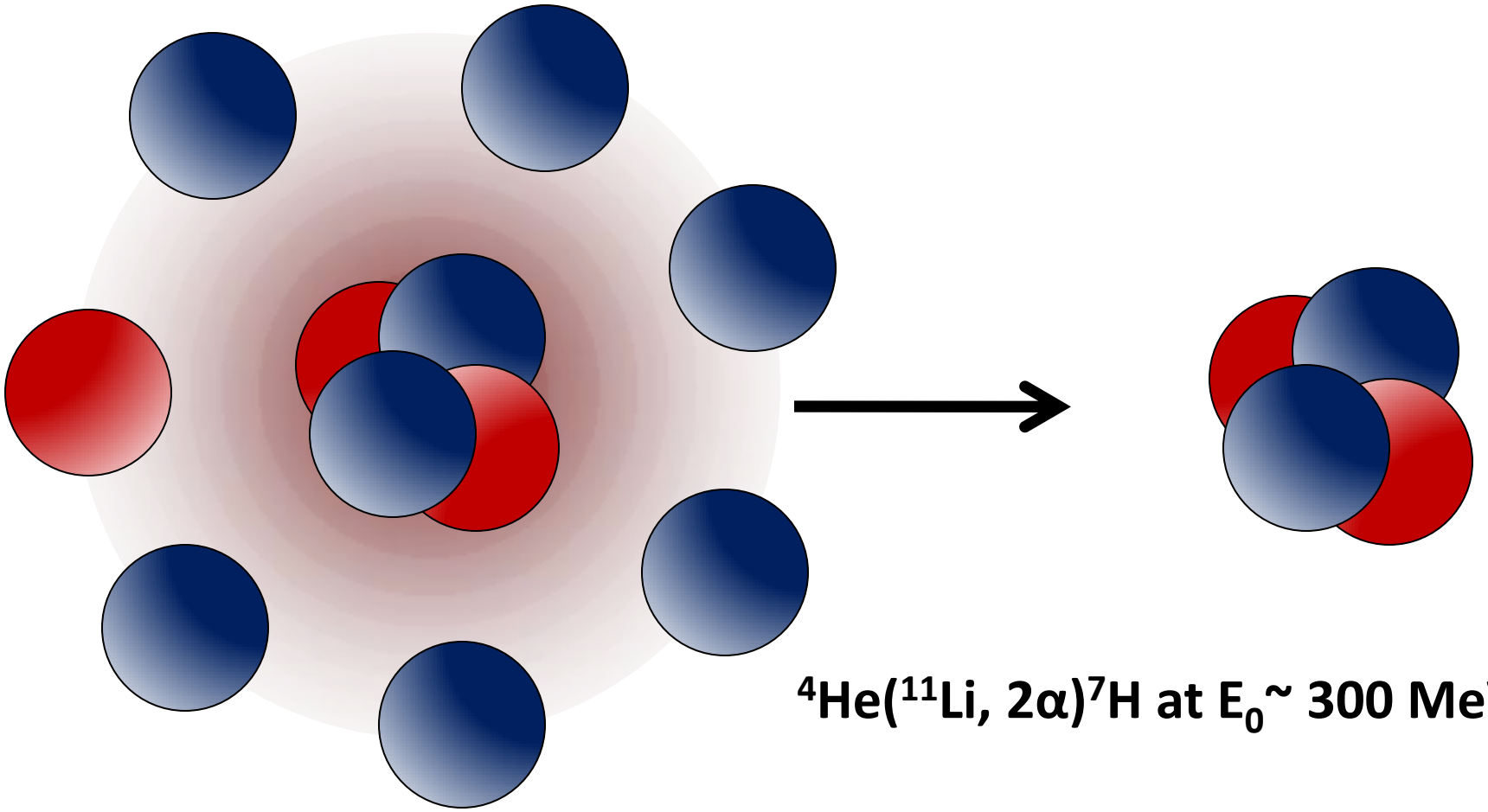

$^{4}He(^{11}Li, 2\alpha)^{7}H$ at E_0~ 300 MeV

Core Knockout Reaction of a Halo Nuclues :-

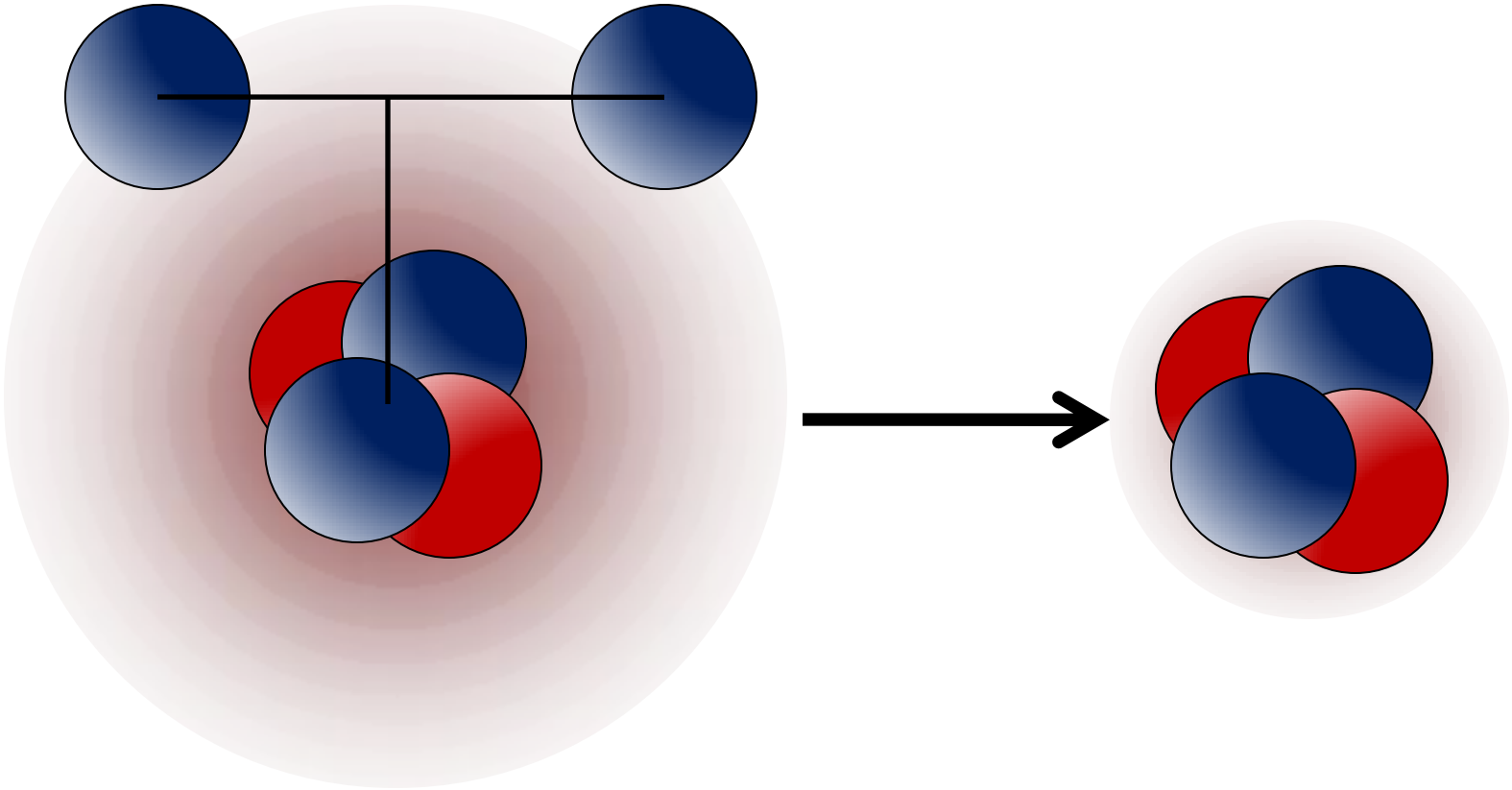

$^{4}He(^{6}He, 2^{4}He)2n$

Core Knockout Reaction of a Halo Nuclues :-

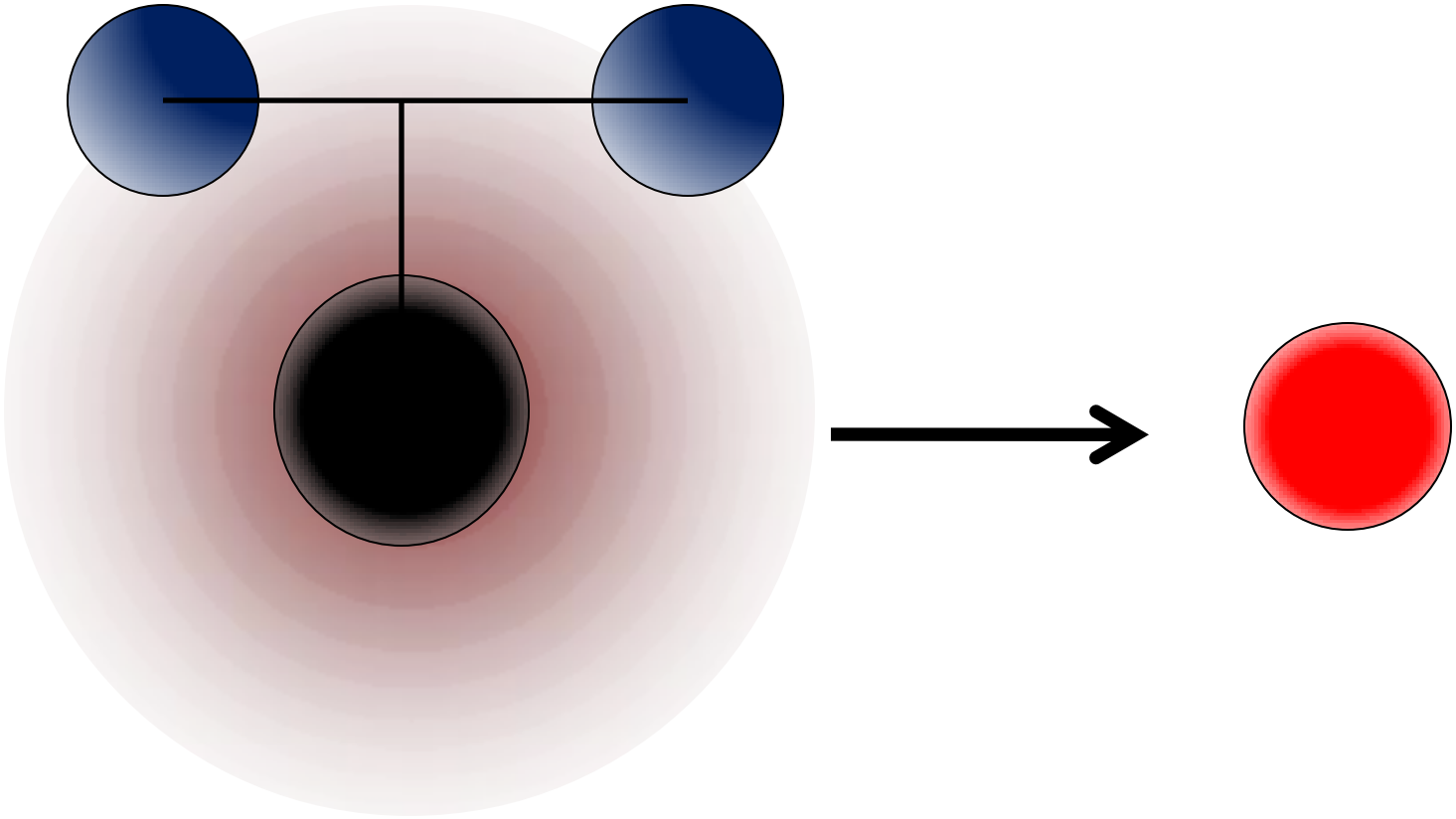

$^{9}Be(^{11}Li, ^{9}Li\ ^{9}Be)2n$

Conclusions:-

1. **In case of (α, 2α) knockout reactions there is a transition from 160 MeV to 200 MeV, where the α-α interaction changes from repulsive to attractive potential.**
2. **One can by explain the sudden change in reaction cross sections considering the strong interaction vertex.**
3. **One can do heavy cluster knockout similar to (C,2C) reaction to study the short distance behaviour of the heavy clusters vertex (Repulsive core radius).**
4. Preliminary data analysis and understanding of the ^{24}Mg(^{12}C, 2^{12}C)^{12}C Reactions at 104 MeV suggest that ^{24}Mg(g.s) can not be described in terms of two Carbon-12 (g.s) clusters.
5. Data also indicated that ^{16}O knockout from ^{24}Mg is very significant leading to ^{24}Mg as ^{16}O+^{8}Be
6. **This also can be used to study the very weakly bound nuclei such as ^{11}Li, ^{8}He, ^{6}He etc by core knockout reaction etc.**
7. **This way one can probably arrive at "HOLLOW" nuclei.**

In the present project we would like to study the heavy ion knockout on ^{28}Si and ^{32}S using ^{24}Mg and ^{28}Si Beams respectively at the Mumbai LINAC in order to compare these reactions with the corresponding $(\alpha,2\alpha)$ reactions.

$^{28}Si(^{24}Mg\ ,2\ ^{24}Mg\ )^{4}He$ *vs* $^{28}Si(\alpha\ ,\ 2\ \alpha\cdot)\ ^{24}Mg$

$^{32}S(^{28}Si\ ,2\ ^{28}Si\ )^{4}He$ *vs* $^{32}S(\alpha\ ,\ 2\ \alpha\cdot)\ ^{28}Si.$

.

This way we will be able to observe the influence of bigger and bigger knockout vertices on the knockout reactions.